PHARMACOKINETICS AND PHARMACODYNAMICS OF OXAZOLIDINONES AND BETA-LACTAMS

By

STEPHAN SCHMIDT

A DISSERTATION PRESENTED TO THE GRADUATE SCHOOL
OF THE UNIVERSITY OF FLORIDA IN PARTIAL FULFILLMENT
OF THE REQUIREMENTS FOR THE DEGREE OF
DOCTOR OF PHILOSOPHY

UNIVERSITY OF FLORIDA

2008

To my family

ACKNOWLEDGMENTS

First and foremost, I would like to thank my supervisor Dr. Hartmut Derendorf for having my as a student, for his continuous support, advice and in times patience. Furthermore, I would also like to thank my committee members Dr. Kenneth H. Rand, Dr. Guenther Hochhaus and Dr. Veronika Butterweck for their constructive guidance of my thesis work.

I would like to thank our current office staff Robin Keirnan-Sanchez, Patricia J. Khan and Marty Rhoden, as well as, our former office staff Andrea Tucker and Jim Ketcham for their consistently excellent support with administrative issues during my stay in the Department of Pharmaceutics.

I wish to give a special thanks to Dr. Olaf Burkhardt, April Barbour and Martina Sahre, Dr. Martin Brunner, Yufei Tang, Dr. Maria Grant, Dr. Christoph N. Seubert, Dr. Robert W. Rout and Dr. Kfir Ben-David for their close collaboration, our study subjects for participating and Shands' GCRC staff for their excellent support of our clinical microdialysis projects.

I would like to thank my co-workers Martina Sahre, April Barbour, Oliver Ghobrial and Dr. Sreedharan Nair Sabarinath, as well as, our German exchange students Katharina Roeck, Sandra Weiss, Matthias Fueth and Sara Dizayee for their support with my *in vitro* experiments.

I want to acknowledge my co-authors April Barbour, Dr. Olaf Burkhardt, Dr. Kenneth H. Rand, Dr. Yanyun Li, Dr. Vipul Kumar, Dr. Edgar L. Schuck, Dr. Martin Brunner, Dr. Maria Grant, Dr. Robert W. Rout, Dr. Kfir Ben-David, Dr. Seubert, Martina Sahre, Katharina Roeck, Rebecca Banks, Yufei Tang, Lars Schiefelbein and Benjamin Ma for their contributions to the manuscripts and publications.

I also would like to thank Dr. Derendorf's group for the all inspiring discussions, as well as, social gatherings in and outside the laboratory. They all have substantially improved the quality of my work and made my time in Gainesville a pleasant memory.

Last but not least, I would like to thank my family and friends, especially my future wife Arielle Pandolph, for all their support and encouragement during my stay at the University of Florida.

Chapter 2 of this thesis has been previously published in Antimicrobial Agents and Chemotherapy, chapter 3 in the Journal of Clinical Pharmacology, chapter 4 in the Journal of Antimicrobial Agents and Chemotherapy and chapter 5 in Expert Opinion in Drug Discovery. Chapter 6 is currently under submission with Antimicrobial Agents and Chemotherapy. These journals have been credited in the respective chapters and permissions for reprint for educational purposes as part of this thesis have been granted.

TABLE OF CONTENTS

LIST OF TABLES

LIST OF FIGURES

LIST OF ABBREVIATIONS

ABS	Adult bovine serum
AIC	Aminoimidazole-4-carboxamide
ALA	Aminolevulinic acid
ANOVA	Analysis of variance
AUC	Area under the curve
AUC_{0-t}	Area under the curve from time zero to time t
$AUC_{0-\infty}$	Area under the curve from time zero to infinity
AUC/MIC	Area under the curve over 24h at steady-state divided the MIC
$AUMC_{0-\infty}$	Area under the first-moment curve
BA	Bioavailability
BAL	Broncho-alveolar lavage
BCC	Basal cell carcinoma
BE	Bioequivalence
BID	Twice daily
BSA	Bovine serum albumin
CE	Conformite Europeene
CDC	Center for Disease Control and Prevention
CFU	Colony forming units
CI	Confidence interval
CLSI	Clinical and Laboratory Standards Institute
CL_{tot}	Total clearance
C_{max}	Peak plasma concentration

C_{max}/MIC	Peak level divided by the MIC
COX-2	Cyclooxygenase 2
CRO	Ceftriaxone
d_g	Delay in the onset of growth
d_{gs}	Delay in the onset of growth of susceptible bacteria
d_k	Delay in the onset of kill
d_{ks}	Delay in the onset of kill of susceptible bacteria
E. coli	*Escherichia coli*
EC_{50}	Concentration necessary to produce 50% of the maximum (kill) effect
ECG	Electrocardiogram
EE	Extraction efficiency
ELF	Epithelial lining fluid
E_{max}	Maximum effect
ERT	Ertapenem
ESBL	Extended-spectrum β-lactamase
f	Free
fC_e	Free concentration in the effect compartment
FDA	Food and drug administration
fu	Fraction unbound
GI	Gastro intestinal
h	Hill factor
H. influenzae	*Haemophilus influenzae*
HSA	Human serum albumin

HP	Human plasma
HPLC	High performance liquid chromatography
ISF	Interstitial space fluid
IRB	Institutional review board
i.v.	Intravenous infusion
k_0	Bacterial growth-rate constant
k_{12}	Transfer-rate constant from the first to the second compartment
k_{21}	Transfer-rate constant from the second to the first compartment
k_{10}	Elimination-rate constant from the first compartment
k_{1e}	Transfer-rate constant from the first in the effect compartment
k_a	Absorption-rate constant
k_d	Natural death-rate constant
k_{e0}	Elimination-rate constant from the effect compartment
K. pneumoniae	*Klebsiella pneumoniae*
k_{max}	Maximum kill effect
k_{ps}	Transfer-rate constant from persistent stage to susceptible stage
k_s	Growth-rate constant of susceptible pathogens
k_{sp}	Transfer-rate constant from susceptible stage to persistent stage
LC-MS-MS	Liquid chromatography coupled with tandem mass spectrometry
LR	Lactated ringer's
λz	Terminal elimination rate constant
MHB	Mueller-Hinton broth
MIC	Minimum inhibitory concentration

MD	Microdialysis
MMM	Metastatic malignant melanomas
MPT	Mechanical pain threshold
MRSA	Methicillin-resistant Staphylococcus aureus
MRT	Mean residence time
MSC	Model selection criterion
MSE	Mean standard error
N	Number of bacteria
n	Number of study subjects
N_0	Starting number of bacteria
NCCLS	National Committee for Clinical Laboratory Standards
N_{MIC}	Number of bacteria at the MIC turbidity threshold
N_p	Number of bacteria unsusceptible to antibiotic
N_s	Number of bacteria susceptible to antibiotic
NSAID	Nonsteroidal anti-inflammatory drug
N_t	Number of bacteria at time t
OFV	Objective function value
P. aeruginosa	*Pseudomonas aeruginosa*
PB	Protein binding
PCV	Penciclovir
PDT	Photodynamic therapy
PG	Prostaglandin
PET	Positron emission tomography

PD	Pharmacodynamic
PK	Pharmacokinetic
QD	Once daily
S. aureus	*Staphylococcus aureus*
SC	Stationary concentration
SD	Standard deviation
SLS	Sodium lauryl sulfate
S. pneum.	*Streptococcus pneumoniae*
SSSI	Skin and skin structure infections
t	Time
$T_{>MIC}$	Cumulative percentage of a 24h period that the drug level exceeds the MIC at steady-state
$t_{1/2}$	Half-life
TB	Tuberculosis
THB	Todd-Hewitt broth
TID	Three times daily
t_{max}	Time to reach peak plasma concentration
V_d	Volume of distribution
VISA	Vancomycin-intermediate susceptible *Staphylococcus aureus*
VRE	Vancomycin-resistant enterococci
VRSA	Vancomycin-resistant *Staphylococcus aureus*
V_z	Apparent volume of distribution during the terminal phase

Abstract of Dissertation Presented to the Graduate School
of the University of Florida in Partial Fulfillment of the
Requirements for the Degree of Doctor of Philosophy

PHARMACOKINETICS AND PHARMACODYNAMICS OF OXAZOLIDINONES AND BETA-LACTAMS

By

Stephan Schmidt

December 2008

Chair: Hartmut Derendorf
Major: Pharmaceutical Sciences

Introduction: The purpose of this thesis was to support optimizing antibiotic drug development by evaluating the effect of protein binding (PB) on 1) the *in vitro* activity of highly bound agents and 2) on the soft tissue penetration, as well as, 3) establishment of a general PK/PD model to characterize the activity of oxazolidinones against methicillin-resistant *Staphylococcus aureus* (MRSA).

Methods: 1) Using *in vitro* microdialysis (MD), free ceftriaxone (CRO) and ertapenem (ERT) concentrations were determined in growth medium with and without bovine/human serum albumin (BSA/HSA), in adult bovine serum (ABS) and in human plasma (HP). Corresponding antimicrobial activity was determined in minimum inhibitory concentration (MIC) and time-kill curve experiments against *E. coli* ATCC25922 and *S. pneum.* ATCC6303. A modified E_{max}-model was fitted to the data and respective EC_{50}s compared. 2) Blood and MD samples from the interstitial space fluid (ISF) of thigh muscle and subcutaneous adipose tissue were obtained from 6 healthy volunteers following a 30min infusion of 1g ERT for up to 12 hours. 3) A two-subpopulation model was simultaneously fitted to the static, as well as, dynamic time-kill curve data of RWJ-416457 and linezolid against MRSA OC2878 and EC_{50}s compared.

Results: 1) For CRO, PB differed between HP (76.8±11.0%) and commercially available BSA (20.2±8.3%) or HSA (56.9±16.6%). Similar results were obtained for ERT (HP: 73.8±11.6%, BSA: 12.4±4.8%, HSA: 17.8±11.5%). MICs and EC_{50}s of both strains were increased for CRO when comparing HSA and BSA, whereas EC_{50}s were not different for ERT. 2) Free concentrations in the ISF of thigh muscle and subcutaneous adipose tissue were consistent with free concentrations in plasma but much lower than those in total plasma. 3) A two-subpopulation model was appropriate to describe the data resulting in a lower EC_{50} of RWJ-416457 (0.41μg/mL) compared to that of linezolid (1.39μg/mL).

Conclusion: Free, unbound concentrations are responsible for antimicrobial efficacy, as well as, tissue distribution and can be measured by microdialysis. Once determined, free concentrations can be linked to the corresponding PD parameters in an appropriate PK/PD model in order to predict clinical outcome. PK/PD modeling and simulation is, consequently, a valuable tool for dose selection.

CHAPTER 1
INTRODUCTION

An infection is defined as the growth of a parasitic organism (e.g. bacteria, fungi, etc.) within the body of a host. The goal of an anti-infective therapy is to eradicate the infecting organism (pathogen) from the host. Generally, this removal process primarily includes the use of anti-infective drugs. Ideally, these drugs eliminate the pathogen without causing toxic side effects or inducing resistance against the anti-infective agent in the pathogen. The selection of an appropriate antimicrobial agent and/or dosing regimen is hereby crucial for success of the therapy and can be governed by pharmacokinetic (PK) and pharmacodynamic (PD) principles.

Hypothesis: Insufficient free, unbound antibiotic concentrations at the site of infection result in therapeutic failure and can, subsequently, lead to the emergence of resistance. Proper selection of an appropriate antibiotic dosing regimen is, therefore, critically important and can be supported by pharmacokinetic/pharmacodynamic (PK/PD) modeling and simulation approaches.

The selection of appropriate antimicrobial agents does not start at the bedside but way early in drug development by evaluating the antimicrobial spectrum of new antibiotic candidates in the laboratory. This is usually done by determining the minimum inhibitory concentration (MIC) against a variety of Gram-positive, Gram-negative and atypical pathogens. The MIC is defined as the lowest concentration that completely inhibits visible growth of the organism, as detected by the unaided eye after overnight incubation at 35^{o}C with a standard inoculum of approximately $5x10^{5}$-10^{6} colony forming units per milliliter (CFU/mL) (228). Although routinely employed, the MIC is a static, mono-dimensional threshold value that does not allow to account for changes of antibiotic concentrations over time or prediction of antimicrobial activity at concentrations apart from the MIC itself (148, 216, 231). More detailed information can be obtained from evaluation of the antimicrobial activity over time (time-kill curves).

In order to facilitate the transition between identification of antibiotic candidates and later, clinical stages of drug development, employed *in vitro* systems should be as predictive as possible of clinical outcome. One approach is to reproduce similar conditions *in vitro* as encountered *in vivo*. For example, addition of protein supplements to the *in vitro* MIC or time-kill curve test systems is intended to mimic plasma protein binding. However, the experimental procedure for the determination of protein binding has not been internationally standardized yet and the use of different supplements might yield different outcomes.

The first specific goal of this thesis work is the evaluation of the antimicrobial activity of two beta-lactams with reportedly high plasma protein binding, ceftriaxone (83-96%) (244, 245, 277) and ertapenem (84-96%) (34), in the presence of various protein supplements.

Binding to plasma proteins does not only reduce the antimicrobial activity but also restricts the distribution of antibiotics into tissues. Since most infections are located in the tissues rather than the blood stream, sufficient penetration into the tissue is essential for an antibiotic to be clinical effective and, subsequently, to avoid the emergence of resistance (251). The traditional approach of linking plasma drug concentrations to observed effects is, consequently, unreliable (185, 251). A more rational approach would be to determine free, active drug concentrations at the site of infection. Microdialysis (MD) is currently the most appropriate sampling technique that can provide this information and has been frequently employed in PK studies determining the tissue concentrations of antibiotics (44, 112, 120). In this sampling technique, a small, semi-permeable membrane (MD probe) is placed into the ISF of the tissue of interest. The MD probe is perfused with a physiological solution (e.g. Lactated Ringer's) at a constant flow-rate of 1-5μL/min and at specified time intervals protein-free compound is collected for analysis (28, 228).

The second specific goal of this thesis work is to determine the distribution of ertapenem into muscle- and subcutaneous adipose fat tissue of 6 healthy subjects following a single 30min infusion of 1g ertapenem using microdialysis.

At this point it is important to realize that in isolation, PK and PD information is of limited usefulness. Only the link of PK and PD allows to sufficiently characterizing and predicting the drug-effect relationship. For antibiotics, a combination of the MIC and free (f), unbound PK parameters to MIC-based PK/PD indices is frequently used to define clinically relevant efficacy breakpoints. To date, three main PK/PD indices are employed and have led to a much better understanding of antibiotic dosing: 1) the time free antibiotic concentrations remains above the MIC (fT$_{>MIC}$), free area under the concentration-time curve over MIC ratio (fAUC/MIC) and free maximum plasma concentration over MIC ratio (fC$_{max}$/MIC) (229). Yet, the previously described drawbacks of MIC (static, highly variable, etc.) (231), limit the reliability of the MIC-based PK/PD indices as well. To overcome these limitations, the use of other PD approaches has been suggested. One of these approaches is the continuous measurement of the antibiotic concentration-effect relationship over time (time-kill curves) (11, 198, 258). Once performed, a mathematical model can be simultaneously fit to the data and outcome parameters, such as the EC$_{50}$ (concentrations necessary to produce 50% of the maximum effect) can be used to characterize the potency of antibiotics. Although the description of these time-kill curves is mathematically somewhat more complex, their capability of describing concentration-effect relationships over time allow the evaluation of sub-MIC, as well as, fluctuating concentrations on bacterial growth and kill. Once a mathematical model is established, it can be applied to the time-kill curve data of other drugs with the same mechanism of action and respective PD outcomes can be compared. In addition, the link of determined PD parameters to PK data of

different doses or dosing regimens allows predicting corresponding clinical outcomes. Modeling and simulation approaches are, consequently, very valuable for dose selection and have been recommended by the Food and Drug Administration (FDA) as tools to streamline the drug development process (84).

The third specific goal of this thesis work is, therefore, to qualitatively and quantitatively compare the antimicrobial activity of RWJ-416457 to that of the first-in-class representative linezolid. For qualitative comparison, MIC and constant, as well as changing concentration time-kill curve experiments of linezolid and RWJ-416457 against MRSA OC2878 will be performed. For quantitative comparison, a general PK/PD model will be established, validated and simultaneously fitted to the time-kill curve data and respective EC_{50} values compared.

CHAPTER 2
THE EFFECT OF PROTEIN BINDING ON THE PHARMACOLOGICAL ACTIVITY OF HIGHLY BOUND ANTIBIOTICS[1]

Introduction

Most drugs bind to proteins or other biological materials such as albumin, α1-acid glycoprotein, lipoproteins, α-, β- and γ globulins and erythrocytes. Thus, free, unbound drug concentration in plasma decreases as the degree of binding to these compounds increases. It is a well recognized fact that, at least for small molecules, only free, unbound drug distributes into the extravascular space and is responsible for pharmacological activity and/or side effects (200, 224, 280). For antibiotics in particular, reduced free, active drug concentrations as a result of protein binding reflect in decreased antimicrobial activity (200). In theory, this effect is most pronounced for antibiotics with extensive protein binding. To date, most studies evaluating the effect of protein binding on the potency of an antibiotic against a certain pathogen determine changes in the respective minimum inhibitory concentration (MIC) (200). Whereas both bacterial growth and kill are dynamic processes, the MIC is a static, highly variable threshold value, incapable of predicting antibiotic activity at concentrations apart from the MIC (183, 229). In comparison, evaluation of growth and antibiotic-induced kill profiles over time (time-kill curves) provides more detailed information than the MIC. Once experimentally determined, time-kill curves can be characterized by simultaneous fit of appropriate mathematical models and quantitatively compared by respective outcome parameters, such as the EC_{50} (229). Time-kill curves have, consequently, been suggested as an experimental method for the evaluation of protein binding effects on the antimicrobial activity (231, 280). In order to account for protein binding in these experiments, bacterial media are spiked with either human serum or protein

[1] Copyright © American Society for Microbiology, [Antimicrob Agents Chemother. 52: 3994-4000, 2008]

supplements. When supplementing with human serum, its actual content frequently has to be limited to ≤ 50% since it may inhibit bacterial growth or modify the antibacterial activity (140, 144, 200). On the other hand, when supplementing with proteins, usually human serum albumin (HSA) or comparatively less expensive animal albumins (20, 101, 111) are employed, as HSA is the main natural binding component of antibiotics (142, 218, 247, 262, 280). Nevertheless, the actual free, unbound antibiotic concentration after either HS or protein supplementation is rarely determined. Instead, literature or protein binding values determined *in vitro* are frequently employed to estimate free, unbound concentrations (36, 141).

The goal of the present study was to evaluate this approach by linking measured free, unbound concentrations of the two highly-bound β-lactams ceftriaxone (83-96%) (244, 245, 277) and ertapenem (84-96%) (34) to their respective antimicrobial activity against Gram-positive *Streptococcus pneumoniae* (*S. pneum.*) ATCC6303 and Gram-negative *Escherichia coli* (*E. coli.*) ATCC25922.

Material and Methods

Organisms

E. coli ATCC25922 and penicillin-sensitive *S. pneum.* ATCC6303 were obtained from the Clinical Microbiology Laboratory at Shands Hospital at the University of Florida, USA. *E. coli* and *S. pneum.* were grown in a CO_2 incubator (Barnstead-Thermolyne, Melrose Park, IL, USA) in Mueller-Hinton broth (MHB) or Todd-Hewitt broth (THB) plus 5% CO_2, respectively. To ensure purity of the bacterial strains, they were subcultured at least three times before either usage or freezing of the stock cultures. The bacterial inoculum was prepared from colonies incubated overnight on 5% sheep blood agar plates (Remel Microbiology Products, Lenexa, KS, USA). The microorganisms were suspended in sterile saline solution 0.9% to a concentration equivalent to a 0.5 value in the McFarland scale (Remel Microbiology Products, Lenexa, KS,

USA) with a turbidimeter (A-JUST™, Abbott Laboratories, North Chicago, IL, USA). This value on the McFarland scale of 0.5 is equivalent to a number of $1x10^8$ viable colony forming units per milliliter (CFU/mL). Further dilution steps to reach a final working inoculum of approximately $5x10^5$ CFU/mL were performed in broth.

Antibiotics and Growth Media

Ceftriaxone disodium was purchased from Sigma-Aldrich (St. Louis, MO, USA) and ertapenem sodium was obtained from Merck & Co., Inc. (Whitehouse Station, NJ, USA). Antibiotics were prepared and stored according to the manufacturer's recommendations. MHB (Becton Dickinson, Franklin Lakes, NJ, USA) and THB (Difco, Detroit, MI, USA) were used as liquid growth media. MHB and THB were both prepared according to the manufacturer's instructions and autoclaved prior to use at 121°C (15 min per 1L). Broth media were supplemented with either 40g/L BSA (Sigma-Aldrich, St. Louis, MO, USA, Cat. No. A3059, Lot. No. 036K0735) or 40g/L HSA (Calbiochem®, La Jolla, CA, USA, Cat. No. 12666, Lot No. B75308-01), filtered through 0.2µm filters (Millipore, Billerica, MA, USA) and the pH adjusted to 7.4.

HPLC Analysis

Instrumentation

The HPLC-system for both ceftriaxone and ertapenem consisted of Agilent 1100 Series (Agilent Technologies, Waldbronn, Germany): a model G1313 autosampler, a model G1311 quaternary pump and G1315 DAD UV detector, an Agilent Chemstation for LC systems and a LiChrospher® 100 Reversed Phase 18 (RP-18, 5µm particle size) analytical column (Merck KGaA, Darmstadt, Germany).

Chromatographic conditions

Ceftriaxone: The ion-pair chromatography assay procedure was adapted from Kovar et al..(133) Reversed phase high-performance liquid chromatography (RP-HPLC) was performed at room temperature at a flow-rate of 1.0mL/min. The mobile phase consisted of a mixture of buffer (7.5mM KH_2PO_4; J.T. Baker Chemical Co., Phillipsburg, N.Y., USA) and acetonitrile (56:44, v/v) with 5mM hexadecyltrimethylammonium bromide (HDTA; Sigma-Aldrich, St. Louis, MO, USA) as the ion-pair reagent. The final pH of the mobile phase was adjusted to 8.8. 25µL of ceftriaxone were injected and detected at 280nm. The run time was set to 16 minutes.

Ertapenem: The chromatography procedure was adapted from Gordien et al. (98). The mobile phase consisted of 10mM phosphate buffer adjusted to pH 6.5 with concentrated orthophosphoric acid and mixed with acetonitrile. A gradient was run at a flow-rate of 1mL/min. 40µL of ertapenem were injected and detected at 305nm. The run time was set to 14 minutes.

Protein Binding

Free, protein-unbound ceftriaxone and ertapenem concentrations were determined in *in vitro* dose-ranging (20, 40, 80, 160 and 320µg/mL) extraction efficiency (EE) microdialysis experiments. Briefly, blank Lactated Ringer (LR; Baxter Health Care, Deerfield, IL, USA) solution is pumped through a flexible CMA 60 microdialysis probe (CMA Microdialysis AB, Solna, Sweden) at a constant flow rate of 2.0µL/min. The relative recovery (RR) of the microdialysis probes were determined in LR only and calculated according to equation 2-1,

$$RR = \frac{C(LR)_{dialysate}}{C(LR)_{sample}} \qquad (2\text{-}1)$$

where $C(LR)_{dialysate}$ is the free concentration recovered from the microdialysis probe and $C(LR)_{sample}$ the concentration in the test tube.

Once RR was determined, free, unbound ceftriaxone and ertapenem concentrations were determined in triplicate at 37°C in THB, THB with BSA, THB with HSA and pooled adult bovine serum (ABS; HyClone®, Logan, Utah, USA) or pooled human plasma (HP; Shands Hospital at the University of Florida, Gainesville, USA), respectively. It was previously reported that serum binding properties can be altered by heat treatment (269). Therefore, untreated pooled HP was used for the *in vitro* protein binding experiments.

Protein binding (%) of the respective samples can then be calculated according to equation 2-2,

$$PB(\%) = 1 - \frac{C(sample)_{dialysate}}{RR \times C(sample)_{total}} \quad (2\text{-}2)$$

where $C(sample)_{dialysate}$ is the concentration in the protein-free dialysate and $C(sample)_{total}$ is the mean concentration of the samples that were collected directly out of the test tube at the beginning and the end of the 30min sampling period. Collected samples were analyzed by the RP-HPLC methods described above.

Protein binding differences within the treatment groups were evaluated using analysis of variance (ANOVA) followed by least square means to test for pair-wise differences. All statistical analysis was performed in SAS 9.1.3 (SAS Institute Inc., Cary, USA). A P-value <0.05 was considered statistically significant.

Pharmacodynamics

MIC

MICs of *E. coli* ATCC25922 and *S. pneum.* ATCC6303 against ceftriaxone and ertapenem were determined six times according to the CSLI guidelines both in presence and absence of BSA and HSA using a serial dilution two-fold Macro Broth Dilution method (258).

Time-kill curves

In vitro 6 hour constant concentration time-kill curves were performed in triplicate for both ceftriaxone and ertapenem against the test strains in the presence and absence of BSA and HSA, respectively (258). Eight 50mL cell culture flasks (Nunc^{TM}, Nunc A/S, Roskilde, Denmark) were filled with 20mL of bateria-containing growth medium and incubated for two hours before adding the antibiotic. The selection of respective ceftriaxone or ertapenem concentrations (Table 3-1) was based on their determined MIC values and covered the entire antimicrobial spectrum, including minimum inhibition of bacterial growth (0.25, 0.5, and 1 times MIC), efficient bacterial killing (2 and 4 times MIC) and maximum bacterial killing (8 and 16 times MIC). Samples were taken at 0, 0.5, 1, 1.5, 2, 3, 4, 5 and 6 hours. Bacterial counts were determined, using an adapted droplet-plate method (258). A control experiment with bacteria and no drug was run simultaneously. After incubation at 37^{o}C for 20-24hours, viable counts were determined on all readable plates.

Mathematical Modeling

A modified susceptibility-based two-compartment model was simultaneously fit to the time-kill curve data of with and without BSA and HSA, respectively (198, 258). In this model, the overall change in the experimentally determined total number of bacteria was defined as the sum of self-replicating, antibiotic-sensitive cells and metabolically inactive, insusceptible persister cells (10). While bacterial growth could be sufficiently described by the growth-rate constant k_s (h^{-1}), antibiotic-induced kill was characterized by the maximum kill-rate constant k_{max} (h^{-1}), the antibiotic concentration C (μg/mL) and the concentration at half-maximum effect EC_{50} (μg/mL). The final shape of the curve fit could be optimized by a Hill or shape factor h.

In order to compare the respective EC_{50} values in the presence or absence of BSA or HSA, k_s, k_{max} and h values were fitted across all treatment groups for each antibiotic and strain. Initial

parameter estimates for k_s, k_{max} and h were obtained from individual curve fits and compared for differences. Since no differences in parameter estimates were observed (data not shown), arithmetic means were used as the initial estimates for the simultaneous curve fits across the treatment groups.

After simultaneously fitting the susceptibility-based sigmoidal E_{max}-model to the experimental time-kill curve data with the non-linear least-square regression software Scientist® 3.0 (Micromath, Salt Lake City, UT, USA), models were characterized by Model Selection Criteria (MSC) and graphs visually inspected for quality of fit. EC_{50} comparisons were done using ANOVA, followed by least square means. A P-value <0.05 was considered statistically significant.

Results

Protein Binding

As shown in Figure 2-1, mean protein binding (±SD) values of both ceftriaxone (76.8±11.0%) and ertapenem (73.8±11.6%) were higher in pooled HP than those in THB with and without BSA or HSA, as well as, pooled ABS, respectively (P<0.05). For ceftriaxone, protein binding was significantly lower in commercially available BSA (20.2±8.3%) and HSA (56.9±16.6%), as well as, pooled ABS (30.7±6.2%). Similar lower protein binding values were also observed for ertapenem (BSA: 12.4±4.8%, HSA: 17.8±11.5%, pooled ABS: 38.3±9.8%).

Pharmacodynamics

MIC

Determined MIC values (presented as modes) are shown in Table 2-1. No differences in MIC values were found for ertapenem against *S. pneum.* both in the presence and absence of BSA and HSA, respectively. However, in the presence of HSA (vs. no albumin), MICs were increased for ceftriaxone against *E. coli* and *S. pneum.*, as well as, for ertapenem against *E. coli.*.

In comparison, when supplementing with BSA (vs. no albumin), no change in MICs was detected for ceftriaxone against *E. coli* and ertapenem against *E. coli*, whereas values were increased for ceftriaxone against *S. pneum.*.

Time-kill curves

Qualitative evaluation of the time-kill curves showed that, in comparison to albumin-free medium, there are no differences in growth of both *E. coli* and *S. pneum.* in the presence of BSA and HSA (Figure 2-2), respectively. However, further evaluation showed differences in anti-microbial activity when comparing samples with and without albumin supplementation. These differences were most apparent at concentrations of 8 times MIC (with respect to albumin-free medium). While the maximum kill effect was not reached at 8xMIC for ceftriaxone when HSA was added, these concentrations were sufficient for ertapenem and ceftriaxone in the presence of BSA as well as for ertapenem supplementing with HSA.

Mathematical Modeling

Simultaneous curve fits of ceftriaxone and ertapenem against *E. coli* and *S. pneum.* with and without BSA or HSA are shown in Figure 2-3 and 2-4. The corresponding model parameters for ceftriaxone and ertapenem against both strains in the presence and absence of BSA and HSA are listed in Table 2-1. For ceftriaxone, calculated EC_{50} values for both strains were higher in the presence of HSA than those with BSA ($P<0.05$) or without albumin ($P<0.05$), respectively. The difference remained significant after adjusting for multiple comparisons. In contrast, no differences in EC_{50} values were determined for ertapenem against both strains when it was supplemented with HSA compared to no albumin and BSA.

Discussion

The clinical significance of protein binding on antimicrobial activity continues to be controversial due to conflicting reports from *in vitro* MIC and/or time-kill curve experiments

(232). In these experiments, bacterial media are spiked with either serum or protein supplements in order to produce and modify protein binding. However, whether the degree of drug binding in these *in vitro* test systems is representative of the respective physiological conditions is often unclear since free, unbound concentrations are frequently not experimentally determined. Instead, reported literature values are commonly used to correct total concentrations for protein binding (36, 141). The results of our study, however, clearly show that this approach can be extremely misleading.

In this study, MICs and constant concentration time-kill curves of two beta-lactams with reportedly high protein binding, ceftriaxone (83-96%) (244, 245, 277) and ertapenem (84-96%) (34), were determined in the presence and absence of BSA and HSA (40g/L), respectively, and outcomes compared. Results indicate that the antimicrobial activity of both ceftriaxone and ertapenem was decreased against both test strains, except for ertapenem against *S. pneum.*, in the presence of HSA. However, MICs remained unchanged, except for ceftriaxone against *S. pneum.*, in the presence of BSA. In theory, these differences in pharmacodynamic outcome could be explained by albumin-induced effects on growth- and maximum kill-rates, as well as, changes in potency (EC_{50}) (188, 200, 231). The evaluation of bacterial growth is, thereby, of particular importance since only dividing cells are susceptible to beta-lactams (200). However, evaluation of the respective growth controls over time revealed that there were no significant differences in growth-rates of both test strains in the presence or absence of BSA and HSA, respectively (Figure 2-2).

Once antibiotic is added, antimicrobial agents kill bacteria more rapidly as concentrations increase.(211) Yet, at concentrations of 2-4 times the MIC, the respective response varies (211). For beta-lactams, the maximum kill effect is already observed. At this point, a further increase

in antibiotic concentrations does not result in increased killing and the kill rate remains constant. The findings of our study are in agreement with these concepts. However, results further revealed that ceftriaxone concentrations of 8 times MIC (with respect to no albumin) are not high enough to reach k_{max} when HSA is added, but are sufficient when BSA is present (Figure 2-2). When further increasing concentrations to 16-32 times MIC, the maximum kill effect was reached and no albumin-related effects on k_{max} were determined. In contrast, saturation in kill was achieved for ceftriaxone and ertapenem in the presence of BSA as well as for ertapenem when adding HSA at 8xMIC.

Nevertheless, substantial differences in mean EC_{50}s were determined for ceftriaxone, whereas, no significant differences in mean EC_{50}s were determined for ertapenem in the presence of HSA. In comparison, no differences in mean EC_{50} values were determined for both strains and antibiotics when it was supplemented with BSA. At this point, it is important to realize that in isolation, the results of the MIC and time-kill curves lead to ambiguous conclusions about the impact of protein binding on the antimicrobial activity. While a two-fold increase in MIC was observed for both ceftriaxone against *S. pneum.* in the presence of BSA and ertapenem against *E. coli* in the presence of HSA, no significant differences in EC_{50}s were determined in the respective time-kill curve experiments. These differences in pharmacological outcome (MIC vs. EC_{50}) are frequently attributed to the immanent high variability of the employed Macro-broth dilution (two-fold) method (188, 229). Nevertheless, the fact that there are tremendous differences in both MICs and EC_{50}s between ceftriaxone and ertapenem against both strains cannot simply be explained by variability or calculated free concentrations, since both antibiotics have very similar reported protein binding (ceftriaxone: 83-96%, ertapenem: 84-96%) values (34, 244, 245, 277). However, the major assumption that the reported *in vivo* protein binding

values reflect also the binding conditions in the *in vitro* system is rarely validated by experimentally measuring free, unbound concentrations.

Different methods, such as, equilibrium dialysis, ultrafiltration, microdialysis, etc. have been used for the determination of protein binding and have shown comparable outcomes (12, 103). In our study free, unbound concentrations were measured by *in vitro* microdialysis and respective protein binding values were calculated (Figure 2-1). Results indicate that the observed differences in antimicrobial activity of ceftriaxone and ertapenem can be explained by differences in their *in vitro* binding to the respective albumin supplements. While ceftriaxone is extensively bound to the tested HSA, it shows only little binding to BSA, and ertapenem hardly binds to either one. The findings of our *in vitro* microdialysis study are in agreement with those from Nix et al., where the binding of ertapenem to purified albumins was determined by ultrafiltration (200). Findings of both studies concurrently indicate that the *in vitro* binding to albumin supplements was substantially lower than previously reported literature protein binding values. Results of the ultrafiltration experiment further showed that the binding of ertapenem to various albumin supplements was greatly dependent on the albumin preparations used and differed substantially between suppliers (200). These observations may be explained by the lack of fatty acids in the albumin supplements (246) and/or the use of rigorous conditions, such as, heat treatment or organic solvents during the purification process that can result in conformational changes in the respective albumin binding sites and, subsequently, reduced protein binding values (200). On the other hand, the significantly lower binding to pooled ABS, compared to pooled HP, indicates that for both antibiotics differences in binding capacities between species may play a role. For ceftriaxone, similar protein binding values have been previously determined in human, rat, baboon and rabbit plasma, whereas substantially lower

binding values were measured in dog plasma (212). This article by Popick et al. further revealed that the initially high protein binding of ceftriaxone (90-95%) at concentrations <100µg/mL is considerably decreased to approximately 60% at higher concentrations (>400µg/mL) (212). In our study, mean protein binding values (ceftriaxone: 76.8±11.0%) were determined at concentrations ranging from 20-320µg/mL and are in agreement with the previously reported range.

At this point, it also should be mentioned that there are other factors that may provide an explanation for the differences in reported outcomes that range from no protein binding effects (88, 141), delay in the onset of activity (36, 41), to only free, unbound drug being responsible for the antimicrobial activity (177, 200, 224, 261, 279, 280). For example, it has been shown that the bacterial density or the state of nutrition are crucial parameters and usually differ in MIC and time-kill curve studies from the physiological conditions. While a lack of nutrition and low bacterial numbers hinder the experimental conduct, very high initial inoculum sizes seem to alter the susceptibility towards antimicrobial agents and might mask protein binding effects (169). It would, therefore, be important to internationally standardize the methodology of protein binding studies in order to minimize the experimental bias.

In conclusion, the results of the constant and changing concentration experiments clearly show that protein binding reduces the *in vitro* antimicrobial activity. The study results further demonstrate that binding to commercially available protein supplements can substantially differ from that of serum or plasma and greatly depends on the supplement used. Correcting total concentrations for reported literature binding values is, consequently, unreliable. Instead, free, active antibiotic concentrations should be experimentally measured in the actual test system. *In vitro* microdialysis is a convenient sampling tool for this purpose. In addition, an international

standardization of the respective test systems might help prevent further misinterpretation of the impact of protein binding on the antimicrobial activity.

Table 2-1. Determined MIC values (presented as modes) and simultaneously fitted model parameters (±SD) of ceftriaxone and ertapenem against *E. coli* and *S. pneum.* in the presence and absence of bovine serum albumin (BSA) and human serum albumin (HSA), respectively.

Parameter (unit)	Ceftriaxone vs. *E. coli* ATCC 25922 w/out albumin	w/ BSA[a]	w/ HSA[a]	vs. *S. pneum.* ATCC 6303 w/out albumin	w/ BSA[a]	w/ HSA[a]
MIC (µg/mL)	0.064	0.064	2.0	0.01	0.02	0.16
k_s (h^{-1})			2.40 (±0.34)			1.56 (±0.08)
k_{max} (h^{-1})			6.34 (±0.13)			3.59 (±0.11)
EC_{50} (±SD) (µg/mL)	0.027[h] (±0.0007)	0.057[h] (±0.007)	1.096[c,b] (±0.00272)	0.004[h] (±0.0004)	0.015[h] (±0.0099)	0.084[c,b] (±0.0147)
h			1.61 (±0.10)			2.18 (±0.14)
MSC			4.24			4.04

[a] At a protein concentration of 40g/L. Significant differences ($P \leq 0.05$) from the value for [c]the control (protein-free), [b]the sample with BSA and [h]the sample with HSA.

Table 2-1. Continued

Parameter (unit)	Ertapenem vs. *E. coli* ATCC 25922			vs. *S. pneum.* ATCC 6303		
	w/out albumin	w/ BSA[a]	w/ HSA[a]	w/out albumin	w/ BSA[a]	w/ HSA[a]
MIC (μg/mL)	0.015	0.015	0.03	0.025	0.025	0.025
k_s (h^{-1})			2.76 (±0.89)			2.28 (±0.13)
k_{max} (h^{-1})			6.02 (±1.00)			3.28 (±0.11)
EC_{50} (±SD) (μg/mL)	0.010 (±0.0035)	0.020 (±0.0029)	0.014 (±0.0046)	0.010 (±0.0019)	0.010 (±0.0015)	0.019 (±0.0101)
h			2.54 (±0.14)			2.65 (±0.25)
MSC			4.71			2.67

[a] At a protein concentration of 40g/L. Significant differences ($P \leq 0.05$) from the value for [c]the control (protein-free), [b]the sample with BSA and [h]the sample with HSA.

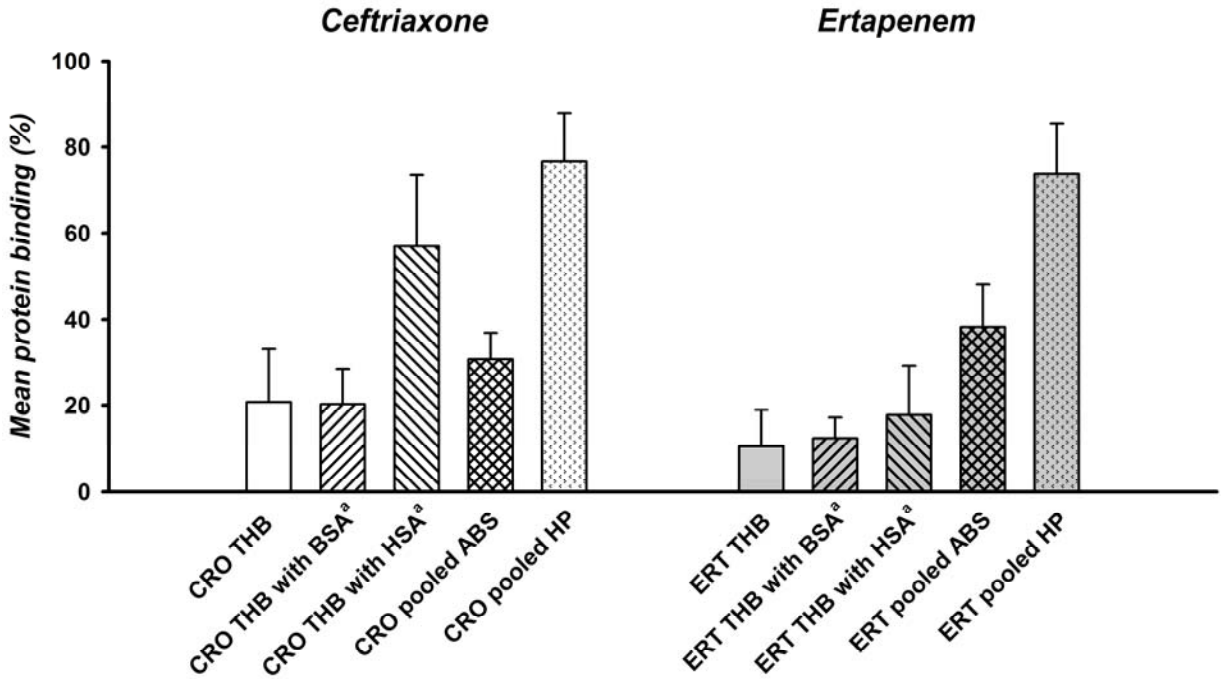

Figure 2-1. *In vitro* protein binding of ceftriaxone and ertapenem. *In vitro* mean protein binding (%) of ceftriaxone (white) and ertapenem (gray) in Todd-Hewitt broth (THB), THB with bovine serum albumin[a] (BSA), THB with human serum albumin[a] (HSA), pooled adult bovine serum (ABS) and pooled human plasma (HP), respectively

[a]At a protein concentration of 40g/L

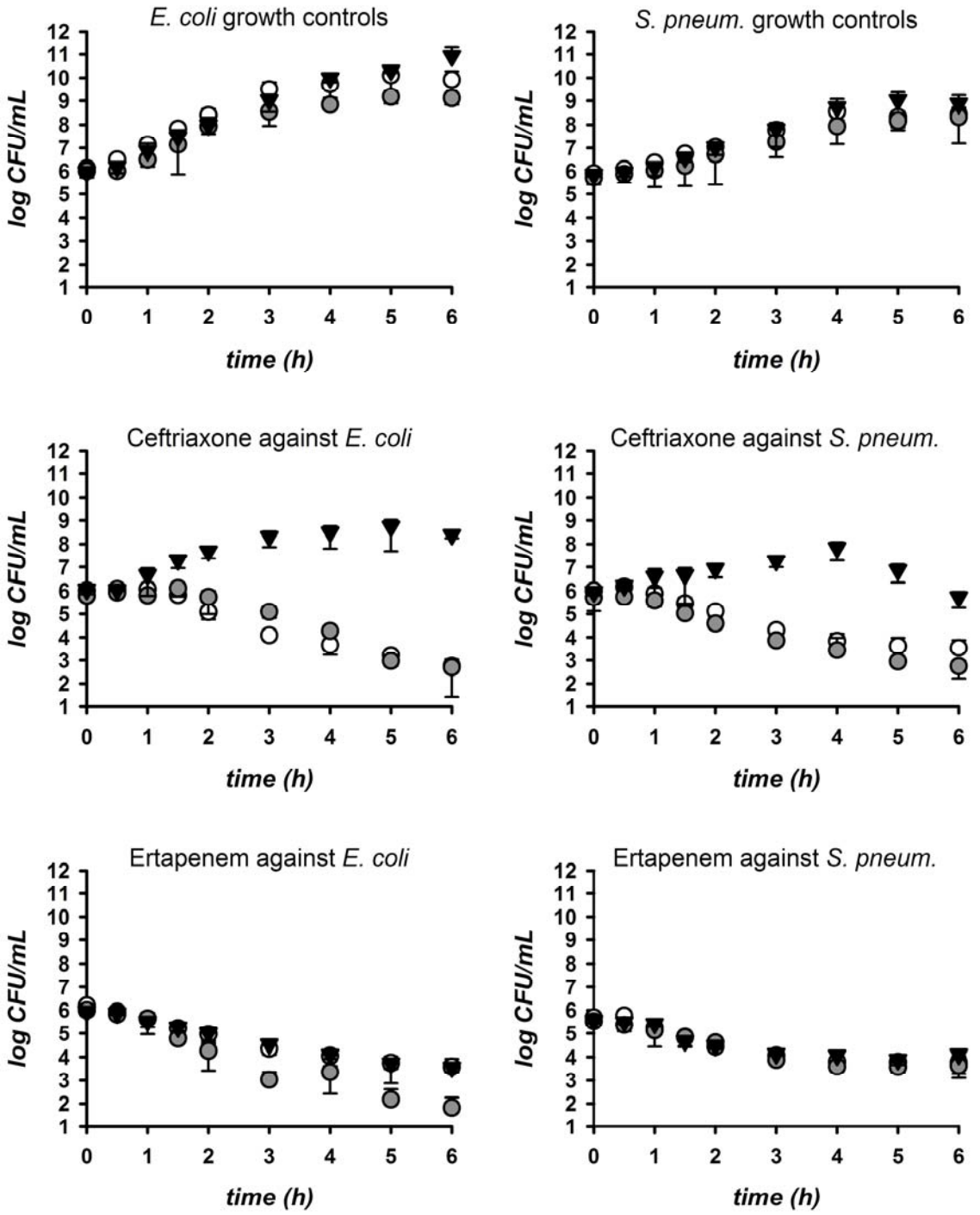

Figure 2-2. Effect of bovine (BSA) and human serum albumin (HSA) on bacterial growth and antibiotic-induced kill. The maximum kill-rate was determined at 8 times MIC (8xMIC, with respect to albumin-free medium) for ceftriaxone and ertapenem against *E. coli* and *S. pneum.*, respectively. (Symbols: without albumin (○), with BSA (●), with HSA (▼))

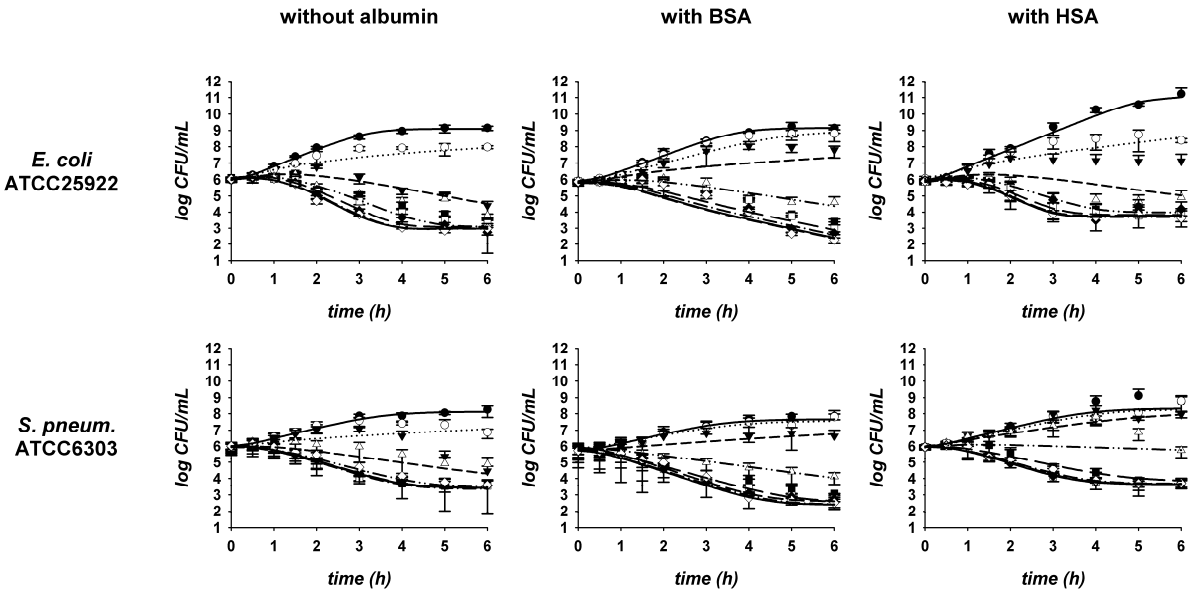

Figure 2-3. Simultaneous curve fits for ceftriaxone against *E. coli* and *S. pneum.* in the presence and absence of bovine serum albumin (BSA) and human serum albumin (HSA). At concentrations of 0.25xMIC (----○----), 0.5xMIC (—▼—), 1xMIC (—··△··—), 2xMIC (—■—·), 4xMIC (—·□·—), 8xMIC (—◆—), 16xMIC (—◇—) plus growth controls (——●——). Symbols represent the experimental data; solid lines represent the simultaneous curve fits based on the PK/PD model.

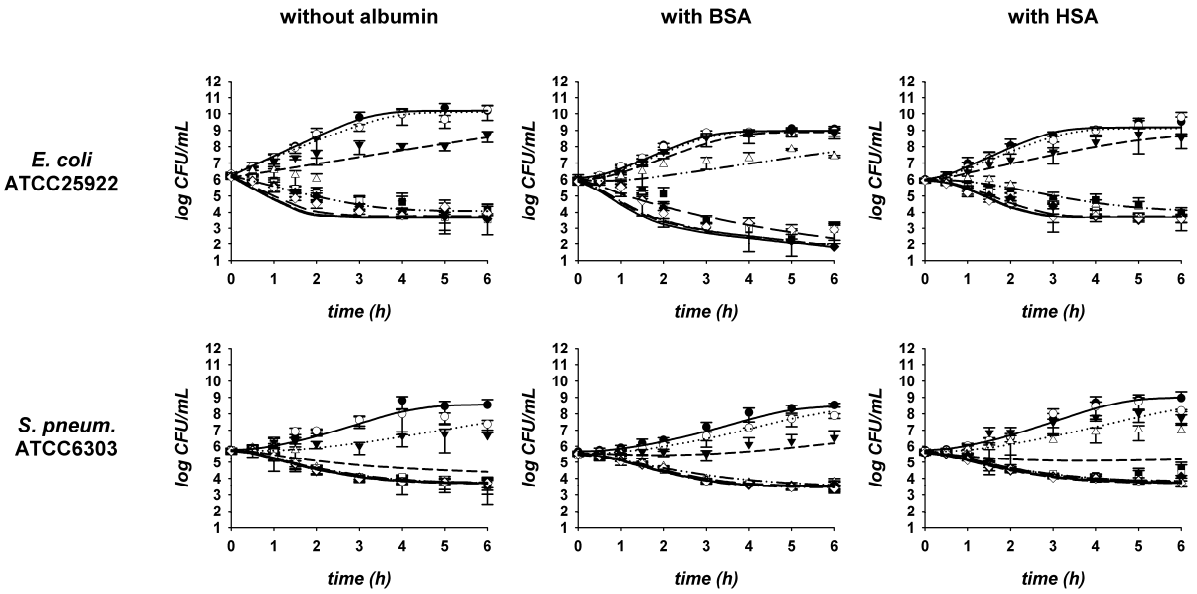

Figure 2-4. Simultaneous curve fits for ertapenem against *E. coli* and *S. pneum.* in the presence and absence of bovine serum albumin (BSA) and human serum albumin (HSA). At concentrations of 0.25xMIC (----○----), 0.5xMIC (— ▼ —), 1xMIC (— ·· △ ·· —), 2xMIC (— ■ — ·), 4xMIC (— · □ · —), 8xMIC (— ◆ —), 16xMIC (—◇—) plus a growth control (——●——).Symbols represent the experimental data; solid lines represent the simultaneous curve fits based on the PK/PD model.

CHAPTER 3
CLINICAL MICRODIALYSIS IN SKIN AND SOFT TISSUES: AN UPDATE[2]

Introduction

Historically, pharmacokinetic/pharmacodynamic (PK/PD) approaches link plasma drug concentrations to observed effects. However, most PD effects are mediated by interaction with enzyme, transporter or receptor systems that are located in the tissues (28, 44). Consequently, linkage of PD effects to tissue drug concentrations at the site of action is a more accurate approach to characterize exposure-effect relationships (44). Closer evaluation of concentration-effect relationships have shown that only free, unbound drug at the target site is responsible for PD efficacy (13, 59). Therefore, continuous sampling of free drug in the tissues is the most rational approach to estimate active drug profiles at the site of action. MD is currently the most appropriate sampling technique that can provide this information (44, 120).

The MD principle was first employed in the early 1960s in order to sample free amino acids and other electrolytes in the extracellular fluid of animal brains (16). Further technical advancement resulted in the development of the "dialytrode" in 1972, the first simple version of today's MD probe (66). In 1974, Ungerstedt and Pycock discussed the use of "hollow fibers" as a superior *in vivo* sampling technique (260). Steady improvement of both MD catheters and methodology allowed not only measurement of neurotransmitters and metabolites in animals, but also application in humans (107). In early clinical trials, glucose levels were determined in subcutaneous adipose tissue (18, 63, 117). The approval of MD catheters for use in humans by the US Food and Drug Administration (FDA) and the European Union Conformite Europeene (CE) has opened the door to further studies in virtually every human tissue, including muscle, skin, lung, myocardium, brain, and even tumors (44). Consequently, in recent years,

[2] Copyright © American College of Clinical Pharmacology, [J Clin Pharmacol 48: 351-64, 2008]

considerable experience has been gained in clinical studies of both healthy volunteers and patients, resulting in more than 2,000 publications as of today.

Rationale for this Review

In 2004, the Food and Drug Administration (FDA) issued its Critical Path Document, "Innovation and Stagnation? Challenge and Opportunity on the Critical Path to New Medical Products" (84). In this report, the FDA critically evaluates reasons for the recent decline of drug launches onto the market despite the increased investment of time and resources. One of the key issues identified in this document is the lack of sufficient safety and efficacy measures for new drugs and drug formulations (84). In the FDA's view, a new product development toolkit containing powerful new scientific and technical methods (i.e. animal or computer-based predictive models, biomarker for safety and effectiveness, and new clinical evaluation techniques) is urgently needed (84).

Recently, the FDA published a list of 'Critical Path Opportunities.' (81) MD is one of these new clinically applicable evaluation techniques that is specifically mentioned in this list. Its capability of determining free, active local drug concentrations qualifies it for site-specific safety and efficacy assessment. This has become of particular interest to industry and regulatory authorities for the evaluation of bioavailability (BA) and bioequivalence (BE) of topically applied drug formulations, especially of dermatological products (81, 82, 85). For systemic drugs, usually the serum concentrations are used in BA and BE studies. However, based on the respective definitions of BA and BE, measurements of exposure at the site of action would be more meaningful (83). The goal of our review is to give an overview of newer clinical BA and BE studies in skin and soft tissues using microdialysis.

Methods

The MD catheter (probe) consists of a small semi-permeable hollow fiber membrane that is connected to inlet and outlet tubing (63). It is constantly perfused with a physiological solution (perfusate) at flow rates of approximately 0.1-5μL/min (44). After insertion into a selected tissue or (body) fluid, solutes can cross the membrane by passive diffusion depending on their concentration gradient (28, 44, 63). Hence, the probe can be used as a sampling tool as well as a delivery tool (44). The solution leaving the probe (dialysate) is collected at certain time intervals for analysis.

Calibration Methods

Since the MD probe is continuously perfused with fresh perfusate, a total equilibrium across the membrane cannot be established. Rather, a steady-state rate of exchange across the MD membrane is rapidly reached. This steady-state exchange rate is described by the extraction efficiency (EE). The EE is the ratio between the loss/gain of analyte during its passage through the probe ($C_{perfusate}$-$C_{dialysate}$) and the difference in concentration between perfusate and the sample of interest such as tissue fluid, *in vitro* analyte, etc. ($C_{perfusate}$-C_{sample}), as shown in equation 3-1.

$$EE = \frac{C_{perfusate} - C_{dialysate}}{C_{perfusate} - C_{sample}} \qquad (3\text{-}1)$$

At steady-state, EE has the same value for all $C_{perfusate}$, no matter if the analyte is being enriched or depleted in the perfusate (44). For this reason, MD probes can be calibrated with either drug-containing perfusate or sample solutions. While various calibration techniques are available (i.e. low-flow-rate method, zero-net-flux method (161), extended zero-net-flux method (207), etc.), retrodialysis by drug (34) is the most commonly employed method in humans.

During retrodialysis, the probe is perfused with drug-containing perfusate prior to or after drug administration, without the drug in the tissue. Since absence of drug in the tissue is required for retrodialysis, this calibration technique cannot be applied to endogenous compounds (44).

The proper selection of an appropriate calibration method is critically important for the success of a MD experiment, so supportive *in vitro* experiments prior to use in animals or humans are recommended (44). The recovery determined *in vitro* might differ from the recovery in humans, therefore, its actual value needs to be determined in every single *in vivo* experiment (241).

Strengths of the Microdialysis Technique

Depending on the molecular cut-off of the MD probe membrane, larger molecules (such as proteins) are prevented from diffusing into the dialysate (241). This allows the analysis of protein-free, active drug concentrations to be performed frequently without further sample preparation (28).

While MD selectively determines free, unbound concentrations in the interstitial fluid of a particular living tissue, other sampling techniques have limited capabilities to distinguish between different sites within the tissue or between free and bound drug. For example, tape stripping is a commonly used method that is well established for evaluating the penetration of topically applied compounds into the upper part of the skin (150). However, this method is limited to the stratum corneum and can, therefore, not be used for the assessment of free, active drug concentrations in deeper tissues such as the dermis. In fact, continuous tape stripping does disturb the barrier function of the skin and can result in artificially increased drug levels in the skin (15). Other tissue sampling approaches also have major limitations. While, for example, broncho-alveolar lavage (BAL) pools data from large segments throughout the lung, concentrations obtained from homogenized tissue, positron emission tomography (PET), and

scintigraphy will include drug that is bound to interstitial and intracellular proteins or to intra- and intercellular membrane structures (28, 44, 241).

In comparison, the skin blister technique is capable of target-site specific sampling. Yet, it reflects concentrations in experimentally induced secretory fluids. The concentrations in these fluids might vary with blister size and surface to volume ratio due to protein and chemokine content and might not be comparable to the interstitial space fluid (28, 48, 61, 189, 222, 241). It was shown, for example, that ciprofloxacin and moxifloxacin accumulated preferably in blister fluid whereas an almost complete equilibration of the free unbound antibiotic plasma fraction with the interstitial space fluid was observed using MD (28, 29, 193).

Another limitation of most of these techniques is that they are usually not capable of continuous measurement of the concentration-time profile. Hence, investigators using, for example, epithelial lining fluid (ELF) and tissue biopsies are forced to pool data from different subjects in order to receive concentration-time profiles (1, 278). In contrast, continuous sampling via MD allows the generation of PK profiles from individual subjects.

Limitations of the Microdialysis Technique

Usually, MD probe insertion is associated with minimal tissue damage. However, some tissue sites such as brain (78, 79), lung (102, 254), bone (253), heart (9), liver (204) or the peritoneal cavity (116) are not readily accessible to the MD procedure. The MD probe must then be surgically implanted into these tissues.

Another limitation of the MD technique is its dependency on flow rate and sensitivity of the analytical assay. As the analyte concentration decreases with increasing flow rate, assays with small sample volumes are restricted to highly sensitive analysis techniques (i.e. HPLC, LC/MS/MS, capillary electrophoresis) (44). However, if very low flow rates are used, the time

resolution might be compromised (44). For this reason, flow rate and analytical procedures require extensive fine-tuning.

MD has emerged as the method of choice to monitor drug concentrations in the extracellular space. If the site of action is located intracellularly, MD is not able to measure that concentration directly. Even in these cases, the respective extracellular concentration resides closer to the site of interest than the respective plasma or blood concentrations.

Bioavailability at the Site of Action

In the FDA "Guidance for Industry", BA is defined as "the rate and extent to which the active ingredient or active moiety is absorbed from a drug product and becomes available at the site of action. For drug products that are not intended to be absorbed into the bloodstream, BA may be assessed by measurements that reflect the rate and extent to which the active ingredient or active moiety becomes available at the site of action." (83) Local site drug levels can become important in, for example, anti-cancer therapy, because tumors might show altered physiology and/or limited drug access compared to normal tissue (114, 115, 213). Knowledge of the active drug concentrations inside the tumor is therefore critically important for the selection of an appropriate drug and/or dosing regimen.

Even though metastatic malignant melanomas (MMMs) respond poorly to drugs due to resistance at a molecular level and impaired transcapillary drug transfer, dacarbazine is an effective treatment of MMMs (121). Transcapillary transfer rates of dacarbazine and its active metabolite 5-aminoimidazole-4-carboxamide (AIC) into the tumor were determined after intravenous administration of dacarbazine at doses of 200mg/m^2 -1000mg/m^2 body surface area in 7 MMM patients using MD. Dialysates (tumor and healthy adipose tissue) and plasma (ultrafiltered) samples were collected over 240min and analyzed using HPLC for free dacarbazine and AIC concentrations. Results indicated that for all doses, AUCs for dacarbazine

and AIC were not significantly different between plasma (free concentration) and tumor interstitium. It was concluded that dacarbazine and its active metabolite AIC showed significant tumor penetration characteristics after i.v. administration. The lack of response to antineoplastic therapy with dacarbazine might be explained by resistance at molecular level rather than by inability of dacarbazine and AIC to penetrate into the interstitium of MMM (121).

Once the drug reaches the systemic circulation, there are no more differences in distribution, metabolism, and elimination between the intravenous and the non-intravenous administration route. Depending on the value of the oral bioavailability (F), oral doses will have to be increased in comparison to the respective intravenous dose in order to achieve similar therapeutic drug levels.

As a case in point, MD was employed to compare free, active ciprofloxacin concentrations in the interstitial space fluid (ISF) of skeletal muscle and subcutaneous adipose tissue, after i.v. or oral ciprofloxacin administration, respectively (29). Each of eight healthy volunteers were studied twice and randomly assigned to initial ciprofloxacin treatment with either 500mg orally or 400mg intravenously, with a washout period of at least 7 days. Free ciprofloxacin concentrations were determined in the ISF of skeletal muscle and subcutaneous adipose tissue, saliva, cantharis-induced skin blister, as well as capillary plasma, and compared to total venous plasma concentrations. Samples were analyzed using HPLC, and respective AUCs were calculated. In order to predict the antimicrobial activity of ciprofloxacin, PK profiles, determined in the ISF after oral and intravenous dosing, were simulated in an *in vitro* PD model against *Enterobacter*, *K. pneumoniae*, and *S. aureus*. Results showed that after oral and intravenous administration, mean *f*AUCs (± SD) of both muscle and subcutaneous adipose tissue were statistically significantly lower than the corresponding AUC for plasma (29). Whereas

$fAUC_{muscle\ i.v.}$ (7.43 ± 1.40 mg·h/L) was significantly higher than $fAUC_{muscle\ oral}$ (4.49 ± 1.41mg·h/L), no significant differences could be detected between $fAUC_{subcutis\ i.v.}$ (4.13 ± 1.63mg·h/L) and $fAUC_{subcutis\ oral}$ (3.85 ± 2.26mg·h/L) (29). However, a closer look at the continuously increasing $fC_{muscle\ oral}/C_{plasma}$ ratio indicates that steady-state conditions have not yet been reached. While a $C_{skin\ blister}/C_{plasma}$ ratio > 4 is an indicator that ciprofloxacin preferably accumulates in inflamed lesions, saliva and capillary blood concentrations were similar to total plasma (29). In addition, results from the *in vitro* PD model showed that a comparable outcome was achieved against selected test strains with ciprofloxacin given either as 400mg i.v. or 500mg orally (29). The above information leads to the conclusion that single i.v. infusion of 400mg and single oral administration of 500mg of ciprofloxacin result in different skeletal muscle and subcutaneous adipose tissue concentrations. Yet, these differences in PK might not be pronounced enough to result in clinically significantly altered PD outcome (29).

In some cases, on the other hand, the absorption of active drug molecules into the blood stream is undesirable, especially when drug-specific systemic adverse events are induced. Topical administration of these compounds might, therefore, be considered as an alternative. For example, nonsteroidal anti-inflammatory drugs (NSAIDs) such as diclofenac are widely prescribed for the treatment of rheumatic diseases (105). Although they are among the most commonly prescribed drugs worldwide, they are also responsible for approximately one-quarter of all adverse drug reactions such as increased risk of severe gastrointestinal (GI) complications (105). Topical diclofenac administration might therefore be superior to oral or intravenous application for the treatment of inflammatory diseases.

MD was used in the following study to determine the relative BA of diclofenac in plasma, subcutaneous adipose and skeletal muscle tissue after application of a novel diclofenac spray gel

formulation (4%), or oral dosing with enteric coated diclofenac tablets, respectively (25). In one study, 12 healthy, male volunteers received two dosing regimens with a 14-day washout period in between. During the first regimen, a diclofenac spray gel formulation (48mg) was applied topically TID for three days (10 doses total). In the 2nd regimen, enteric-coated diclofenac tablets (50mg) were administered orally TID for three days (10 doses total). In both cases, after administration of the 10th dose, blood and MD (from subcutaneous adipose and skeletal muscle tissue) were collected in 1-hour intervals for 10 hours post dose and at 48h. Diclofenac concentrations in dialysate and plasma samples were determined using LC-MS-MS and the respective AUCs calculated. While the relative BA of diclofenac in skeletal muscle (209%) and subcutaneous adipose tissue (324%) was higher after topical compared to oral administration, the relative BA in plasma was 50-fold lower (Table 3-1) (25). In addition, results showed that maximum plasma concentrations ($C_{max,plasma}$) after topical administration were approximately 250-fold lower than the $C_{max,plasma}$ values after oral administration. These data lead to the conclusion that the spray gel formulation is a good alternative to oral diclofenac formulations for the treatment of inflammatory soft tissue conditions due to the favorable penetration characteristics and low systemic availability (25).

Although the results of the previous study indicate topical diclofenac formulations are appropriate for treatment of rheumatic diseases, there is still uncertainty whether these concentrations are sufficient in the target tissues (215, 217, 235). The aim of another MD study was to investigate transdermal penetration of diclofenac after local topical administration into superficial and deep tissue layers (191). Two MD catheters – one into a superficial (3.9 ± 0.3mm) and one into deep (9.3 ± 0.5mm) - were inserted into the tissue of 20 healthy, male volunteers. The correct position (distance between skin surface and MD tip) was determined by

high frequency ultrasound scanning. Diclofenac gel (approximately 300mg/100cm^2) was applied onto skin above the inserted MD membrane. Dialysate was collected every 30 min for up to 4 h and respective free AUCs were calculated. Results showed that diclofenac concentrations could be determined in both sampling sites in just 7 volunteers and could not be correlated to the insertion depth. Linkage to the IC_{50} (0.5µg/mL) of cyclooxygenase 2 (COX-2) showed that effective levels in underlying tissue layers were reached in only 8 out of 20 subjects (179, 191). In contrast to the previous study, it was therefore concluded that due to insufficient deep tissue penetration, a generalized use of transdermal diclofenac formulations, at least single doses, is often not justified and may be greatly dependent on individual skin properties (191).

The effect of NSAIDs is triggered by inhibition of key enzymes (cyclooxygenase 1 and 2) of the prostaglandin (PG) synthesis. PGs are mediators and are involved in a number of physiological and pathophysiological effects including the evolvement of pain (31). However, it is still debated whether antihyperalgesic effects of NSAIDs include both peripheral (inflammation site) and central sites of action (31).

MD was used to determine PG levels in the skin after topical and oral diclofenac administration. All of the 10 healthy volunteers were treated in three consecutive treatment periods. Each treatment period was randomly assigned and could contain the following combinations: a) oral formulation (93mg) plus topical formulation (placebo), b) oral formulation (placebo) plus topical formulation (65mg) or c) oral formulation (placebo) plus topical formulation (placebo), respectively. While MD samples were taken every 0.5h after administration for up to 6 h, blood samples were drawn for 24h and analyzed using LC-MS-MS. In addition, antihyperalgesic action of diclofenac was assessed using an inflammatory model of cutaneous hyperalgesia (freeze lesion). The response was quantified by estimating mechanical

pain threshold (MPT) before and after dosing at 0.5h intervals for up to 6h. Study results showed that both topical and oral diclofenac formulations are significantly more effective than placebo. While higher tissue levels were measured for topical treatment during the first hour after the application compared to oral administration (46.1ng/mL vs. 11.4ng/mL), oral administration resulted in higher tissue levels at time points 2 and 2.5h (Figure 3-1) (31).

However, after topical administration, diclofenac could not be detected in plasma. Even though the area under the curve in tissue ($fAUC_{tissue}$) after oral dosing was lower than after topical application (32.2ng·h/mL vs. 40.7ng·h/mL), the overall pain relief was 1.7 fold higher after oral administration during the first three hours. Accordingly, the authors suggested that an additional centrally mediated antihyperalgesic effect is involved in the analgesic effect of systemically administered diclofenac (31).

Insufficient BA at the tissue site, in addition to the occurrence of adverse events, might limit the use of oral or IV formulations (250). Instead, topical administration can overcome these limitations and is employed to deliver drugs at, or close to, the point of application (221). Topical drug formulations can be applied to the eye, nose and throat, ear, vagina, lung, etc.; however, the vast majority of topical medications is applied to the skin (221). Dermal drug formulations are thus commonly used for the treatment of skin diseases such as urticaria, psoriasis or skin cancer.

In the area of skin cancer treatment, photodynamic therapy (PDT) has shown promising results for the treatment of basal cell carcinoma (BCC), the most common type of non-melanotic skin cancer (266). During PDT therapy, an intravenously or topically administered photosentisizer such as Protoporphyrin IX accumulates in the cancer tissue (266). After exposure to light of a specific wavelength, this photosensitizer releases cytotoxic singlet oxygen.

MD was used to assess the BA of Delta-Aminolevulinic Acid (δ-ALA), a prodrug, that is specifically metabolized by tumor cells to Protoporphyrin IX, in BCC (n = 14) and normal skin (n = 4) after dermal application (266). In addition, the skin blood flow was mapped and skin amino acid content determined using laser Doppler perfusion imaging and MD, respectively. Results indicated that interstitial ALA concentration in BCC increased from 0 to 3.1 ± 1.7mmol/L (mean ± SEM) within 15 min of application, whereas no ALA could be detected in healthy skin. In contrast, amino acid levels were found to be similar in both healthy and BCC tissue and blood flow was 2.5-fold increased in BCC compared to normal skin during treatment (266). It was concluded that MD is an appropriate technique for the determination of ALA PK in the skin. However, the rapid penetration of ALA into tumor tissue and increased blood flow in BCC might lead to faster elimination from the tumor and warrants further investigation.

Factors Affecting Bioavailability

Despite great interest in the skin as an application route for therapeutic agents, the availability of clinical BA studies evaluating the mechanisms of transdermal absorption and factors affecting the disposition of topically applied drugs is limited (15, 21, 55). In order to address this lack of information, an increasing number of human studies have been performed evaluating factors (e.g. skin barrier function, blood flow, degree of ionization, etc.) that can alter the BA after dermal drug application. The ability of MD to continuously monitor the change of free, unbound drug in the ISF of different layers of the skin or subcutaneous adipose tissue has made it a valuable tool for investigating these factors. MD has, for example, been used to study the effect of skin barrier perturbation by repeated tape stripping, treatment with 1% sodium lauryl sulfate (SLS) or 2% SLS, and treatment with acetone on the penetration of salicylic acid into the skin (15). Findings show that there was an approximate 150-fold difference between

unmodified and tape-stripped/SLS (2%) treated skin, indicating a massive disturbance of the skin barrier function (Figure 3-2). In comparison, penetration increased approximately 46-fold after SLS (1%) and 2.2-fold after acetone treatment, respectively.

The BA of topically applied drugs in skin and soft tissue is not only dependent on the integrity of the skin barrier but also highly correlated to the local blood flow (17, 19, 21, 44, 119, 219, 234). An increase, as well as a decrease, in local blood flow can be due to physiological or drug-induced changes. Whereas an increase in blood flow enhances the penetration of a compound into the respective tissue, a decrease slows down its tissue uptake (19, 21, 30, 44, 119).

This situation was demonstrated in a MD study evaluating the BA of penciclovir (PCV) in the skin after a single oral dose (250mg) of its prodrug famciclovir (19). Three MD probes were implanted into the left forearm of seven healthy volunteers. While all three probes were perfused with Ringer solution, vasoconstriction was additionally induced in the tissues around probes #2 and #3 by either supplementation with adrenaline (0.2mg/mL) or cooling (20^{o}C), respectively (19, 108). Results (Figure 3-3) indicate that penetration of PSV into untreated skin was statistically significantly higher than into skin with decreased microcirculation due to either adrenaline or cooling, respectively (19). In comparison, local warming of the dermis (40^{o}C) was shown to enhance the microcirculation in soft tissues and was correlated with an increased penetration of ciprofloxacin into these tissues (119).

However, physiological or pathophysiological conditions determine not only the BA of a drug in the soft tissue, but the physicochemical properties of the drug itself. It was shown in both *in vitro* and *in vivo* experiments that unionized drug penetrates more efficiently through the stratum corneum than ionized drug (145). Whereas chemical modifications of the drug molecule

(e.g. ester, ion pairs, etc.) are frequently employed to increase the lipophilicity of the parent compound, the molecule's charge can also be actively used (e.g. in iontophoresis) for active drug delivery (55, 240). Yet, these chemical modifications can result in different penetration behavior and consequently altered relative BA (55). Altered BA can become an issue when two different drug formulations of the same parent compound are used and can be addressed in BE studies.

Bioequivalence

In the case of systemically active drugs, although both BA and BE evaluate the release of a drug substance from a drug product and the subsequent absorption into the systemic circulation, BE is a more formal comparative test between two drug products using specified criteria. In the FDA "Guidance for Industry", BE is defined as "the absence of a significant difference in the rate and extent to which the active ingredient or active moiety in pharmaceutical equivalents or pharmaceutical alternatives becomes available at the site of drug action when administered at the same molar dose under similar conditions in an appropriately designed study." (83) However, the determination of BE for locally acting and targeted delivery products has confronted both industry and regulatory authorities with problems during the approval process since plasma concentrations are usually inappropriate surrogates of pharmacological activity (81).

A recent study compared the applicability of MD for BE determination of two topical lidocaine formulations (cream 5%, ointment 5%) to the tape stripping method (14). Multiple MD and tape stripping samples were taken at two different application sites. Results of both methods showed that these two formulations were not bioequivalent, and consequently, not interchangeable. In addition, further statistical analysis of the applied study design indicated that BE studies (90% CI and 80-125% BE limits) using two formulations in each subject need a minimum of 27 subjects (when 2 probes are used per application site), or 18 subjects (when 3 probes are used per application site), respectively (14). In comparison, it has been estimated that

approximately 40 to 50 subjects are required for BE studies using the tape stripping method and up to 300 subjects, using the current clinical BE study design (14, 44).

PK/PD Indices

Besides assessment of BA and/or BE, the actual information on free drug concentrations obtained from the MD experiments can be further used to predict treatment outcome. This approach is frequently employed during drug development of anti-infective agents. In the following clinical MD studies, measured free, active antibiotic concentrations were linked to the respective PD outcome parameters of the most prevalent skin and skin structure pathogens in order to predict their clinical efficacy.

Infections of skin and soft tissue can be caused by a variety of gram-positive and gram-negative pathogens and are routinely treated with antibiotics. Whereas penicillins and cephalosporins are drugs of first choice, agents of different classes (e.g. oxazolidinones, glycopeptides, macrolides, tetracyclines, etc.) have to be used in case of adverse events or emergence of β-lactam resistance. In order to increase the chances of clinical success and to decrease the likelihood of toxic side effects as well as resistance development, selection of an appropriate antibiotic dosing regimen is extremely important (229). The most rational approach is to link active drug concentrations to the respective PD outcome. However, outcome predictions based on total plasma concentrations might be misleading since most infections are not located in the blood stream, but rather in the interstitial space fluid (ISF) of tissues (193). In fact, it is free, unbound drug in the ISF that is responsible for antimicrobial efficacy (222). Once free antibiotic concentrations have been determined at the infection site, outcome should be predictable from the respective susceptibility breakpoints of the infection-causing pathogens (26).

To date, the minimum inhibitory concentration (MIC) has served as a well-established and routinely determined susceptibility breakpoint parameter for antibiotics. According to the Clinical and Laboratory Standards Institute (CLSI, formerly National Committee for Clinical Laboratory Standards NCCLS), the MIC is defined as the lowest concentration of drug that completely inhibits visible growth of the organism as detected by the unaided eye after an 18-24 hour incubation period with a standard inoculum of approximately $5x10^5$–10^6CFU/mL (188, 229). Combinations of this PD marker with free (*f*), unbound PK parameters to MIC-based PK/PD indices such as $fT_{>MIC}$, fAUC/MIC and fC_{max}/MIC have led to a much better understanding of antibiotic dosing (229).

The first PK/PD index was developed for penicillins. It correlates *in vivo* efficacy with the amount of time free drug levels stay above the MIC of the target organism ($fT_{>MIC}$) (229). Although a further index differentiation within the drug class was suggested, a common threshold of $fT_{>MIC} \geq 40\%$ seems to be sufficient for the clinical efficacy of β-lactam antibiotics (229). While fC_{max}/MIC index values of 10-12 seem to be a good predictor for aminoglycosides, the magnitude of the fluoroquinolone index is still controversial (89, 125, 180, 214). Nonetheless, target $fAUC_{24}$/MIC values of 100-125 (Gram-negatives), 25-35 (Gram-positives) and fC_{max}/MIC index values of 10 have been identified for fluoroquinolones (76, 89, 205). In comparison, $fAUC_{24}$/MIC values 50-100 or $fT>MIC \geq 85\%$ were good outcome predictors for oxazolidinones (168). Once these MIC-based PK/PD indices are identified, they can support the identification of optimised dosing regimens and the prediction of treatment outcome (229).

Knowledge of the free antibiotic concentration-time course in the ISF is necessary in order to establish the respective $fT_{>MIC}$, fC_{max}/MIC and $fAUC_{24}$/MIC index values. Whereas various

techniques are available for determination of free, unbound concentrations, they are not all capable of characterizing dynamic changes in free ISF concentrations. Only MD combines these two properties. Consequently, it is therefore a very valuable sampling tool and has become an inherent part of evaluation and establishment of PK/PD indices.

$fT_{>MIC}$

Although clinical studies have demonstrated the effectiveness of ertapenem in SSSI treatment, few studies on the *in vivo* penetration of ertapenem into ISF of soft tissues, such as skeletal muscle and subcutaneous adipose tissue, and resulting free, active concentrations, have been available (34, 99, 151).

In a single center, prospective, open label study, free, unbound ertapenem concentrations in the ISF of skeletal muscle and subcutaneous adipose tissue were measured using MD (34). After determination of the individual probe recoveries, six healthy volunteers received 1g ertapenem as a single 30 min short-term i.v. infusion. Plasma and MD samples were collected over 12 h post-dosing and analyzed using LC-MS-MS. Results indicate that free, unbound ertapenem profiles in the ISF of both skeletal muscle and subcutaneous adipose tissue are lower than corresponding total plasma concentrations as shown in Figure 3-4. While free ISF concentrations of the skeletal muscle correlated well with free, unbound concentrations in plasma (4-16% of total plasma concentration), they were comparably higher than free ISF concentrations in subcutaneous adipose tissue. This phenomenon was observed in other studies as well, and might be explained by differences in blood flow in these two tissues (27). Free ertapenem concentrations of 1.13 ± 0.68mg/L in the muscle, observed 12h after single dose i.v infusion of 1g ertapenem, exceeded the MIC_{90}s of methicillin susceptible *S. aureus* (0.25mg/L), *Streptococcus spp* (0.5mg/L), extended-spectrum b-lactamase (ESBL)-producing *Enterobacteriaceae* (0.03-0.06mg/L), *Bacteroides fragilis* and other anaerobic bacteria (≤ 1.0mg/L) for at least 50% of the entire

dosing interval. In comparison, free levels of 0.31 ± 0.16mg/L in the subcutaneous adipose tissue (at 12h) exceeded the MIC_{90} of the same SSSI pathogens for at least 30% of the dosing interval. The authors concluded that free, active ertapenem concentrations reached sufficient levels in non-infected interstitial fluid of muscle and subcutaneous adipose tissue and that previous clinical findings were supported by this data (34).

fAUC$_{24}$/MIC

Linezolid, the first oxazolidinone, is approved by the FDA for the treatment of nosocomial pneumonia and complicated skin and skin structure infections. It shows good antimicrobial activity against various resistant gram-positive bacteria, including methicillin- and glycopeptide-resistant *S. aureus* (282). Despite the fact that 1) only free, unbound data is considered for antimicrobial efficacy and 2) most relevant pathogens are located in the ISF, most of the available linezolid PK data is based on total plasma concentrations (33, 64, 243). Therefore, a clinical MD study was performed that evaluated the penetration of linezolid into soft tissues of 10 healthy volunteers after single and multiple dose administration (64). On day one of this study, MD catheters were placed into the subcutaneous adipose tissue and the skeletal muscle of each volunteer. After calibration and baseline determination, 600mg linezolid were infused intravenously over 30min. MD and blood samples were taken for up to eight hours. After withdrawal of the MD probes, volunteers were started on oral linezolid (600mg) BID for five consecutive days (64). The second set of MD experiments was started simultaneously with the last oral dose. This time, probes were calibrated after the 8-hour sampling period. The AUC_{0-8} was calculated by using the trapezoidal rule, the AUC_{24} by extrapolation to 24 hours. In addition, AUC_{24}/MIC ratios were calculated for pathogens with MICs of 2mg/L and 4mg/L, respectively. Results show that after single i.v. administration of linezolid, fAUC$_{0-8}$ of both skeletal muscle (65.3 ± 18.2mg·h/L) and subcutaneous adipose (75.8 ± 24.2mg·h/L) tissue were

statistically significantly higher than the $fAUC_{0\text{-}8}$ of plasma (53.0 ± 11.6mg·h/L). However, at steady-state no significant differences between concentrations in the ISF of skeletal muscle and subcutaneous adipose tissue could be detected (64). The findings further indicated that steady state concentrations in both muscle ($fAUC_{24\ muscle}$/MIC 58.9 ± 33.0mg·h/L) and adipose subcutaneous tissue ($fAUC_{24\ tissue}$/MIC 46.6 ± 15.9mg·h/L) were sufficient to treat infections that are caused by pathogens with MICs of up to 4 mg/L (64).

fC_{max}/MIC

According to the CDC (Center of Disease Control), surgical site infections (SSI) include skin and subcutaneous tissue infections and are the second most common cause of serious nosocomial infections (23, 195). These SSI can be caused by various pathogens (e.g. *S. aureus*, *P. aeruginosa*, *Klebsiella ssp.*) and are frequently treated with β-lactam antibiotics (195, 263). In patients with confirmed allergy or adverse reaction to β-lactam antibiotics, gentamicin can be used in combination with either clindamycin or metronidazole (24). Gentamicin is a broad-spectrum antibiotic that shows good antimicrobial activity against gram-positive *S. aureus* and gram-negative bacteria including *Enterobacteriaceae* and *Pseudomonaceae* (162). Its short half-life of 2-3 hours in patients with normal renal function requires a well-designed dosing regimen in order to prevent concentrations from dropping rapidly to subtherapeutic levels (24). Since it is oftentimes unclear whether surgical procedures change free, active drug levels in the ISF, the most rational approach is to measure respective free concentrations directly at the surgical site using MD.

After insertion of the MD catheter into the subcutaneous fat layer of the abdominal wall (10cm lateral to the umbilicus), seven healthy volunteers, with normal renal function, received 240mg gentamicin as an IV bolus (162). For the first hour, plasma and MD samples were taken every 20min, followed by 60min sampling intervals for up to six hours. Samples were analyzed

using a spectrophotometric immunoassay. PK parameters were determined by compartmental analysis. Free peak concentrations in tissue ($fC_{max\ tissue}$) of 6.7 ± 2.0mg/L, which is equivalent to 39.1% of the total peak serum concentration (C_{max}), were reached within 10 to 30min of administration (162). Since the fC_{max}/MIC ratio was identified as the best predictor of aminoglycoside efficacy, fC_{max}/MIC values were calculated for common SSI pathogens such as *P. aeruginosa* (7.4:1, MIC: 0.9mg/L), *S. aureus* (33.5:1, MIC: 0.2mg/L) and *Klebsiella ssp.* (4.8:1, MIC: 1.4mg/L), respectively (162). The authors concluded that 1) MD could be successfully used to measure gentamicin concentrations in subcutaneous tissue and 2) determined gentamicin concentrations were sufficient to treat infections with the most common SSI pathogens (162).

In some cases, the antibiotic dosing regimen does not result in sufficient concentrations in the ISF. If they fail to outreach the MIC thresholds of respective SSSI pathogens, they cannot be used for treatment.

Telithromycin, for example, is typically used as a reserve antibiotic for the treatment of respiratory tract infections since it shows high concentrations in inflammatory fluids, bronchopulmonary tissues, tonsillar tissue, and saliva (74, 97, 128). However, its good activity against some *Streptococci ssp.* has lead to speculation on its applicability in the treatment of SSSI (94, 97). Hence, a MD study was designed to evaluate the PK profile of telithromycin in the ISF of soft tissues after single dose administration. In this study, commercially available 800mg telithromycin tablets were given orally to 10 healthy male volunteers (94). Blood and dialysate concentrations were determined. Areas under the concentration time curve from zero to eight hours ($AUC_{0\text{-}8}$) were calculated for free concentrations in the ISF of muscle and subcutaneous adipose tissue as well as free and total plasma concentrations, respectively.

Results showed that there were no statistically significant differences between areas under the mean free concentration-time curve from zero to eight hours (fAUC$_{0\text{-}8}$) in muscle (0.6 ± 0.3mg·h/L), subcutaneous adipose tissue (0.9 ± 0.6mg·h/L) and plasma (0.5 ± 0.2mg·h/L). However, fAUC$_{0\text{-}8}$s of muscle and subcutaneous adipose tissue were significantly lower than the mean AUC$_{0\text{-}8}$ of total plasma (4.1 ± 1.5mg·h/L) as shown in Figure 3-5. Since antimicrobial efficacy of ketolides correlates best with fAUC$_{0\text{-}24}$/MIC ratio, the fAUC$_{0\text{-}24}$ was additionally calculated. Using the MIC where the growth of 90% of the SSSI-causing pathogens is inhibited (MIC$_{90}$), the fAUC$_{0\text{-}24}$/MIC$_{90}$ ratios indicated that bacteria highly susceptible to telithromycin such as *S. pyogenes* might be eradicated from tissues and plasma (54, 276). Nevertheless, these fAUC$_{0\text{-}24}$/MIC$_{90}$ ratios further indicated that telithromycin shows insufficient concentrations against other prevalent SSSI pathogens such as *S. aureus* or bite pathogens such as *Prevotella canis*. The authors concluded, that telithromycin shows limited activity against common SSSI-causing pathogens and should therefore not be used for their treatment (94).

Conclusion

Despite the fact that most pharmacological events take place in tissues, PK data is usually still based on blood or serum concentrations (44). However, free, unbound drug concentrations can differ significantly between blood and tissues. Measurement of free, active drug concentrations in the tissue of interest is consequently the most rational approach, but has frequently been restricted by insufficient sampling/analysis techniques. With MD, a well-accepted, relatively inexpensive, semi-invasive sampling technique that is able to sample free, active drug directly from the extracellular space fluid of tissues has become available. The resulting tissue concentration-time profiles reflect both rate and extent of drug absorption from the respective application site and can, therefore, be used for BA and BE assessment. In fact,

MD has been recommended by the FDA as a sampling tool for BE evaluations of topical dermatological products (14, 44, 81, 134, 135, 173).

To date, most of the current BA studies are performed in healthy volunteers. However, physiological processes can be altered in patient populations compared to healthy volunteers. Consequently, the assessment of BA in patients can be expected to become more important in the future. Initial progress has already been made in this area by determining free, active drug concentrations in diseased tissue (e.g. tumors, diabetic food, psoriasis, etc.) using MD. Once free, active drug concentrations have been determined, they then can be further correlated with appropriate biomarkers in order to predict clinical efficacy.

Table 3-1. Pharmacokinetic parameters for diclofenac in plasma and subcutaneous and skeletal muscle tissue.

Parameters	Topical		Oral	
	Median	95% Cl	Median	95% Cl
Plasma (n=12)[a]				
AUC_{∞}, AUC_{τ} ($ng \cdot h \cdot mL^{-1}$)	32.8	(22.7-52.9)	1569.7	(1255.8-1849.8)
C_{max} (ng/mL)	4.9	(3.4-7.7)	1240.2	(787.0-1388.9)
Subcutaneous tissue (n=12)[b]				
AUC_{∞}, AUC_{τ} ($ng \cdot h \cdot mL^{-1}$)	21.5	(19.4-50.5)	8.6	(7.0-10.6)
C_{max} (ng/mL)	13.1	(9.3-33.6)	1.9	(1.6-2.5)
Skeletal muscle (n=12) [b]				
AUC_{∞}, AUC_{τ} ($ng \cdot h \cdot mL^{-1}$)	18.2	(11.8-28.1)	8.8	(7.8-12.3)
C_{max} (ng/mL)	12.3	(6.2-22.0)	2.6	(2.0-4.0)

Data from 12 healthy males after multiple dose regimens of either topical (diclofenac spray gel 4%) or oral (50mg enteric-coated tablets) diclofenac. CI = confidence interval; AUC_{∞}, AUC_{τ} = area under the plasma or tissue concentration vs. time curve of diclofenac approximated to infinity (AUC_{∞}) or evaluated in the last dosage interval (0-8h; AUC_{τ}); C_{max} = maximum plasma or tissue concentration. [a]Total drug. [b]Free drug

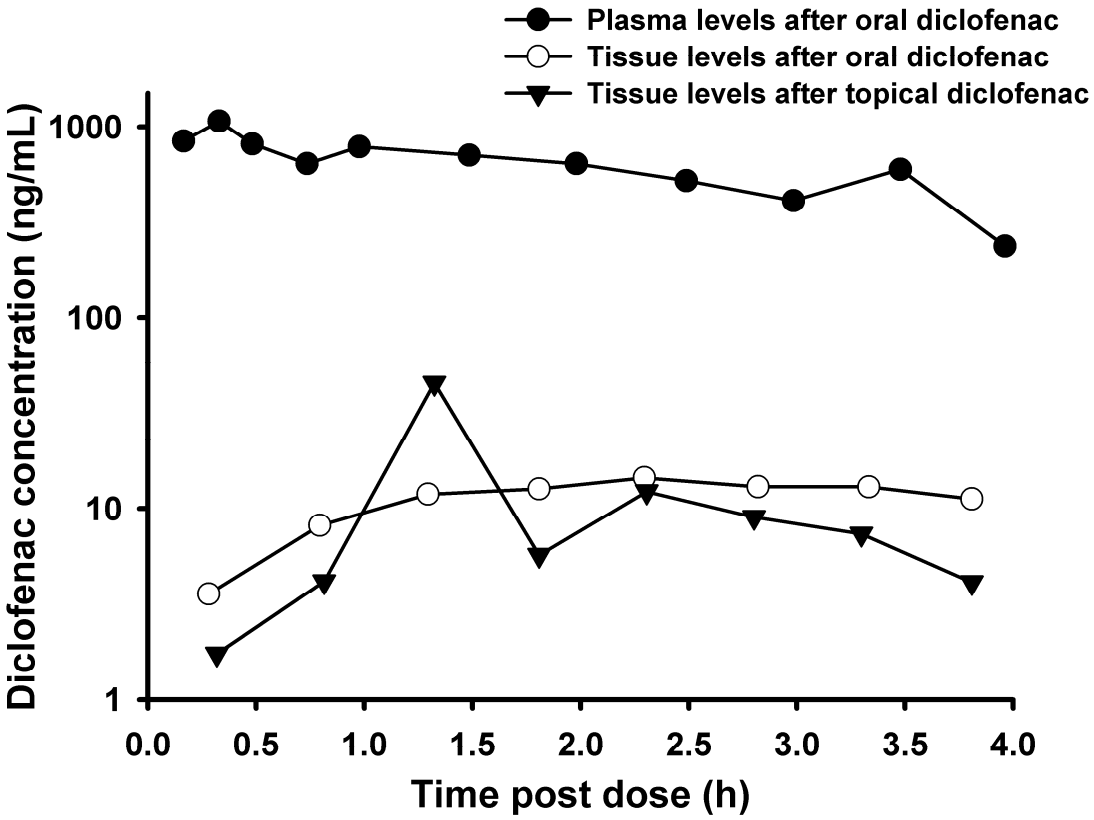

Figure 3-1. Mean concentration-time profile of diclofenac after oral and topical administration in subcutaneous tissue and plasma.

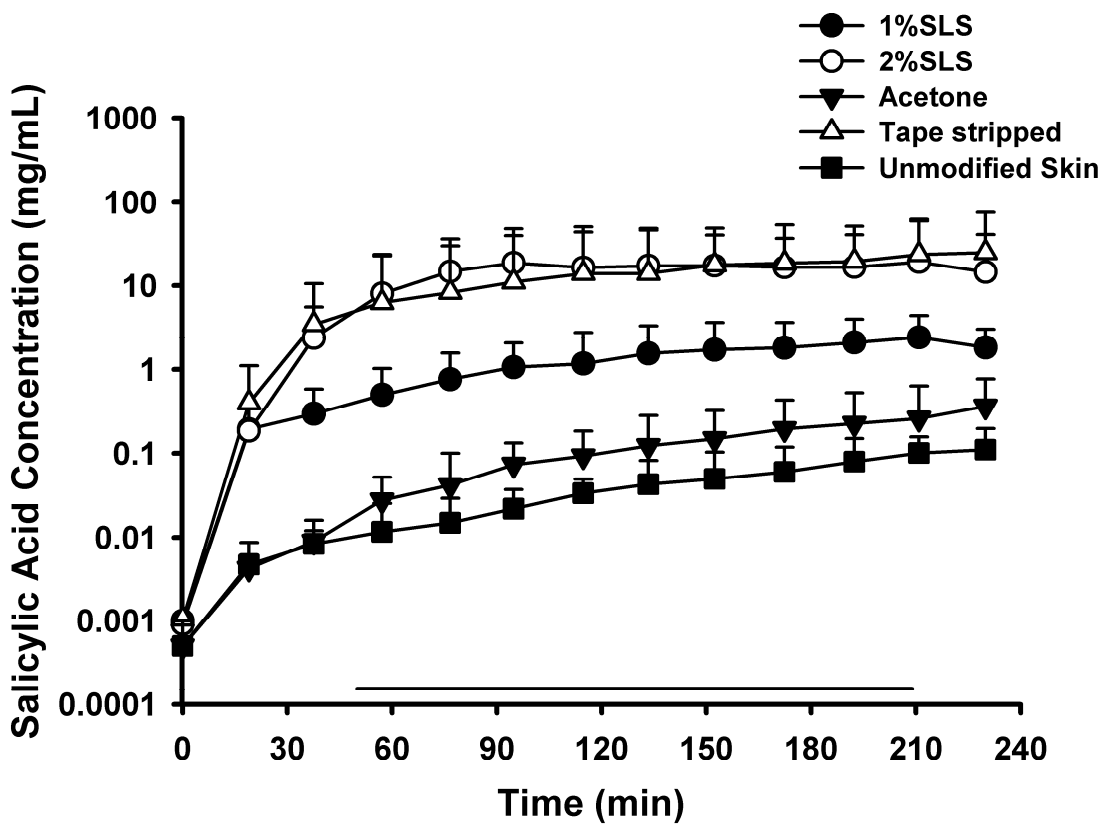

Figure 3-2. Concentration (mean ±SD)-time plots demonstrating differences in dermal salicylic acid (SA) penetration sampled by MD probes, inserted in the 4 barrier-pertubated skin areas (n=16).

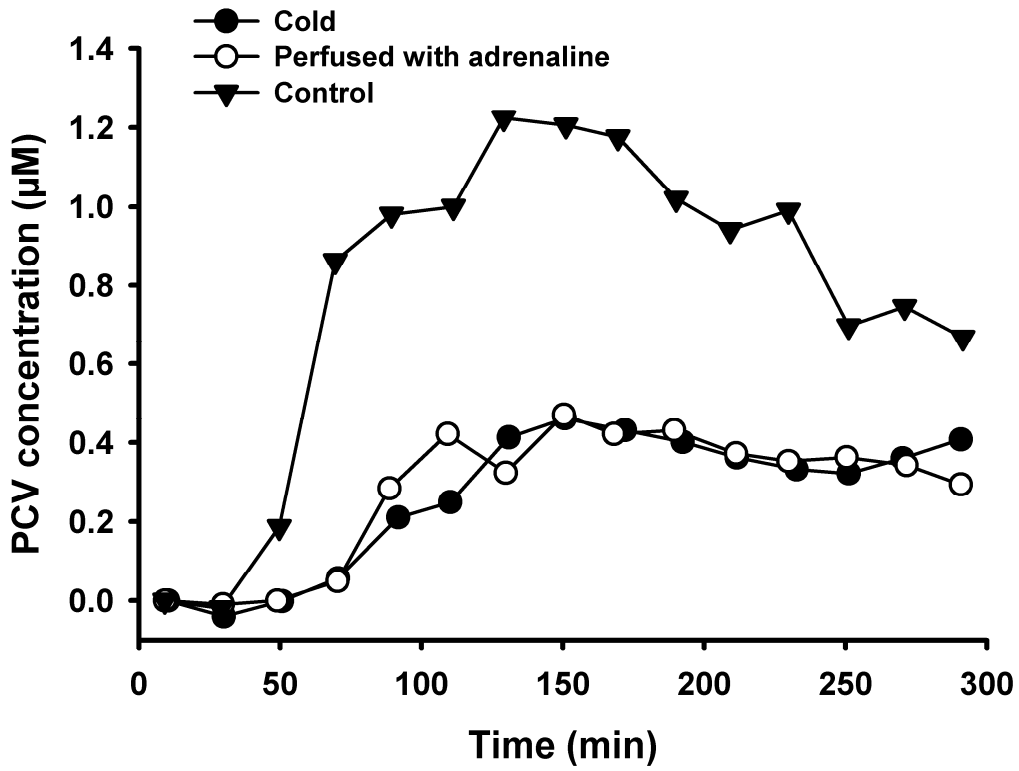

Figure 3-3. Median concentration-time profiles for penciclovir (PCV) in skin for control, solution perfused with adrenaline, and cold skin following single oral administration of 400mg famciclovir (prodrug) in healthy volunteers (n=4).

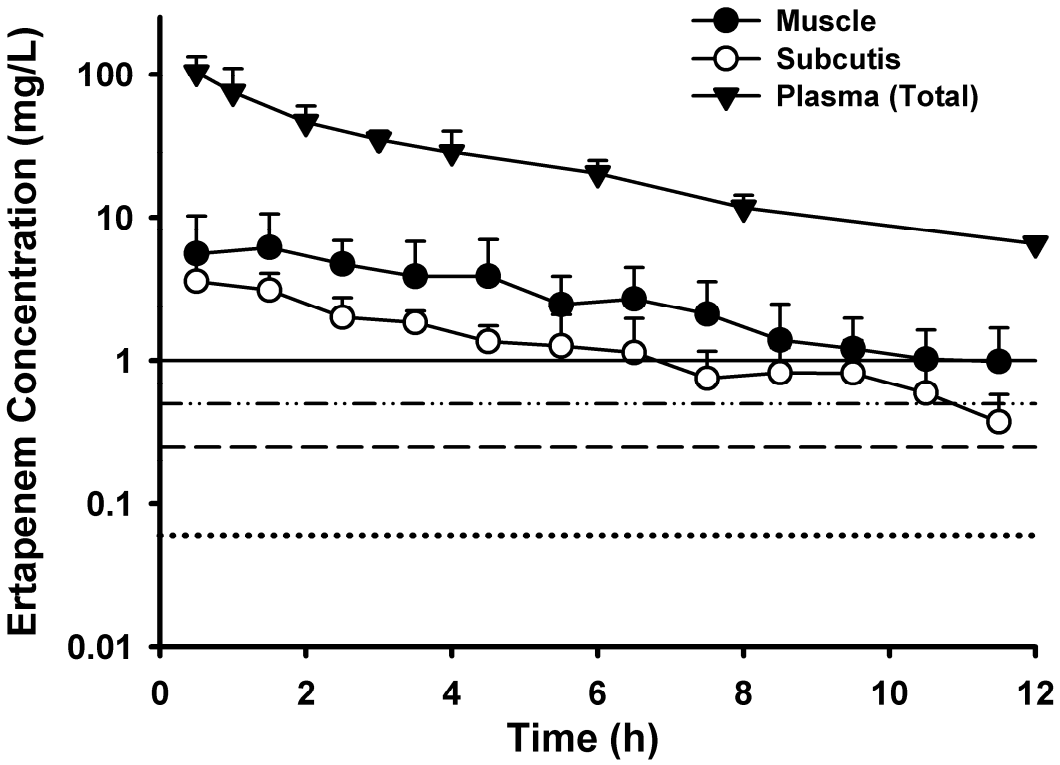

Figure 3-4. Ertapenem concentration (mean ±SD)-time profiles in total plasma, skeletal muscle fluid, and interstitial adipose tissue (subcutis) following 1g infusion for 30min in healthy volunteers (n=6). Horizontal lines indicate MIC_{90} values for methicillin susceptible S. aureus (———), Streptococcus spp (—··—), extended-spectrum b-lactamase (ESBL)-producing Enterobacteriaceae (·····), Bacteroides fragilis and other anaerobic bacteria (——).

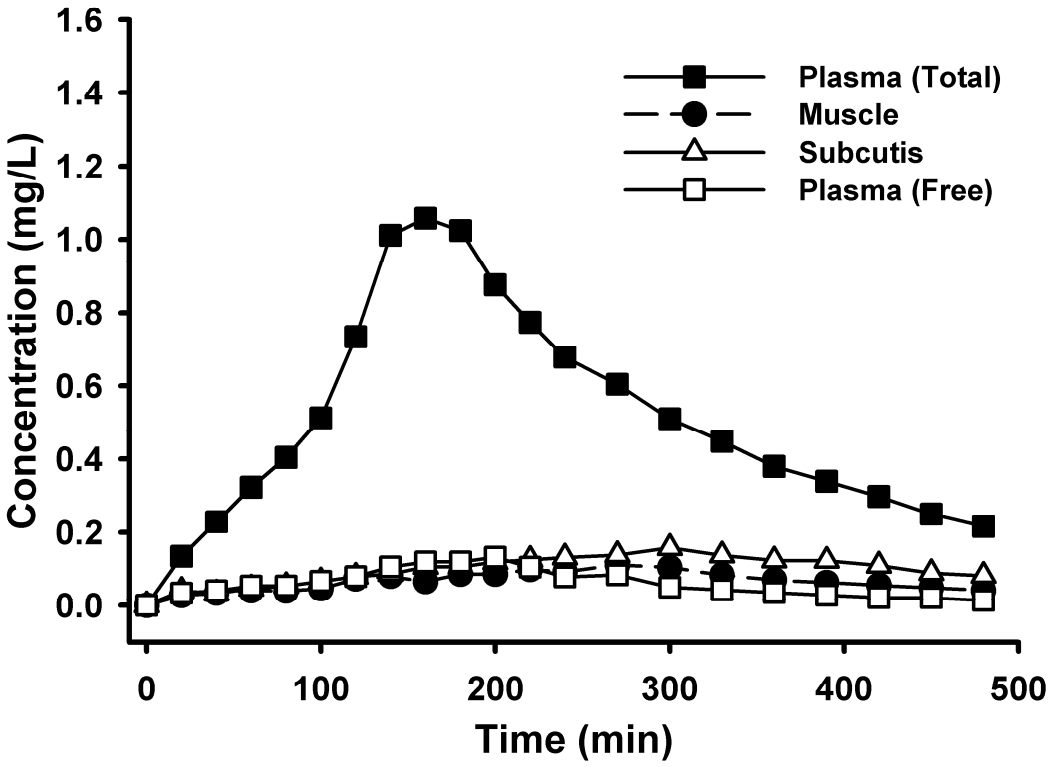

Figure 3-5. Telithromycin concentration-time profiles in plasma (total and free), muscle, and subcutaneous adipose tissue after a single 800mg dose in healthy volunteers (n=10).

CHAPTER 4
PENETRATION OF ERTAPENEM INTO SKELETAL MUSCLE AND SUBCUTANEOUS ADIPOSE TISSUE IN HEALTHY VOLUNTEERS MEASURED BY *IN VIVO* MICRODIALYSIS[3]

Introduction

In clinical practice, empiric antibiotic therapy is initiated as the first measure dealing with bacterial infection. In case of therapeutic failure, however, it may become necessary to measure the susceptibility of the causative agent and to adjust antibiotic dosage schedules with the aim to attain serum drug concentrations above the MIC for the respective pathogen throughout the dosing interval (53). Although this approach is suitable for conditions, where the central compartment is the main site of infection, e.g. septicemia, for localized organ or tissue infections drug concentrations in the interstitial space rather than in serum determine the clinical outcome of antimicrobial therapy (152, 188). This is particularly relevant for skin and skin-structure infections (SSSI), which may occur due to surgical wound contamination, after trauma or in diabetic patients and may result in severe necrotizing limb- and even life-threatening infections (32, 92, 96). Hence, to be clinically effective an antibiotic should reach pharmacologically active, i.e. unbound, soft tissue concentrations high enough to eradicate the causative pathogen (136, 177). A class of antibiotics which was shown to qualify for the treatment of SSSI are carbapenems. Ertapenem is a long-acting parenteral 1-β-methyl-carbapenem, which was selected for clinical development partially based on its pharmacokinetics (56, 156, 281). Owing to its long plasma half-life, which reflects a high plasma protein binding, ertapenem can be administered once daily (199). Although clinical studies have demonstrated the effectiveness of ertapenem for SSSI-treatment, the *in vivo* penetration and the resulting free protein-unbound concentrations in interstitial space of soft tissues, such as skeletal muscle and subcutaneous

[3] Copyright © Oxford Journals, [J Antimicrob Chemother 58: 632-6, 2006]

adipose tissue have not been reported, mainly due to a lack of appropriate methodology (99, 151). One technique, which has been proven suitable for the measurement of target tissue concentrations of a variety of substances *in vivo* in humans, is clinical microdialysis (122). This method is a minimal invasive technique for the measurement of unbound drug concentrations in virtually every tissue and organ. The present microdialysis study was conducted to measure and compare the free protein-unbound ertapenem concentrations in the interstitial space fluid of two peripheral target sites, skeletal muscle and subcutaneous adipose tissue, following the administration of 1 g infusion, and to compare them with the respective plasma concentrations.

Volunteers and Methods

Volunteers

Six healthy volunteers (3 men, 3 woman, 4 Asians, 2 Caucasians), between 22 and 37 years old, average height 160.0 ± 8.8 cm, average body weight 64.7 ± 8.6 kg, average body mass index 25.3 ± 2.4 kg/m^2, and average body surface area 1.68 ± 0.16 m^2, participated in the study. All had normal renal and hepatic function; the mean creatinine clearance was 100.5 ± 21.1 ml/min 1.73 m^2. All volunteers included in the study had normal findings from physical examination, electrocardiogram and laboratory tests (including haematological and biochemical parameters, urinalysis, and negative pregnancy test). The mean albumin serum concentration was 4.43 ± 0.29 g/L, the mean total protein concentration 7.50 ± 0.24 g/L. Further exclusion criteria were regular use of medications, abuse of alcoholic beverages, symptoms of significant illness within 3 months before the study period, history of liver or kidney disease potentially interfering with metabolism or excretion of the drug, history of central nervous system disorders, allergy or hypersensitivity to the study drug, blood donation of more than 500 ml during the previous 3 months, participation in a clinical trial within 3 months before the study period and pregnancy. The study was conducted in the General Clinical Research Center at Shands

Hospital, University of Florida, was approved by Shands' Hospital Institutional Review Board (IRB-01), and was performed in accordance with the Declaration of Helsinki. All volunteers were given a detailed description of the study, and their written consent was obtained.

Study Design and Protocol

The study was conducted as a single-center, prospective, open-label trial. Volunteers were hospitalized from the evening before start of the study until 12 h post dosing. On the study day, the volunteers were kept under fasting conditions for 10 h prior to the start of the experiments until 2 h after drug administration. Each volunteer received one dose of 1g ertapenem as an intravenous infusion over 30 min. Tolerability and safety assessments, clinical chemistry, haematological tests and urinalysis, and the measurement of vital signs (blood pressure, heart rate) and ECG were included in the study. Vital signs were taken before administration of the drug and 15 min, 1, 2, 12 h thereafter. All data relating to drug safety were recorded throughout the study. Each volunteer recorded a diary protocol of possible adverse events.

Sample Collection

To measure the unbound fraction of ertapenem in the interstitial space fluids, microdialysis probes (CMA 60; CMA, Stockholm, Sweden) with a molecular cutoff of 20 kDa were used. Microdialysis probes were inserted after cleaning and thorough disinfection of the skin. One dialysis probe was inserted into the medial vastus muscle and one was inserted into the subcutaneous layer of the thigh. The microdialysis probes were secured in place by holding a plastic flap at the base of the probe while the needle was removed. The microdialysis system was flushed with lactated Ringer's solution and then connected to a microinfusion pump (Precidor; Infors-AG, Basel, Switzerland). The principles of microdialysis have previously been described in detail (27, 190, 192). Briefly, microdialysis is based on sampling of the non-protein-bound fraction and, therefore, the pharmacologically active fraction of analytes from the

interstitial space with a semipermeable membrane at the tip of a microdialysis probe. The probe is constantly perfused with a physiological solution (perfusate) at a flow rate of 2 μL/min. Once the probe is implanted into the tissue, substances present in the extracellular fluid at a particular concentration (C_{tissue}) are filtered out of the interstitial space fluid by perfusion into the probe, resulting in a concentration ($C_{dialysate}$) in the perfusate. Samples are collected and analyzed. For most analytes, equilibrium of the concentration between extracellular tissue fluid and the perfusion medium is incomplete; therefore, $C_{tissue} > C_{dialysate}$. The factor by which the concentrations are interrelated is termed recovery. To obtain absolute concentrations in the interstitial space fluid from the concentrations in unbound dialysate, microdialysis probes were calibrated for *in vivo* recovery rates by the retrodialysis method (242). The retrodialysis procedure is performed in each subject before dosing of the drug. The principle of this method relies on the assumption that the diffusion process is quantitatively equal in both directions through the semipermeable membrane. Therefore, ertapenem was added to the perfusate at a concentration of 5.0 mg/L, and the disappearance rate (delivery) through the membrane was taken as the *in vivo* recovery. The *in vivo* percent recovery was calculated as

$$\text{Recovery}(\%) = 100 - \left(\frac{\text{Concentration}_{\text{dialysate}}}{\text{Concentration}_{\text{perfusate}}} \times 100 \right) \qquad (4\text{-}1)$$

After a 30-minute baseline perfusion period, *in vivo* calibration was performed as described previously for a period of 60 minutes, during which two samples were collected (at -30 and -60 minutes) (27). Concentrations in both retrodialysis samples were averaged and used to calculate the *in vivo* recovery. After the calibration period was completed, a 60-minute washout period was observed. Microdialysis sampling was performed at 60-minute intervals up to 12 hours post dose.

Blood samples (5 mL) were collected in lithium heparinate-coated tubes, via a venous plastic cannula (JELCO; Johnson-Johnson, Arlington, Tex), before ertapenem infusion, and 0.5, 1, 2, 3, 4, 6, 8, and 12 hours after the start of infusion. Samples were centrifuged at 1.300 g for 10 min at 4°C. Plasma was separated and stored at -80°C until analysis.

Drug Assay

Quantitative determination of ertapenem in plasma and in interstitial space fluid of skeletal muscle and subcutaneous adipose tissue were determined by validated SPE-Liquid chromatography–tandem mass spectrometry methods (LC-MS-MS) (132). The HPLC analytical column used was Synergi 4µ Polar-RP 10·2.0 mm. The flow rate was 0.5 mL/min, with a gradient mobile phase of A = 2 mM ammonium acetate/0.1% Acetic Acid, pH = 3.2 and B = 100% methanol, starting from 100% A to 90% B in 5 minutes and change back to 100% A in 3 minutes, keep it there for 6 minutes, total of 14 minutes for each injection. MS-MS equipment and related parameters are: Micromass Quattro LC-Z, with negative electro spray ionization, MRM scan function for two channels: 474.00 > 265.00 (ertapenem) and 466.00 > 422.00 (ceftazidime, as internal standard), cone voltage was 25 volts, collision energy was 20 for ertapenem and 10 for I.S.. The limit of quantification was 0.04 mg/L.

Pharmacokinetic Analysis

Pharmacokinetic parameters were calculated by non-compartmental analysis with Kinetica pharmacokinetic software program (Kinetica 4.3, Innaphase). The maximum observed plasma concentration (C_{max}) and time to reach C_{max} (T_{max}) after drug administration were determined directly from the concentration-time curves. The area under the plasma concentration curve from time 0 (the start of infusion) until the last quantifiable plasma concentration ($AUC_{0\text{-}last}$) was calculated by using the log-linear trapezoidal rule. $AUC_{0\text{-}\infty}$ was derived by adding $C_{last}/\lambda z$ to $AUC_{0\text{-}last}$. The terminal elimination rate constant (λz) was estimated from the slope of terminal

exponential phase of the logarithmic plasma concentration-time profile using no fewer than 3 data points. The apparent terminal elimination half-life ($t_{1/2z}$) was calculated as $0.693/\lambda z$. The mean residence time (MRT) was calculated $AUMC_{0-\infty}/AUC_{0-\infty}$, where $AUMC_{0-\infty}$ is the area under the first moment of concentration-time curve, determined by integrating the product of time and concentration from zero to infinity. Apparent total clearance (CL_{tot}) was calculated as dose/$AUC_{0-\infty}$. The apparent volume of distribution during the terminal phase (V_z) was calculated as ($CL_{tot/\lambda z}$). Protein-unbound ertapenem concentrations in the extracellular skeletal muscle and subcutaneous adipose tissue fluid were calculated from measured microdialysate concentrations and individual probe recovery, determined in our *in vivo* experiments. The parameters, such as C_{max}, T_{max}, AUC_{0-last}, $AUC_{0-\infty}$, and $t_{1/2z}$ were calculated using the same formula as for plasma samples. The tissue penetration was calculated as the ratio of the unbound $AUC_{0-\infty}$ in skeletal muscle or subcutaneous adipose tissue fluid to the total $AUC_{0-\infty}$ in plasma ($AUC_{tissue, free}/AUC_{plasma, total}$). All data are presented as geometric means ± standard deviations, with the exception of T_{max}, for which median and minimum-maximum ranges are given only.

Results

Safety

All six enrolled volunteers completed the study in accordance with the protocol. The microdialysis procedure and treatments were well tolerated. No serious or severe adverse events or microdialysis-associated side-effects were observed. Two volunteers reported headache, not related to study drug. There were no clinically significant changes in electrocardiograms, blood pressure or pulse. Similarly, there were no clinically important findings in haematology, clinical chemistry or urinalysis.

Pharmacokinetics

The time versus concentration profiles of ertapenem in plasma (total concentration) and in the interstitial space fluid of skeletal muscle and subcutaneous adipose tissue after administration of a single intravenous dose of 1 g over 30 min to healthy volunteers (n = 6) are shown in Figure 4-1. Pharmacokinetic parameters are listed in Table 4-1.

Discussion

Bacterial skin and skin-structure infections are among the most frequently seen infectious diseases in the community and occasionally in the hospital setting (32, 71). Larger and profound lesions are usually secondarily mixed-infected with aerobic Gram-positive and Gram-negative bacteria including *Staphylococcus aureus*, Streptococcus species, Enterobacteriaceae, and anaerobic bacterial pathogens (71, 92, 96). Apart from surgical and general care measures (wound cleaning) a therapy with highly effective antimicrobial agents is indicated, because infected SSSI are often starting point of phlegmonous inflammations and in worst case also of a septic syndrome (32, 71, 92, 96). For the selection of a suitable antibiotic drug the antibacterial spectrum and the concentrations reached at the site of infection are very important (152, 188). Many studies have shown that plasma concentrations may not be an ideal parameter for the prediction of the clinical efficacy of antibiotics because most infections occur at the tissue sites. Additionally, it has been found that only free protein-unbound antibiotic concentrations at the infection sites are responsible for the antibacterial activity (136, 177). Therefore, inadequate interstitial tissue concentrations can lead to therapeutic failure and bacterial resistance (152, 188).

Due to its wide range of antibacterial activity against most Gram-positive, Gram-negative and anaerobe bacteria, ertapenem is a candidate for the treatment of skin and skin-structure infections (56, 156, 281). However, there is only limited information on the ability of ertapenem

to penetrate into different organ tissues, such as lung or pancreatic tissue (35, 273). With reference to the treatment of SSSI, one study investigated ertapenem penetration into suction-induced skin blister fluids in 12 healthy young volunteers (139). Drug concentrations in skin blister fluids exceeded 4 mg/L (the MIC at which 90% of isolates tested are eliminated) throughout the entire dosing interval of 24 hours. However, extrapolation of these data to the concentrations in infected tissues should be done with extreme caution (27). One problem is that skin blisters are formed before the administration of the antibiotic. The blister thus serves as a large third compartment with a surface-to-volume ratio, which is hardly representative of that for tissue. Besides, other variables must be taken into account, such as the barrier between the blister and the skin, which may change over time and the presence of proteins in blister fluid.

The main purpose for our study was to measure the concentrations of the non-protein-bound ertapenem in interstitial fluids of two different SSSI target sites (skeletal muscle and subcutaneous adipose tissue) by microdialysis after administration of a single intravenous standard dose (1g/day). The results show that ertapenem reaches measurable concentrations in both target tissues. As expected, time versus concentration profiles indicate that free ertapenem concentrations in interstitial space fluids were lower than the corresponding total concentrations in plasma (Figure 4-1). The tissue levels measured in our study corresponded approximately to the free protein-unbound fraction of ertapenem in plasma (4-16%). Free interstitium / total plasma concentrations ratios for skeletal muscle and subcutaneous adipose tissue were not congruent, a finding that has been observed previously and that might be explained by differences in local blood flow between the two tissues (27).

Finally, the question arises: Are the free, protein-unbound ertapenem concentrations in the interstitial space fluids of muscle and subcutaneous adipose tissue high enough to kill the

bacteria effectively? Like other β-lactam antibiotics, carbapenems exert their killing effect in a time-dependent manner (53, 231). In this category of antibacterial drugs, increasing the concentrations above 4 – 5 times the MIC of the bacteria no longer adds a proportional increase in the killing effect. Therefore, maximum killing is obtained by optimizing the time of exposure of the drug to the bacteria so that the concentrations remain above the MIC as long as possible. The main pharmacokinetic/pharmacodynamic (PK/PD) parameter for β-lactams is the proportion of time of the dose interval during which the drug concentration exceeds the MIC ($T_{>MIC}$). For carbapenems a $T_{>MIC}$ of 30 to 40% of the dose interval has been previously suggested to be effective due to their rapid bactericidal activity (186). *In vitro* studies demonstrated that ertapenem inhibited 90% (MIC_{90}) of methicillin-susceptible *Staphylococcus aureus* strains at 0.25 mg/L (91, 154). Against *Streptococcus spp.*, ertapenem had a MIC of 0.5 mg/L and against extended-spectrum β-lactamase (ESBL)-producing Enterobacteriaceae MIC_{90} values ranged from 0.03-0.06 mg/L (91, 154, 155). Ertapenem MIC_{90} values for *Bacteroides fragilis* and other anaerobe bacteria were ≤1.0 mg/L (154). In this study, protein-unbound ertapenem concentrations 12 h after a single intravenously administration of 1 g were 1.13 ± 0.68 mg/L for muscle tissue and 0.31 ± 0.16 mg/L for subcutaneous adipose tissue. Therefore, a 1 g dose once daily results in muscle tissue concentrations higher than MICs of most above-mentioned SSSI pathogens for at least 50% of the entire dosing interval. Also the mean concentrations in subcutaneous adipose tissue exceeded the time above the MIC_{90} of SSSI pathogens by at least 30% (Figure 4-1).

From this finding we can conclude, that the data obtained in this study suggest adequate free, protein-unbound ertapenem concentrations in the non infected interstitial fluid of muscle

and subcutaneous adipose tissue. Our results support the previously observed clinical efficacy of ertapenem in the treatment of skin and skin-structure infections.

Table 4-1. Non-compartmental pharmacokinetic analysis of ertapenem after 1 g single intravenous dose

Parameters	Plasma	Muscle	Subcutis
C_{max} (mg/L)	103.3 ± 26.3	6.71 ± 4.14	3.96 ± 1.63
T_{max} (h)	0.5 (NA)	2.0 (1.0 – 3.0)	1.0 (1.0 – 2.0)
C_{12} (mg/L)	7.93 ± 4.15	1.13 ± 0.68	0.31 ± 0.16
$AUC_{0\text{-last}}$ (mg·h/L)	316.1 ± 49.1	36.7 ± 23.4	17.4 ± 4.0
$AUC_{0\text{-}\infty}$ (mg·h/L)	359.7 ± 66.5	41.1 ± 26.0	19.5 ± 4.9
Terminal half-life (h)	3.77 ± 0.60	3.38 ± 0.68	3.63 ± 0.85
MRT (h)	4.58 ± 0.88	ND	ND
V_z (L)	15.5 ± 3.4	ND	ND
Cl_{tot} (L/h)	2.88 ± 0.51	ND	ND
$AUC_{interstitium}/AUC_{total\ plasma}$	-	0.13 ± 0.10	0.05 ± 0.01

Data are presented as geometric mean ± standard deviation, with the exception of T_{max}, for which median and minimum-maximum ranges are given. C_{12} = Ertapenem concentrations obtained 12 h after start of infusion.

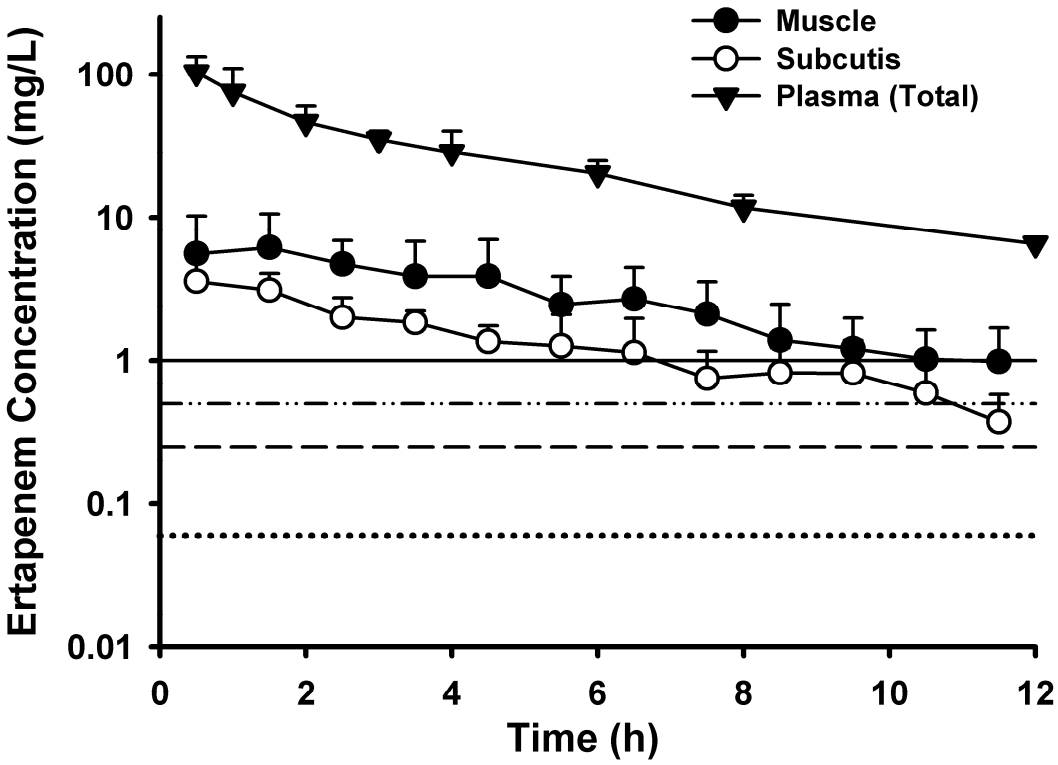

Figure 4-1. Comparison of ertapenem concentration profiles in plasma (total concentration) with unbound tissue concentrations in skeletal muscle fluid and interstitial adipose tissue fluid in healthy volunteers (n = 6) after a single intravenous dose of 1 g (infusion period 30 min). Horizontal lines indicate MIC_{90} values for *Bacteroides fragilis* (——), *Streptococcus spp.* (−···−), methicillin-susceptible *Staphylococcus aureus* (— — —), and extended-spectrum β-lactamase (ESBL)-producing Enterobacteriaceae (·····).

CHAPTER 5
INTEGRATION OF MODELING AND SIMULATION IN DEVELOPMENT OF NEW ANTI-INFECTIVE AGENTS – MIC VS. TIME-KILL CURVES[4]

Introduction

Historically, clinical pharmacology is divided into two main areas – pharmacokinetics (PK) and pharmacodynamics (PD). While PK describes what the body does to the drug, PD evaluates what the drug does to the body. In isolation, PK and PD are of limited usefulness and a mechanism-based linkage of PK and PD is essential in order to design a rational drug development plan (68, 69, 175, 176). In practice, numerous complex interactions between drug, patient and disease state can make this task quite challenging. Identification of specific, consistent and reliable biomarkers offers a solution to this challenge and is commonly employed in rational drug development (47). Once suitable biomarkers are identified, they are incorporated into PK/PD modeling and simulation approaches in order to predict clinical endpoints of new doses and dosing regimens. In the area of infectious diseases, to date, minimum inhibitory concentration (MIC) has fulfilled this role as a well-established and routinely determined PD parameter for antibiotics. According to the Clinical and Laboratory Standards Institute (CLSI, formerly National Committee for Clinical Laboratory Standards NCCLS), MIC is defined as the lowest concentration of drug that completely inhibits visible growth of the organism as detected by the unaided eye after an 18-24 hour incubation period with a standard inoculum of approximately 10^5 CFU/mL (188). MIC-based PK/PD indices such as $T_{>MIC}$, AUC/MIC and C_{max}/MIC have been introduced into anti-infective drug therapy (182, 183). Although this use of MIC combined with pharmacokinetic parameters has led to a much better understanding of antibiotic dosing, the MIC is still an imprecise threshold with several

[4] Copyright © Informa Pharmaceutical Science, [Expert Opin. Drug Discov. 2: 849-860, 2007]

limitations (e.g. inter MIC test variability, inability to account for changes in free antibiotic concentration over time) that does not allow prediction of antimicrobial activity at concentrations apart from the MIC itself (148, 216, 231).

The purpose of this review paper is to 1) evaluate MIC and MIC-based PK/PD indices, 2) introduce an alternative PK/PD modeling approach, 3) discuss strengths and weaknesses of both approaches and 4) give a perspective for future research in the field.

PK/PD Strategies for Anti-Infectives

Effect of Drug Binding

Most drugs can be bound to proteins or other biological material and hence are present in the body in bound and free form. It is a well-recognized fact that for small molecules only free drug is pharmacologically active (13, 59, 200). Therefore, for PK/PD modeling, the use of free drug is recommended and indicated by the prefix *f* in the PK input function (183). In most cases, free, unbound drug concentrations in well-perfused tissue seem to correlate well with unbound concentrations in plasma and can therefore be estimated from total plasma concentrations (59). Since alteration of the fraction unbound (fu) does not necessarily result in changes in free steady-state concentrations (45, 255), oversimplifications estimating free, unbound concentrations especially of highly bound drugs might lead to wrong conclusions. This scenario becomes even more complex in patient populations where altered physiological conditions such as liver function, uremia or hypoalbuminemia need to be taken into consideration. It has further been shown that protein binding results determined *in vitro* might need to be interpreted with care (200). Therefore, a close evaluation including metabolic and disease status is necessary. The actual measurement of free, unbound concentrations at the site of action/infection using microdialysis is an alternative way to precisely determine the PK input function.

MIC-Based PK/PD Indices

MIC-based indices are intended to normalize the drug exposure (PK) to the respective sensitivity (MIC). The first PK/PD index was developed for penicillins where *in vivo* antimicrobial efficacy was correlated to the time free or total drug levels stay above the MIC ($fT_{>MIC}$ or $T_{>MIC}$, respectively) of the target organism. Other commonly used indices are the free or total maximum plasma concentration over MIC ratio (fC_{max}/MIC or C_{max}/MIC) and free or total area under 24 hour plasma concentration time curve over MIC ratio ($fAUC_{24}$/MIC or AUC_{24}/MIC) (147, 183, 225). Although some authors suggest a further index differentiation within the drug class (6, 52, 272), $fT_{>MIC} \geq 40\%$ of the dosing interval seems to be sufficient for clinical efficacy of β-lactam antibiotics (49-51, 90, 167, 170, 237). In comparison, C_{max}/MIC values of 10-12 seem to be a good predictor for aminoglycosides (125, 180, 223, 256). For fluoroquinolones, AUC_{24}/MIC or C_{max}/MIC ratios seem to be the best index (8, 113, 201, 205, 223, 272). Target AUC_{24}/MIC values of 100-125 have been identified for gram-negative bacteria (39, 49, 89, 252), 25-35 for gram-positives pathogens (49) and C_{max}/MIC values of 10 (205). The magnitude of the fluoroquinolone PK/PD index needed is still controversially discussed and seems to vary with type of infection, fluoroquinolone, pathogen, immune status and degree of protein binding (6, 205). At this point, we strongly agree with other authors stating that only free, unbound and pharmacologically active fraction should be used and appropriately marked to calculate respective PK/PD indices (4, 183, 272).

Based on these MIC-based PK/PD indices dosing, regimens can be optimized to ensure efficacy and minimize the emergence of resistance. This becomes particularly important in special patient populations, such as neonates or elderly, where there is a lack of sufficient data on the efficacy of dosing regimens (62). In drug development, the good correlation of clinical

outcome with $fT_{>MIC}$, fC_{max}/MIC and fAUC/MIC makes them a valuable predictor for the efficacy of new drugs or dosing regimens. For example, treatment of drug-resistant pulmonary tuberculosis (TB) with ofloxacin 10mg/kg QD was successfully suggested to be sufficient based on determined fC_{max}/MIC ratios (7.7-15.4) and a long β half-life (46).

However, relationships based on MICs suffer from numerous drawbacks. While antibacterial activity is a dynamic process, MIC is a crude mono-dimensional threshold value that shows a high variability due to its determination (202). Depending on the method used (E-test, Kirby Bauer test, broth/agar dilution method, etc.), results can vary dramatically. As a consequence, MICs are often reported as a range of concentrations instead of a single value. Consequently, MIC-based indices and predictions are highly variable as well. Hence, it was suggested that for any calculation or expression of the MIC a description of the method by which the MIC was determined should be mentioned (182, 183). At present, regulatory authorities are also working on global standardization of MIC methods (183).

Time-Kill Curve-Based PK/PD Indices

To overcome limitations of the MIC, subsequent sampling of bacterial counts *in vitro* or in animals can be used to provide a time course of antimicrobial action (time-kill curve). In general, there are two different types of time-kill curves, based on constant concentrations, or on fluctuating concentrations (dynamic models) (226, 230, 231). The constant concentration model simulates the steady-state concentration obtained *in vivo* after constant rate infusion. In this approach a set of culture flasks containing bacteria and nutrient are exposed to different antibiotic concentrations, usually multiples of the MIC, for a certain incubation time. Samples are taken at preset time points and plated on appropriate agar plates. Bacterial counts are taken and then plotted as CFU/mL against time.

Dynamic models try to reflect the change in drug concentration that occurs *in vivo* (Figure 5-1) (164). In order to simulate the half-life, drug- containing medium is removed from the flask and replaced by fresh medium. This can either be done manually using syringes or automatically by employing pumps. Microfilters (0.2μm) placed between flask- and pump system prevent the bacteria from washout. Additional flasks can be used to simulate a multi-compartment scenario. This ability to mimic the PK of a drug for one- and multi-compartment-body models makes the dynamic model a very powerful PK/PD prediction tool (231). Detailed descriptions of the experimental setting of these models and their applications can be found elsewhere (164, 188, 198, 206). Once the time-kill curve experiments are performed, a mathematical model can be identified to describe the data. Before discussing these models in greater detail, a general concept of how they link PK and PD together is provided in the following section.

The rationale for PK/PD-modeling is to link PK and PD in order to establish and evaluate dose-concentration-response relationships and subsequently describe and predict the effect-time courses resulting from certain doses (69, 175). Keeping in mind that "all models are wrong, but some are useful", PK/PD models represent a simplification of the real physiological process (22). They can either be purely descriptive, regardless of the actual mechanism of action, or they can be mechanism-based appreciating the underlying physiological events (69). In any case, PD effects can either be directly correlated to plasma concentrations (direct link model) or show a time delay (indirect link model). Plotting effect vs. plasma concentration results in a single curve for direct link or a hysteresis loop for indirect link models, respectively (38). Definition of a hypothetical effect-compartment (Figure 5-2) offers an elegant solution for this problem and leads to a collapse of the hysteresis loop in the concentration-effect relationship (69, 109, 110). Hence, either the measured or calculated free plasma concentration (direct link model) or free

concentration in the effect compartment fC_e (indirect link model) serves as the PK input function. This PK input function is then combined with an appropriate PD model. However, drug interacting with its target at the effect site may not necessarily result in a "direct response". Whenever, the mechanism of action involves a time-dependent physiological process (e.g. the down-regulation or synthesis of receptors or transporters), the response will occur with a certain time delay. In such cases, indirect response models are fitted to the data accounting for the temporal dissociation between concentration- and effect-time courses.

Pharmacodynamic Models

To appropriately describe effects over time relationships, different PK/PD models have been established (67). Of those, E_{max}- and sigmoidal E_{max}-models are most commonly used in PK/PD modeling. Especially modified sigmoidal E_{max}-models have found great acceptance in describing PK/PD of antibiotics. An example is shown in equation 5-1

$$\frac{dN}{dt} = \left(k_0 - \frac{k_{max} \times fC_e^h}{EC_{50}^h + fC_e^h} \right) \times N \qquad (5\text{-}1)$$

where dN/dt represents the change in number of viable bacteria, usually given as colony forming units per millilitre (CFU/mL) over time (188, 258). Growth in the absence of antibiotic is characterized by the bacterial growth rate constant (k_0) reflecting the rate of multiplication of a given pathogen in its surrounding environment. However, in the presence of antibiotic, bacterial kill can be described by an E_{max}-model with the maximum killing rate constant (k_{max}), the free concentration of antibiotic necessary to produce 50% of the maximum effect (EC_{50}) and the free concentration of antibiotic in the effect compartment (fC_e) at any time (t). The general curve fit can be further optimized with a Hill or shape factor h that modifies the steepness of the curve. A delayed onset in growth and/or kill might make the addition of further factors necessary (258).

A brief outline of the mathematical relationships underlying time-kill curve modeling was provided by Mueller et al. and is illustrated in the following scenario (188). Starting out with an initial inoculum N_0 of $5x10^5$CFU/mL, a hypothetical bacterial strain X grows in the absence of antibiotic ($fC_e = 0$) with k_0. Plotting the number of bacteria at time t (N_t) vs. time on a semi-log scale results in a straight line with a growth rate of k_0 as the slope as shown in equation 5-2 and Figure 5-3.

$$\text{slope} = \frac{\ln N_t - \ln N_0}{t} = k_0 \qquad (5\text{-}2)$$

However, it should be noted that Figure 5-3 shows ideal growth behavior. In practice, the *in vitro* exponential growth phase is limited by nutritional and environmental constrains resulting in slower growth rates that can be modelled by additional parameters (258). These factors are dependent on strain(s), antibiotic(s) and experimental conditions used (172, 194, 258, 264). For didactic reasons, these factors were not included in the simulations presented in Figure 5-3.

Addition of an antibiotic A to the inoculum results in a diminished net-growth. From a certain drug-specific fC_e, a maximum effect will be reached, where a further increase in fC_e does not contribute to the antimicrobial efficacy any longer. Solving equation 5-1 for $fC_e >> EC_{50}$ leads to equation 5-3.

$$\frac{dN}{dt} = \left(k_0 - \frac{k_{max} \times fC_e^h}{fC_e^h} \right) \times N \qquad (5\text{-}3)$$

At such high antibiotic concentrations the antimicrobial effect is not dependent on fC_e any longer. The slope of this "maximum effect curve" is defined by equation 5-4 as the difference of k_0 and k_{max} (Figure 5-3).

$$\frac{dN}{dt} = (k_0 - k_{max}) \times N \tag{5-4}$$

Since EC_{50} is defined as the concentration of antibiotic necessary to produce 50% of the maximum effect k_{max}, it can be illustrated as the bisecting line of the angle formed by growth control (zero effect) and maximum kill effect as shown in Figure 5-3. A general statement whether the EC_{50} is equal to, smaller or bigger than the MIC cannot be made. A special case occurs when antibiotic induced kill equals growth and so the number of bacteria stays constant resulting in a horizontal line. The respective concentration of antibiotic in this scenario is referred to as stationary concentration (SC) (187). It can be calculated using equation 5-5 and is different than the MIC.

$$SC = \left[\frac{k_0}{k_{max} - k_0} \right]^{\frac{1}{h}} \times EC_{50} \tag{5-5}$$

However, to date, MIC is more commonly used as a pharmacodynamic measure than SC. Being defined as the lowest concentration of drug that completely inhibits visible growth of the organism as detected by the unaided eye after an 18-24 hour incubation period, the MIC value is linked to a turbidity threshold. This threshold is reached for most bacteria at concentrations of approximately 10^7 CFU/mL (Figure 5-3) (188, 202). Substitution of fC_e by the MIC in equation 5-1 leads to equation 5-6.

$$\frac{dN}{dt} = \left(k_0 - \frac{k_{max} \times MIC^h}{EC_{50}^h + MIC^h} \right) \times N \tag{5-6}$$

Rearranging and integration of equation 5-6 on both sides results in equation 5-7.

$$\int_{N_0}^{N_t} \frac{1}{N} \times dN = \int_{0}^{t} \left(k_0 - \frac{k_{max} \times MIC^h}{EC_{50}^h + MIC^h} \right) \times dt \tag{5-7}$$

As shown in Figure 5-3, the MIC turbidity limit is reached after an incubation time t of 18 hours. Solving the integral in equation 5-7 with a lower limit N_0 of $5.5x10^5$CFU/mL and an upper limit N_{MIC} of 10^7CFU/mL leads to equation 5-8.

$$\frac{\ln N_{MIC} - \ln N_0}{t} = k_0 - \frac{k_{max} \times MIC^h}{EC_{50}^h + MIC^h} \tag{5-8}$$

Rearranging for the MIC leads to equation 5-9.

$$MIC = \left[\frac{k_0 - \frac{1}{t} \ln \frac{N_{MIC}}{N_0}}{k_{max} - \left(k_0 - \frac{1}{t} \ln \frac{N_{MIC}}{N_0} \right)} \right]^{\frac{1}{h}} \times EC_{50} \tag{5-9}$$

Considering that the concentration of antibiotic remains constant throughout the entire MIC experiment, k_{max}, EC_{50} and h remain the only variables in equation 5-9. Since k_0 is a constant for a given strain X in a given medium as well, k_0, N_0, N_{MIC} and t can be combined to a drug independent constant d as shown in equation 5-10 (188).

$$MIC = \left(\frac{d}{k_{max} - d} \right)^{\frac{1}{h}} \times EC_{50} \tag{5-10}$$

The resulting MIC equation has three unknowns and hence it cannot unambiguously describe the effect-time course for a given antibiotic concentration. Consequently, k_{max}, EC_{50} and h have to be determined separately to clearly specify the antimicrobial properties of a drug

against a certain pathogen. Equation 5-10 clearly illustrates that the same MIC value can be a product of different combinations of k_{max}, EC_{50} and h.

Once these relationships have been evaluated and validated, time-kill curve based indices can be used to compare different doses, dosing regimens or dosage forms. The suitability of a new ciprofloxacin extended-release dosage form (1000mg, QD) was compared to the outcome of the standard dose (500mg, BID) (230). Ciprofloxacin PK parameters were determined from mean serum concentrations (N=19) using non-compartmental and compartmental data analysis and linked to PD parameters determined from *in vitro* time-kill curve experiments against *E. coli*. Comparison of expected kill curves with the immediate-release versus extended-release treatments showed similar outcome. Therefore, a once daily dosing regimen was suggested, due to its similar efficacy but superior patient compliance compared to traditional immediate release.

PK/PD Simulations

Monte Carlo simulation

Both MIC and time-kill curve parameter do not account for variability in either patient or bacterial population. Instead, mean values or concentration ranges are evaluated. One approach to incorporate variability among clinical PK and PD is using Monte Carlo simulation (MCS) as an advanced statistical modeling tool. MCS allows prediction of therapeutic outcome based on an integrated PK/PD stochastic model for a drug or dosing regimen (2, 197). The first step in a MCS is to estimate mean PK parameters and their associated variability for a desired patient population and dosing regimen. This can be done by using analysis tools such as population pharmacokinetics (POPPK) (231). From this multivariate distribution data pool, values are randomly picked and a PK profile is simulated. This random selection process is repeated multiple (e.g. 5,000) times and respective PK profiles for these hypothetical patients are obtained (159). Together, they give a range of possible PK profiles. This information can now be used to

estimate the probability with which a predefined PK/PD index (e.g. $fT_{>MIC}$ = 40%) is reached for that particular MIC. Whether this target is attained for a range of MICs can be calculated by summing up the products of frequency of specific MIC values and their respective probability of target attainment (159). This ability of predicting the likelihood of a certain outcome to occur has been used by numerous investigators to optimise dosing of drugs or drug combinations in both pre- and post-marketing studies (137, 159, 184, 231). This approach has also been applied to compare potencies of different drugs, determine susceptibility break points for initial human trials and help selecting drugs (5), doses and dosing regimens (65, 77, 138, 160) in healthy, renal impaired (248) and elderly patient populations (3, 160, 203).

In a recent study, PK modeling and MCS (10,000 subjects) were performed to describe the PD profile of cefepime in plasma and cerebrospinal fluid (CSF) (158). PK data of 7 hospitalised patients with external ventricular drains was used for MCS in order to estimate the probability of attaining targets of $f\text{cefepime}_{plasma}$ (20% plasma protein binding) and total cefepime_{CSF} of 50 to 100%$T_{>MIC}$ for MICs of 0.06-8mg/L. Calculations were performed for short-term infusions (0.5 hours) of 2g cefepime TID and BID or QD plus continuous infusion (250mg/h). Results indicate that in plasma, targets attainment rates of $fT_{>MIC}$ 60-70% were high at each MIC (0.03-8mg/L) for all dosing regimens examined. However, at MICs > 0.5mg/L, indices of $T_{>MIC}$ 50-100% were not reached for more than 80% of the patients. As shown, MCS is an important simulation tool employed in the establishment of new dosing regimens.

To date, most MCS are performed using MIC rather than model based PK/PD indices as the therapeutic target. Since the MIC is not an intrinsic property of a microorganism, its use as a single point estimate oversimplifies the dynamic process of growth and natural or antibiotic

induced kill (187, 226). In future approaches the use of time-kill parameters in MCS approaches might provide more detailed information than the MIC.

Time-kill curve based simulations

The relationships derived in the previous sections are not only of theoretical interest but can also be used to simulate clinical outcome. In the following it will be shown that time-kill curve based indices provide more reliable information than MIC based indices.

Simulations were performed for the β-lactam antibiotics faropenem and ceftriaxone for a TID and BID dosing regimen, respectively. It has been shown for β-lactams that the free antibiotic concentration has to exceed the MIC for at least 40% of the dosing interval in order to be clinically effective. Maximal efficacy for cephalosporins in several animal infection models was shown for Enterobacteriaceae and Streptococci when $fT_{>MIC}$ in serum exceeded 60%-70% of the dosing interval (51). Therefore, breakpoint values of $fT_{>MIC}$ = 40% and $fT_{>MIC}$ = 67% (2/3 of the dosing interval) have been chosen for our simulation. Intravenous doses necessary to maintain steady state concentrations above these breakpoints were calculated from PK data given in the literature, using a one-compartment body model with a first order elimination rate constant k_e and correcting for plasma protein binding (130, 244). Mean plasma protein binding for ceftriaxone and faropenem was assumed to be 90% (211, 212) and 96% (20), respectively. Respective PD parameters of *Streptococcus pneumoniae* CDC 145, *Streptococcus pneumoniae* ATCC 6303 and *Haemophilus influenzae* ATCC 10211 were determined and are listed in Table 5-1 (129, 130, 153).

In the first scenario (A), kill-curves of faropenem against *Haemophilus influenzae* ATCC 10211 and ceftriaxone against *Streptococcus pneumoniae* CDC 145 were simulated and the outcomes were compared. For $fT_{>MIC}$ = 40%, failure in antimicrobial treatment is predicted for both drugs (Figure 5-4 A). In comparison, treatment with faropenem is able to reduce the

number of *H. influenzae* by ~ 3 log steps (Figure 5-4 B), while treatment with ceftriaxone still remained ineffective against *S. pneumoniae* for $fT_{>MIC}$ = 67%. Faropenem given TID appeared to be more effective against *H. influenzae* ATCC 10211 than ceftriaxone given BID against *S. pneumoniae* CDC 145. However, a direct comparison of both dosing regimens is rather difficult, since *S. pneumoniae CDC 145* and *H. influenzae* ATCC 10211 show different growth rates (equation 5-9, Table 5-1).

Hence, a second set of simulations (B) was performed evaluating the antimicrobial potency of faropenem (TID) and ceftriaxone (BID) against *S. pneumoniae* ATCC 6303 for $fT_{>MIC}$ = 40% and $fT_{>MIC}$ = 67%, respectively. Simultaneous simulations of scenario B predicted a failure of the treatment with ceftriaxone for both dosing regimens (Figure 5-4 C and 5-4 D). The $fT_{>MIC}$ = 40% dosing regimen is predicted to be ineffective for faropenem, while total eradication of *S. pneumoniae* ATCC 6303 is predicted after 36 hours, adjusting for $fT_{>MIC}$ = 67% (Figure 5-4 D). Based on $fT_{>MIC}$ = 40%, a false positive treatment outcome is predicted for both treatment regimens.

Discussion and Conclusion

In comparison to the single endpoint MIC, modelled time-kill curve parameters provide more detailed information. These parameters describe the antimicrobial effect over time. This additional information can then be further used to optimise the dosing regimen. However, time-kill curve analysis is a very labour intensive method. Due to the fact that quite a large number of time-kill curves are necessary to allow sufficient evaluation of concentration- and time-effect relationships, time and manpower are limiting factors. Considering the current speed of technical development, these limitations are likely to be counterbalanced by improved experimental analysis techniques and automation in the future.

Since MIC and time-kill curves are performed *in vitro*, both have limitations with respect to their predictability of *in vivo* situations. Conditions simulated *in vitro* are much less complex than the actual *in vivo* situation. Drug can be bound to proteins, growth-rates might be altered in human fluids and infection is usually affected by the immune system. *In vivo* protein binding and altered growth can be simulated by performing time-kill curves in human serum or animal experiments (75). In many cases, the immune system of the test animal has to be knocked out in order to facilitate an infection. However, a complete suppression of the host defense may only apply to a special patient population undergoing chemotherapy (e.g. HIV, cancer, transplants). Therefore, an extrapolation of results determined *in vitro* to *in vivo* can lead to an overestimation of the antibiotic effect (231). Although these experiments cannot fully reflect the situation in humans, valuable data can be generated for the development of dosing regimens and therefore have become inexpensive alternatives to clinical trials (143, 268). However, the above discussion assumes a homogenous population of bacteria with a single MIC or EC_{50}, respectively. In reality this is rarely the case and more complex approaches are needed to adequately evaluate these situations (37, 75, 146, 230).

Based on data from *in vitro*, animal experiments and clinical trials, mathematical models can be developed that provide insight into the population dynamics underlying the emergence of antimicrobial resistance. Models accurately predicting the outcome of antimicrobial therapy can then be used to evaluate different dosing regimens that are able to prevent resistance development (37, 100). While emergence of resistance is indicated by increasing MIC values, only with continuous sampling over time, distinct evaluation of resistance development can be assessed. However, models needed to describe these resistance scenarios can become fairly complex and much more work needs to be done to develop and validate new time-kill curve

based resistance models. Once these models have been established and validated, much more information can be extracted from them than from MIC indices (230).

In conclusion, both MIC and time-kill curve approaches have limitations but their introductions into antimicrobial therapy were milestones in making educated dose recommendations compared to previous empirical treatment of most likely disease causing pathogens.

Table 5-1. Pharmacokinetic and pharmacodynamic parameters for ceftriaxone and faropenem used for the simulations.

Parameter	Scenario A Faropenem versus *H. influenzae* ATCC 10211	Ceftriaxone versus *S. pneumoniae* CDC 145	Scenario B Faropenem versus *S. pneumoniae* ATCC 6303	Ceftriaxone versus *S. pneumoniae* ATCC 6303
MIC determined (mg/L)	0.5	0.64-1.28	0.01-0.02	0.01-0.02
MIC calculated (mg/L)	0.42	1.09	0.01	0.018
Dosing interval (h)	8	12	8	12
V_d (L)	15.9	7	15.9	7
k_e (h^{-1})	0.693	0.087	0.693	0.087
f_u in plasma	0.04	0.1	0.04	0.1
k_0 (h^{-1})	0.98	1.44	1.67	1.5
k_{max} (h^{-1})	1.79	2.47	3	2.6
EC_{50} (mg/L)	0.5	1.063	3	2.6
h	1	2.5	1	2.5

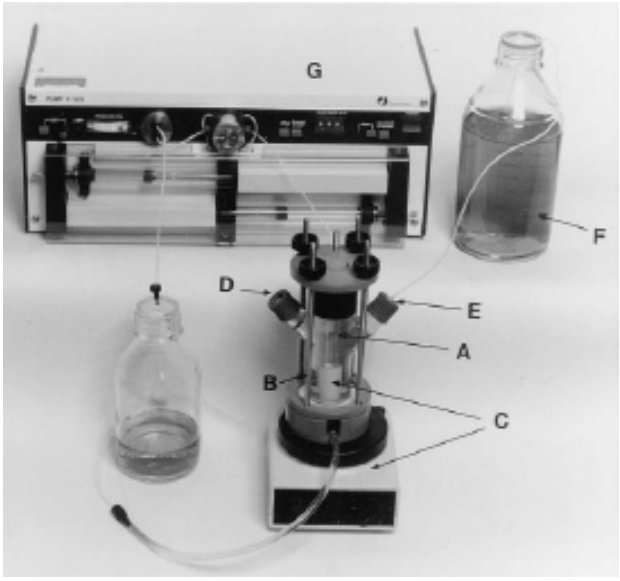

Figure 5-1. Design of *in vitro* model. (A) Culture vessel; (B) construction to clamp the upper and bottom part together; (C) magnetic stirrer; (D) side arm for sampling; (E) side arm for supplying fresh medium; (F) vessel containing fresh medium; (G) pump.

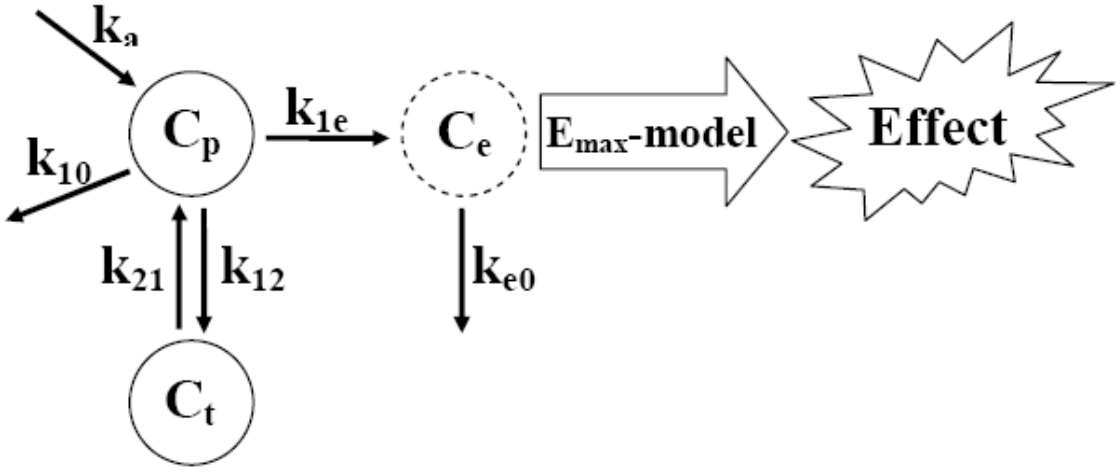

Figure 5-2. Two-compartment body model with additional effect compartment

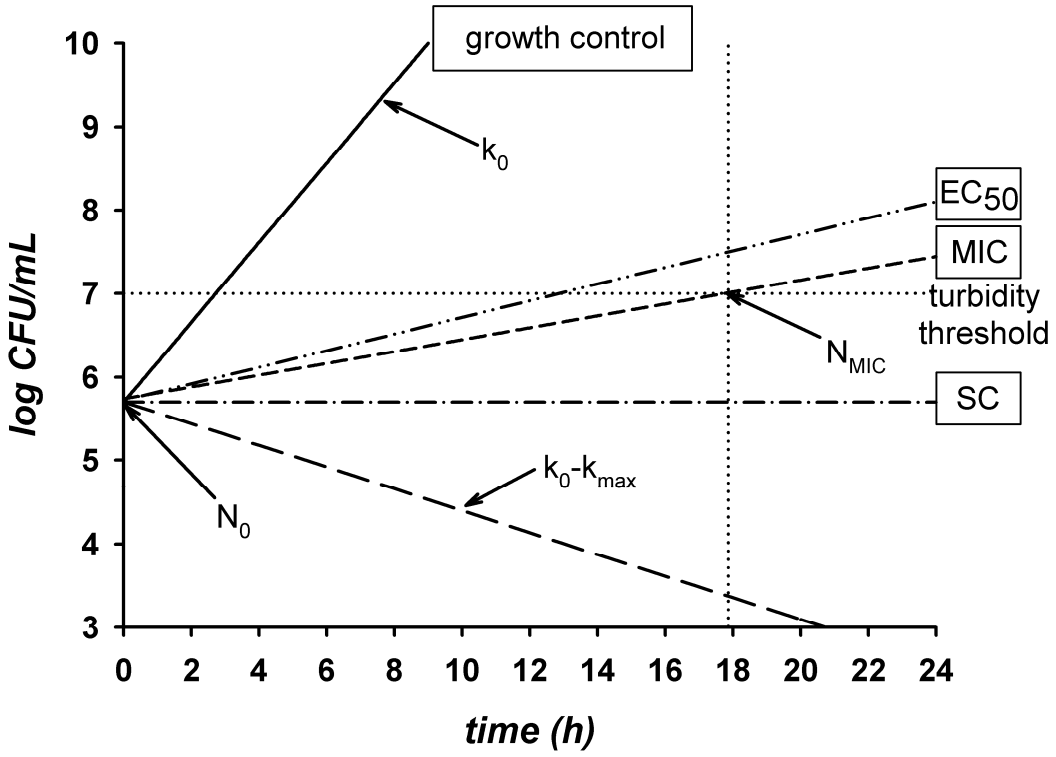

Figure 5-3. Growth/kill curves at different drug concentrations to illustrate k_0, kmax, EC_{50}, MIC and SC relationship

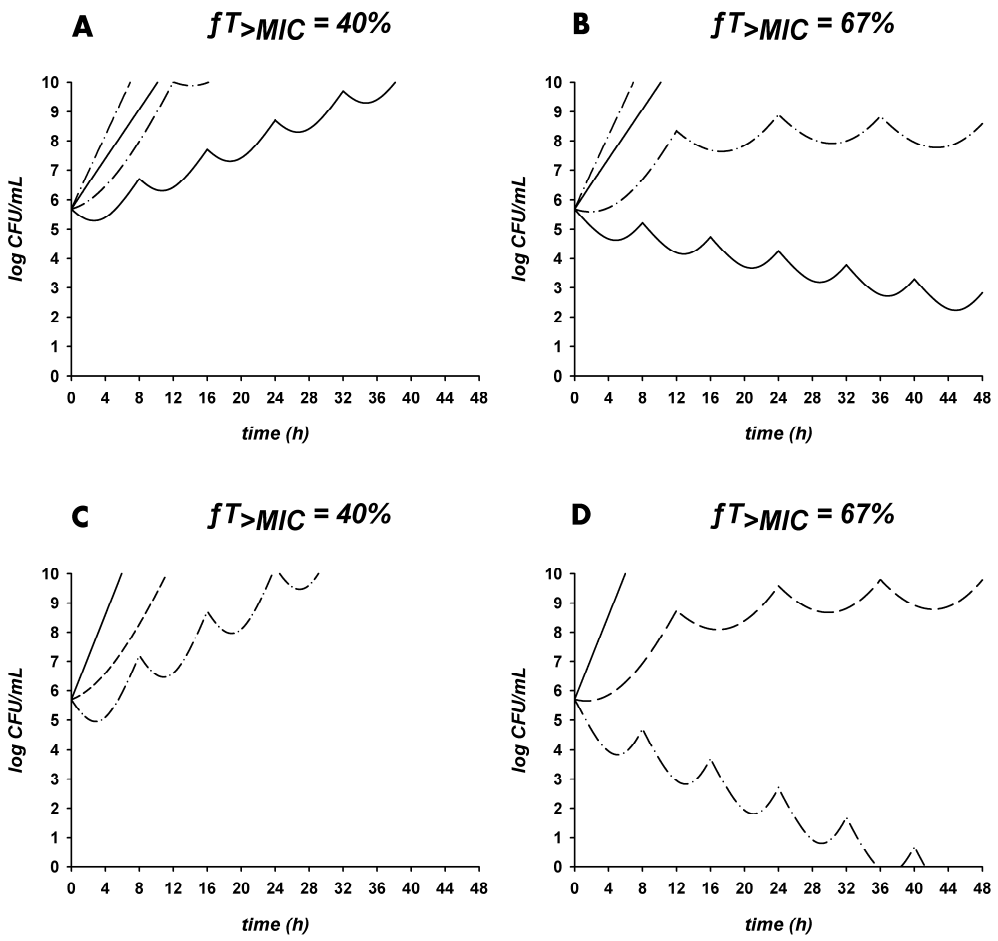

Figure 5-4. Simulated time-kill curves and respective growth controls of faropenem against *Haemophilus influenzae* ATCC10211 (solid line) and ceftriaxone against *Streptococcus pneumoniae* CDC145 (dotted line). For the therapeutic target A) $T_{>MIC}$ = 40% and B) $T_{>MIC}$ = 67%, as well as, faropenem (dash-dotted line) and ceftriaxone against *Streptococcus pneumoniae* for the therapeutic target C) $T_{>MIC}$ = 40% and D) $T_{>MIC}$ = 67% compared to growth control (solid line).

CHAPTER 6
PHARMACOKINETIC/PHARMACODYNAMIC MODELING OF THE *IN VITRO* ACTIVITY OF OXAZOLIDINONE ANTIBIOTICS AGAINST METHICILLIN-RESISTANT *STAPHYLOCOCCUS AUREUS*[5]

Introduction

Gram-positive pathogens are a major cause of a wide range of infections, including skin and skin structure infections (SSSI) and life-threatening infections like bacteremia, endocartitis and pneumonia (163, 227). Treatment of these infections has become increasingly challenging due to the rapid development of resistance against "first choice" antibiotics. In many cases, physicians are left with no other choice than using highly potent "last resort" antibiotics, such as vancomycin, on a daily basis. However, with the appearance of vancomycin-resistant strains, for example vancomycin-resistant *Staphylococcus aureus* (VRSA) or vancomycin-resistant enterococci (VRE), the once powerful antibiotic arsenal has become ineffective (42, 124). Therefore, it is critically important to develop new potent antibiotics or antibiotic classes to successfully treat these infections.

In 2000 the FDA approved with linezolid the first representative of a novel class of antibiotics, the oxazolidinones. At the time of approval, linezolid was one of the few agents that showed activity against vancomycin-resistant strains (40, 72). However, resistances against linezolid have been reported as early as 2002 (104, 259). In addition, toxic side effects such as reversible thrombocytopenia, neutropenia or rarely neuropathy have occurred during prolonged use (43, 149, 239). Due to these limitations there is a definite opportunity to develop new oxazolidinones with improved pharmacokinetic/pharmacodynamic (PK/PD) properties. RWJ-416457 is a new investigational oxazolidinone that is being developed as both an oral and an intravenous formulation for the treatment of infections caused by clinically important Gram-

[5] Manuscript under submission with Antimicrob Agents Chemother.

positive bacteria. Compared to linezolid, RWJ-416457 has a Minimum Inhibitory Concentration (MIC) that is two- to four-fold higher antimicrobial activity against multidrug resistant Gram-positive pathogenic bacteria, including methicillin-resistant *Staphylococcus aureus* (MRSA), vancomycin-intermediate susceptible *Staphylococcus aureus* (VISA), VRSA, VRE, and penicillin-resistant streptococci (87, 157). Although the MIC is routinely determined in clinical settings and has contributed much to the understanding of antibiotic dosing, it does not provide any information on the time course of bacterial growth or antibiotic-induced kill (188, 231). More detailed information can be obtained from the evaluation of growth and kill profiles over time (time-kill curve). A major strength of the time-kill curve approach is its capability of simulating the effect of changing concentrations on the antimicrobial outcome. Changing concentration time-kill curves can, subsequently, be used to evaluate the efficacy of antibiotics with different half-lives ($t_{1/2}$). Once these experiments have been performed, a mathematical model can be simultaneously fitted to the data and respective PD parameters calculated. These PD parameters can then be linked to *in vivo* PK information to predict clinical outcome.

The aim of this study was to 1) establish a general mathematical model that is appropriate for characterizing the *in vitro* PD of oxazolidinones determined in constant, as well as, changing concentration time-kill curve experiments and 2) to apply this model in order to compare the *in vitro* potencies of investigational RWJ-416457 ($t_{1/2}$ ~ 24h) and first-in-class representative, linezolid ($t_{1/2}$ ~ 5h).

Material and Methods

Antibiotics and Growth Media

RWJ-416457 and linezolid were provided by Johnson & Johnson Pharmaceutical Research & Development L.L.C. (Raritan, NJ, USA). Compounds were stored at 4^{o}C in the original opaque vials. RWJ-416457 and linezolid stocks were prepared fresh daily prior to use, kept at

room temperature and diluted to the desired concentrations with Mueller-Hinton broth (MHB; DIFCO, Lawrence, KS, USA). MHB was prepared according to the manufacturer's manual and autoclaved prior to use at 121^{o}C (15 min per 1L).

Organisms

MRSA OC2878 was obtained from Johnson & Johnson Pharmaceutical Research & Development L.L.C. (Raritan, NJ, USA). To ensure purity of the MRSA strain, colonies were plated on 5% sheep blood agar plates (Remel Microbiology Products, Lenexa, KS, USA) at least three times from overnight cultures before usage.

Bacterial inocula for MIC and time-kill curve experiments were prepared in sterile saline solution and adjusted with MHB to a final concentration of approximately 5x10^{5} colony forming units per milliliter (CFU/mL).

MIC Determination

MIC values of RWJ-416457 and linezolid against MRSA OC2878 were determined in 24-well plates (Corning Inc., NY, USA) using a modified Macrodilution Broth method (258). The first dilution where no visual turbidity appeared after a 20-hour incubation period was determined to be the MIC. The procedure was repeated six times per bacterial strain and antibiotic. Positive controls (with bacteria, no drug) and negative controls (no bacteria, no drug) were run simultaneously in order to assess the method.

Constant Concentration Time-Kill Curves

An *in vitro* model was used to investigate the effect of constant RWJ-416457 and linezolid concentrations on MRSA OC2878. This *in vitro* model consisted of eight 50mL cell culture flasks (Nunc^{TM}, Nunc A/S, Roskilde, Denmark). Flasks were filled with 20mL MRSA OC2878-containing MHB (~5 x 10^{5} CFU/mL) and incubated for two hours before adding the antibiotic. Selection of the RWJ-416457 and linezolid concentration range tested was based on their

respective MIC values and included minimum antimicrobial activity (0.25xMIC, 0.5xMIC, 1xMIC), efficient bacterial killing (2xMIC, 4xMIC), as well as, maximum kill effect (8xMIC, 16xMIC) (258). In addition, a growth control (no antibiotic) was also run simultaneously. Culture flasks were incubated and bacterial counts were subsequently determined at predefined time points for up to 24 hours. Samples (20µL) were taken directly out of the flasks, diluted in ten-fold increments and plated onto 5% sheep blood agar plates using an adopted droplet-plate method (258). Bacterial counts were determined on all countable plates (limit of bacterial quantification 15-200 CFUs) after a 20-hour incubation period. All constant concentration time-kill curve experiments were run in triplicate on separate occasions.

Changing Concentration Time-Kill Curves

An *in vitro* syringe model was used to study the effect of changing antibiotic concentrations on MRSA OC2878. This dynamic *in vitro* model was based on that used in the constant concentration experiment and consisted of eight cell culture flasks, each equipped with an additional syringe system. These syringe systems allowed simulating the human half-lives of RWJ-416457 (~24h) and linezolid (~5h) (95, 127) by subsequent replacement of antibiotic-containing MHB with fresh, antibiotic-free medium. To avoid dilution of the bacterial inoculum during the removal/replacement process, sterile filters (0.22µm, Millipore, Billerica, MA, USA) were placed between flasks and syringes. Prior to the start of the experiment, flasks were filled with 20mL MHB and incubated overnight to test for contamination. At the day of the experiment, flasks were spiked with MRSA OC2878 (~$5x10^5$ CFU/mL) and incubated for 2 hours before adding the respective antibiotic. Initial RWJ-416457 and linezolid concentrations in the changing concentration experiment were similar to those employed in the constant concentration time-kill curve and ranged from 0.25 to 16xMIC. The antibiotic inoculum was diluted during the 24-hour time course of the experiment by replacing 2.2mL RWJ-416457-

containing MHB every 4 hours or 4.8mL linezolid-containing MHB every 2 hours with fresh antibiotic-free medium. Samples were taken directly out of the flasks, diluted with sterile saline solution and plated onto 5% sheep blood agar plates using an adopted droplet-plate method (258). Bacterial counts were determined on all countable plates (limit of bacterial quantification 15-200 CFUs) after a 20-hour incubation period. All changing concentration time-kill curve experiments were run in triplicate.

Drug Stability

To ensure stability of RWJ-416457 and linezolid during the 24-hour time course of the experiment, samples (500μL) were taken every 8 hours directly out of the flask containing the highest antibiotic concentration (16xMIC) and immediately frozen at minus 80^{o}C. Samples were analyzed by a validated high-performance liquid chromatographic-quadrupole mass spectrometric (LC-MS/MS) method.

Mathematical Modeling

A susceptibility-based two-compartment model (Figure 6-1) was used to characterize the constant, as well as, changing concentration time-kill curve data of both RWJ-416457 and linezolid. In this model, the overall change in the experimentally determined total number of bacteria (N) was defined as the sum of bacteria susceptible to antibiotic (N_S) and insusceptible persister cells (N_P) as shown in equation 6-1.

$$N = N_S + N_P \tag{6-1}$$

Bacteria from both susceptibility stages can transform into each other with the transformation-rate constants k_{sp} (h^{-1}) and k_{ps} (h^{-1}), respectively, as shown in Figure 6-1. The initial fraction of bacteria in the susceptible or persister stage, respectively, was defined as F ($0<F<1$).

The change in number of susceptible bacteria over time dN_S/dt could be sufficiently described by equation 6-2,

$$\frac{dN_S}{dt} = \left(k_S \times \left(1 - \frac{N_s}{N_{max}} \right) \times \left(1 - e^{-dg \times t} \right) - \frac{k_{max} \times C}{EC_{50} + C} \times \left(1 - e^{-dk \times t} \right) - k_{SP} - k_d \right) \times N_S + k_{PS} \times N_P \qquad (6\text{-}2)$$

where k_S (h^{-1}) characterizes the growth-rate constant, k_d (h^{-1}) the natural death-rate constant, N_{max} (CFU/mL) the maximum number of bacteria, d_{gs} (h^{-1}) the delay in the onset of growth, k_{max} (h^{-1}) the maximum kill-rate constant, C (mg/mL) the antibiotic concentration, EC_{50} (mg/mL) the concentration necessary to produce 50% of the maximum effect and d_{ks} (h^{-1}) the delay in the onset of kill.

In comparison, the change in persister cells over time dN_P/dt could be described as a function of susceptible cells entering the persister stage, as well as, persistent bacteria re-entering the susceptible stage and natural death of bacteria in the persister stage (equation 6-3).

$$\frac{dN_P}{dt} = k_{SP} \times N_S - k_{PS} \times N_P - k_d \times N_P \qquad (6\text{-}3)$$

Data Analysis

This susceptibility-based two-compartment model was simultaneously fitted to the log transformed data of the constant, as well as, changing concentration time-kill curve experiments using a first-order conditional estimation (FOCE) method algorithm as implemented in NONMEM® 6 (Globomax, Hanover, MD, USA, ADVAN6). Between-experiment variability was estimated on the model parameters using exponential error models. The residual variability, which includes the within experimental variability and model mis-specification, was estimated using a log error model.

EC_{50} comparisons were performed using a two-sided, two-sample T-test. A *P* value of < 0.05 was considered statistically significant.

Model Validation

Evaluation of the model performance included diagnostic plots, Akaike information criterion (AIC), precision of the parameter estimates, as well as, visual inspection for the quality of fit. The robustness of the final model was assessed in Wings for NONMEM 6 by a nonparametric bootstrap. In the nonparametric bootstrap procedure, bacterial samples corresponding to one strain and concentration were sampled 1000 times with replacement from the original data set in order to obtain a new data set containing the same number of samples. The final model was fit individually to each of these new data sets and all population model parameters were estimated. Results from the successful runs were determined and median bootstrapped parameter values (including a 90% bootstrap confidence interval) were compared to the final model predicted parameter estimates (80).

Results

MIC

Using a modified Macrodilution broth method, a two-fold difference in MIC values (modes) against MRSA OC2878 was determined for RWJ-416457 (0.5μg/mL) and linezolid (1.0μg/mL), respectively.

Constant Concentration Time-Kill Curves

Constant concentration time-kill profiles of both RWJ-416457 and linezolid are shown in Figure 6-2A. After an initial lag phase of about 2 hours, a ~2-2.5 log reduction in bacterial counts could be observed after 24 hours of antibiotic exposure at concentrations greater than eight times the MIC (8xMIC). Concentrations necessary to produce this maximum kill effect were approximately two-fold lower for RWJ-416457 (4μg/mL) compared to linezolid (8μg/mL).

Changing Concentration Time-Kill Curves

Changing concentration time-kill profiles (Figure 6-2B) show that after an initial ~2 log kill, all linezolid concentrations fail to prevent bacterial re-growth within 8 hours of exposure. In contrast, RWJ-416457 concentrations of greater than eight times the MIC exhibit sufficient bacteriostatic activity after 24 hours of exposure.

Drug Stability

While linezolid was completely stable, approximately 10% of RWWJ-416457 degraded over the time course of 24 hours during the experiment (data not shown). Hence, the degradation-rate constant of RWJ-416457 was determined (assuming first-order degradation kinetics) and incorporated into the mathematical model.

Mathematical Modeling

The final PK/PD model was capable of describing the constant (Figure 6-2A), as well as, changing concentration (Figure 6-2B) time-kill curves of RWJ-416457 and linezolid against MRSA OC2878 reasonably well. Corresponding model parameters (±MSE) are listed in Table 6-1. In the final model, N_{max}, d_{gs} and k_d were estimated from the growth control data and assumed to be constant. Furthermore, k_{ps} was fixed to zero (198). Since the addition of a Hill factor did not significantly improve the overall fit, an E_{max}–model rather than a sigmoidal E_{max}-model was used. In addition, allowing for between-experiment variability on k_{ps}, F, k_{max} and EC_{50} using a log error model did significantly improve the final model fit.

Model Validation

Mean final model-predicted parameter estimates (±MSE) and results of the nonparametric bootstrap runs (n=1000) are in good agreement as shown in Table 1. All parameter estimates from the final model lay within the 95% bootstrap CI. When plotted against the data, population predicted values (Fig. 3A), as well as, individual predicted values (Fig. 3B) are uniformly and

randomly distributed around the line of identity. In addition, no trend was observed when plotting weighted residual versus individual model predicted (Fig. 3C) and weighted residuals versus time (Fig. 3D). In combination with the results of the nonparametric bootstrap run, the diagnostic plots indicate that the model is robust and shows good predictability.

Discussion

The selection of an appropriate dose and dosing regimen is a fundamental step for therapeutic success with any pharmacological agent (178). For antimicrobial agents, the selection of the best drug and dosing scheme for a specific pathogen not only increases the chances of cure while preventing toxic side effects, but also decreases the probability of the infecting pathogen becoming resistant to the antimicrobial agent (123, 249). With a good understanding of the dose-exposure relationship, or PK, and the exposure-response relationship, or PD, it may be possible to identify a quantitative link between the dose/dosing regimen on one hand, and the desired, as well as, undesired drug effects on the other hand. For antibiotics, this link has been established by correlating PK parameters that are based on free (f) plasma or serum concentrations to the MIC of the respective pathogen. To date, three main MIC-based PK/PD indices have been identified for antimicrobials: the cumulative percentage of the dosing interval that the free drug concentration exceeds the MIC at steady-state conditions ($f\mathrm{T}_{>\mathrm{MIC}}$), the area under the free concentration-time curve at steady-state divided by the MIC (fAUC/MIC) and the free peak level divided by the MIC ($f\mathrm{C}_{\mathrm{max}}$/MIC) (183). However, the MIC as single point in time estimate is not capable of characterizing the time course of neither growth nor antibiotic-induced kill or the antibiotic effect at concentrations besides the MIC (188, 198, 231). In addition, the methodology to determine the actual MIC value has not yet been internationally standardized and is a source of variability between different MIC determination methods (183). To overcome these limitations, other susceptibility breakpoints, such as, the EC_{50} have been

suggested as the PD input for PK/PD indices. The EC_{50} can be obtained, together with parameters characterizing bacterial growth and maximum antibiotic-induced kill, from continuous measurement of the antibiotic concentration-effect relationship over time (time-kill curves) (11, 198, 258). In general, there are two different types of time-kill curves, based on the concentration profile used in these *in vitro* models, constant and changing concentration experiments (229). While constant concentration models represent steady-state concentrations obtained after constant-rate infusion, changing concentration models try to simulate the change in antibiotic concentrations that occurs *in vivo*. During changing concentration experiments, the desired concentration-time profile can either be generated manually by using syringes or automatically by employing pump systems. However, it has been shown in previous experiments, that the flow-rate necessary to simulate a RWJ-416457 half-life of approximately 24 hours is so slow that bacteria can actually grow back into the broth only reservoir and cause contamination. In this case, the use of the pump systems is not desirable and, consequently, syringes have been used.

Once the time-kill curve experiments have been performed, evaluation of the respective outcomes allows comparing the antimicrobial activity of RWJ-416457 and linezolid against MRSA OC2878 over a wide range of concentrations. Qualitative analysis of the constant concentration time-kill curves revealed that the bacterial counts in these experiments are reduced by less than 3 log steps indicating that both RWJ-416457 and linezolid are bacteriostatic rather than bactericidal antibiotics (210). It could be further shown that linezolid concentrations (8µg/mL) necessary to reach the maximum kill effect were approximately two-fold higher than the respective RWJ-416457 concentrations (4µg/mL). These two-fold differences in the concentration-effect relationship were consistent with the observed two-fold differences in the

MICs (linezolid: 1.0µg/mL, RWJ-416457: 0.5µg/mL). In theory, the increased antimicrobial activity could be explained by a higher potency or a larger number of molecules at the effect site. Yet, the molecular weights of linezolid (337.35g/mol) and RWJ-416457 (377.41g/mol) are not substantially different. As a result, the increased activity of RWJ-416457 against MRSA OC28768 is explained by a higher potency rather than the number of molecules.

In order to evaluate the effect of decreasing concentrations (according to the physiological half-life) on the antimicrobial outcome, changing concentration time-kill curves were performed. Findings indicate that initial RWJ-416457 concentrations of 4µg/mL were sufficient to obtain bacteriostatic activity, whereas even four-fold higher initial linezolid concentrations (16µg/mL) failed to prevent bacterial regrowth after 24 hours of incubation. These findings imply that, compared to linezolid, the increased potency and prolonged half-life of RWJ-416457 may support a lower dose and/or increased dosing interval. In order to identify an appropriate dosing regimen for RWJ-416457, time-kill curve-based modelling and simulation approaches can be used. Although the description of time-kill curves is mathematically somewhat more complex, PD parameters derived from this *in vitro* model can then be combined with *in vivo* PK data to simulate the antimicrobial efficacy of the respective doing regimen(s). Once a general mathematical model is established, it can be applied to the time-kill curve data of other investigational oxazolidinones and respective outcome parameters between drugs and/or dosing regimens can be compared. Modelling and simulation approaches are, consequently, very valuable for dose selection and have been recommended by the U.S. Food and Drug Administration (FDA) as tools to streamline the drug development process (84). In fact, model-based comparison of a new drug candidate to the approved first-in-class representative may allow demonstrating superiority rather than non-inferiority.

The model that was found appropriate to simultaneously characterize the static, as well as, dynamic time-kill curve data of both RWJ-416457 and linezolid has structural similarities to previously described models (126, 198, 275). In this susceptibility-based model, bacteria can exist in two different metabolic stages, an active, growing state (S) and a dormant resting stage (P) as shown in Fig. 6-1. In addition, the model allows accounting for naturally occurring deaths, saturation in growth and delays in the onset of growth, as well as, antibiotic-induced kill. When simultaneously fitted to the data, the final model was capable of describing the experimentally determined time-kill curve data reasonably well (Fig. 6-2). The overall model fit could be improved by incorporating drug degradation during the 24-hour course of the experiment. The final model was internally validated by nonparametric bootstrapping and showed good robustness and predictability (Fig. 6-3). Comparison of the obtained EC_{50} values revealed that RWJ-416457 (0.41µg/mL) is approximately 3.4-fold more potent than the first-in-class representative linezolid (1.39µg/mL). The parameter estimates obtained from this *in vitro* model can then be used in combination with PK data to predict clinical outcome and provide guidance for the selection of appropriate doses or dosing regimens.

In conclusion, a general PK/PD model has been developed that is appropriate for characterizing the *in vitro* time-kill curve data of oxazolidinone antibiotics. Simultaneous fit of the developed model to static, as well as, dynamic time-kill curve data revealed that RWJ-416457 has a 3.4-fold increased *in vitro* potency compared to the first-in-class representative, linezolid. Combined with appropriate PK data, this model may provide valuable guidance for dose or dosing regimen selection of new, investigational oxazolidinones.

Table 6-1. Comparison of the final model parameter estimates (±MSE) and estimates (95%CI) from 1000 nonparametric bootstrap runs

Parameter and Model	Final Model	Bootstrap Estimates (n=1000)
Structural model		
k_s (h^{-1})	1.19 (±0.061)[a]	1.21 (1.11-1.35)[b]
k_{max} (h^{-1})	1.65 (±0.065)[a]	1.65 (1.51-1.82)[b]
EC_{50}(RWJ-416457) (μg/mL)	0.41 (±0.057)[a]	0.32 (0.22-0.45)[b]
EC_{50}(linezolid) (μg/mL)	1.39 (±0.207)[a]	1.13 (0.80-1.53)[b]
N_{max} (CFU/mL)	Fixed to $3.39*10^9$	Fixed to $3.39*10^9$
d_{gs} (h^{-1})	Fixed to 0.24	Fixed to 0.24
d_{ks} (h^{-1})	0.50 (±0.049)[a]	0.54 (0.47-0.63)[b]
k_{sp} (h^{-1})	0.004 (±0.002)[a]	0.001 (0.000-0.003)[b]
k_{ps} (h^{-1})	Fixed to zero	Fixed to zero
k_d (h^{-1})	Fixed to 0.015	Fixed to 0.015
F	0.83 (±0.023)[a]	0.83 (0.79-0.88)[b]
Variance model		
η (k_s)	0.013 (±0.005)[a]	0.11
η (N_{max})	0.219 (±0.082)[a]	0.51
η (d_{gs})	0.184 (±0.071)[a]	0.43
η (d_{ks})	0.079 (±0.029)[a]	0.26
Residual variability	0.29 (±0.027)[a]	0.53

[a]MSE. [b]95%CI

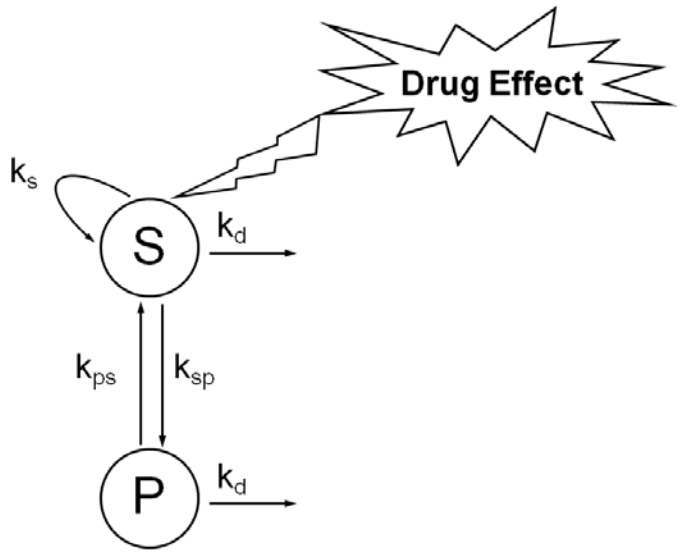

Figure 6-1. Susceptibility-based two-subpopulation model. S = pool of metabolically active and self-replicating bacteria. P = pool of dormant persister cells. k_S = growth-rate constant. k_d = natural death-rate constant. k_{sp} = transfer rate-constant from active to resting stage. k_{ps} = transfer rate-constant from resting to active stage.

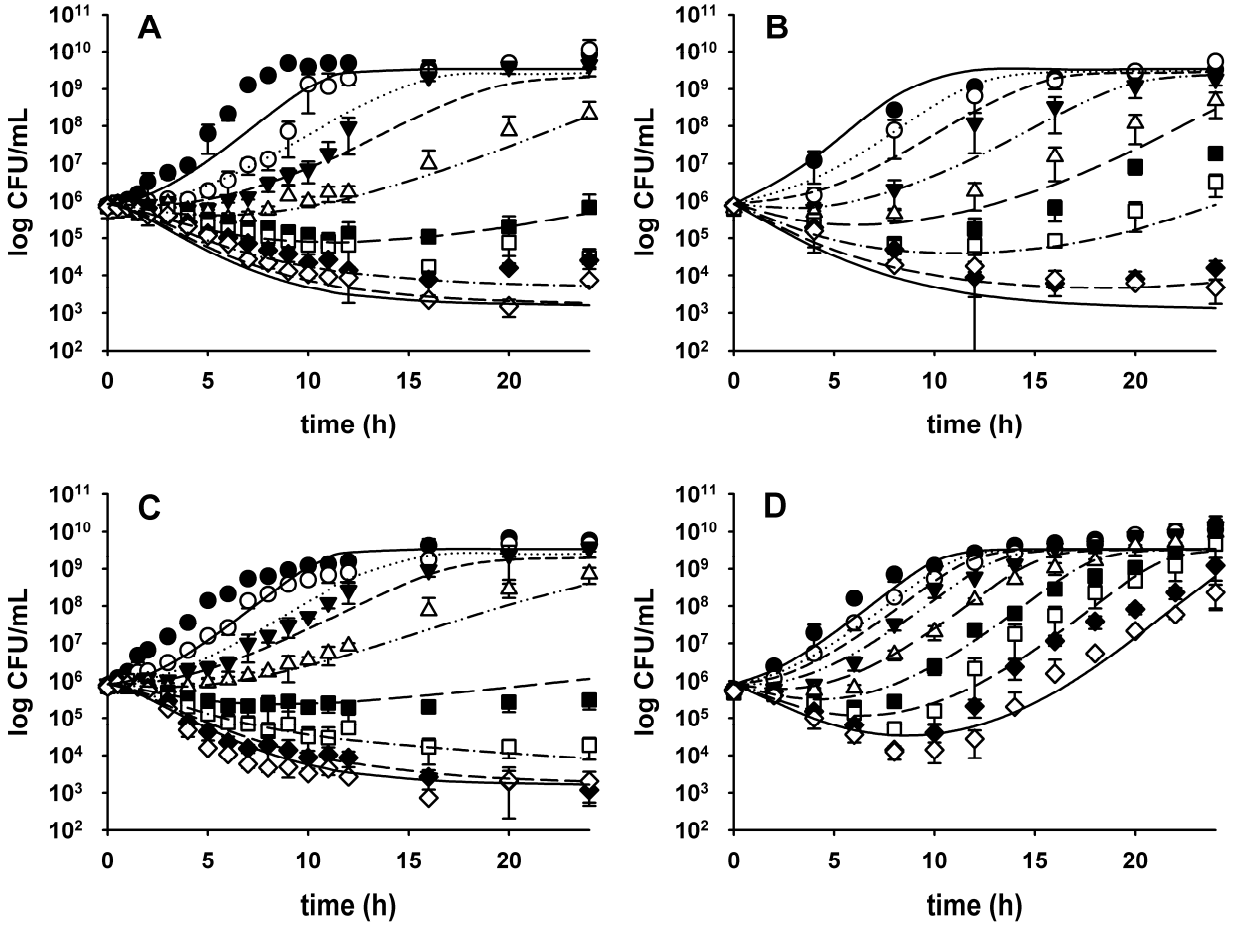

Figure 6-2. Simultaneous curve fits of the susceptibility-based two-compartment model to the experimental data. A) constant concentration time-kill curve of RWJ-416457 against MRSA, B) changing concentration ($t_{1/2}$~24h) of RWJ-416457 against MRSA, C) constant concentration time-kill curve of linezolid against MRSA, and D) changing concentration ($t_{1/2}$~5h) of linezolid against MRSA at initial concentrations of 0.25xMIC (----○----), 0.5xMIC (— ▼ —), 1xMIC (— ·· △ ·· —), 2xMIC (— ■ — ·), 4xMIC (— · □ · —), 8xMIC (— ◆ —) and 16xMIC (—◇—) plus a growth control (——●——). Symbols represent the experimental data, lines the model predicted curve fits.

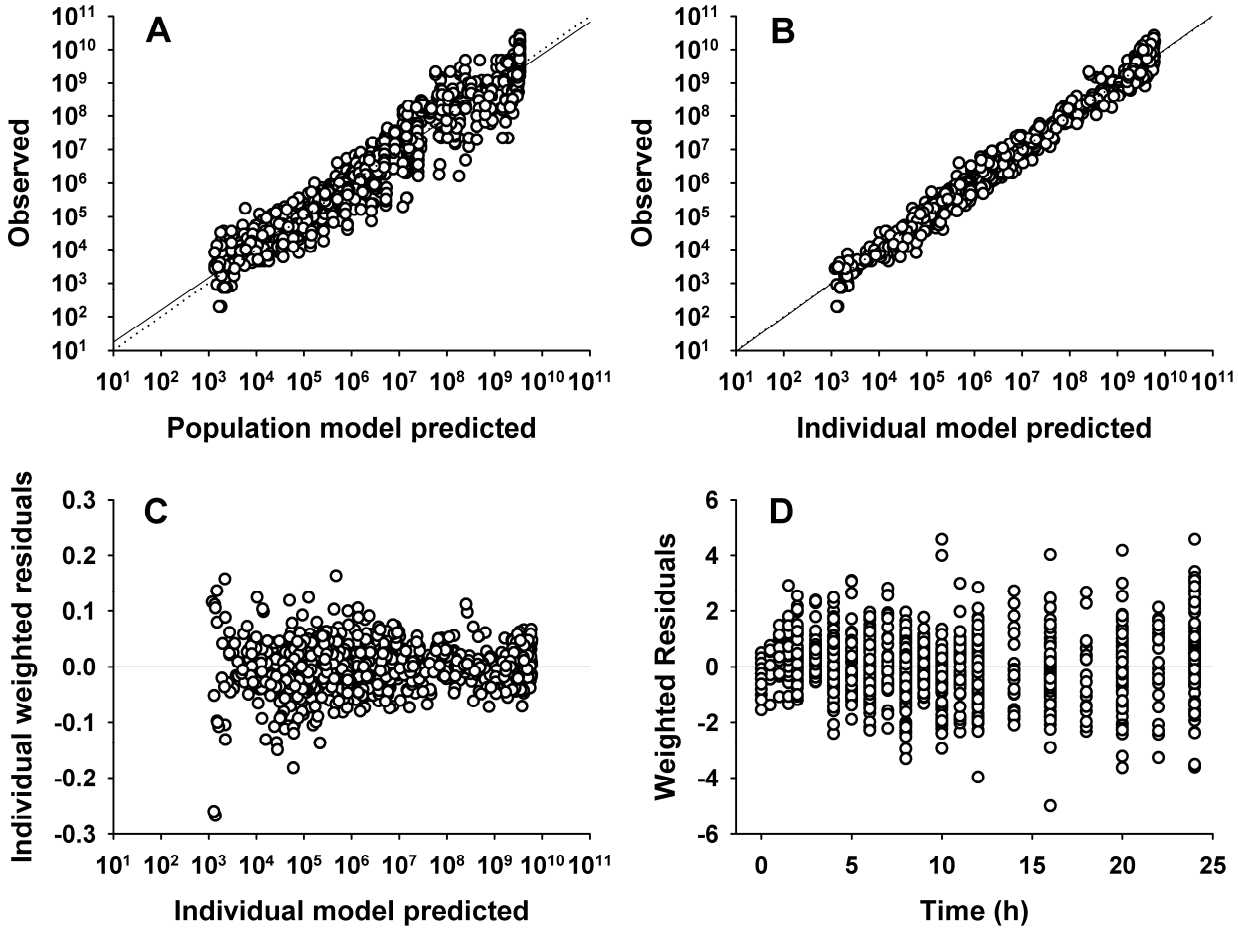

Figure 6-3. Basic diagnostic plots. A) observed versus population model predicted, B) observed versus individual model predicted, C) weighted residual versus individual model predicted and D) weighted residuals versus time. The dotted line represents the line of identity; the solid line represents the linear regression line.

CHAPTER 7
DISCUSSION

Since the discovery of the penicillin by Sir Alexander Fleming in 1928, antibiotics have effectively been used for decades to treat bacterial infections (208, 274). However, due to an over-/misuse of "first choice" antibiotics (e.g. for minor infections or in food-producing animals), the failure to complete treatment, and the substantial increase in the availability and ease of travel within/between countries has contributed to a rapid emergence and spread of resistance during the second half of the 20th century (165, 171, 270). Resistance against antibiotics, as stated in the annual CDC reports and results of the SENTRY study, is a major cause of morbidity and mortality in the United States and all over the world (70, 106, 118, 163, 257, 271) and accounts for excess days of illness and hospitalization (257), as well as, increased health care costs (209).

In order to increase the chances of clinical success and minimize the risk of resistance development, it is critically important to improve antibiotic therapy by optimizing current dosing regimens and developing newer and more potent antibiotics. The most comprehensive approach of achieving this goal is to apply PK/PD principles throughout the optimization/development process. On the other hand, disregard of these principles may result in conflicting outcomes, failure in later and more costly clinical stages and potential harm to the patient. Chances of success are increased when these principles are employed early on in the drug development process. For example, commercially available protein supplements are used in pre-clinical test systems to produce and modify protein binding. However, if the actual binding in these *in vitro* test systems represents physiological binding conditions is frequently not determined.

The first specific goal of this thesis work was to evaluate this approach by experimentally measuring free, unbound ceftriaxone (protein binding: 83-96%) (244, 245, 277) and ertapenem

(protein binding: 84-96%) (34) concentrations using *in vitro* microdialysis. Findings of this study clearly indicate that the protein binding values achieved by supplementing with commercially available albumins can substantially differ from those in serum/plasma. It was concluded that in order to avoid experimental misconduct and further misinterpretation of the effect of protein binding on the antimicrobial activity, free, unbound concentrations need to be measured in the actual *in vitro* test system.

Traditionally, the effect of protein binding is taken into account by linking free, unbound concentrations in plasma to the respective PD outcome. However, since most bacterial infections are located in the extracellular fluid of tissues, a more comprehensive approach would be to measure free, active concentrations in the interstitial space fluid of tissues rather than the blood. Microdialysis is currently the only technique that can provide this information and has been extensively been used in tissue distribution studies.

The second specific goal of this thesis work was to measure free, active concentrations in the interstitial space fluid of muscle and subcutaneous adipose tissue of six healthy subjects following a single intravenous infusion of 1g ertapenem using clinical microdialysis. Results of this microdialysis study indicate that free, unbound ertapenem concentrations in the interstitial space fluid of muscle are comparable to free concentrations in plasma but are higher than those in subcutaneous adipose tissue. Nevertheless, free concentrations in both tissues were sufficient to exceed the MICs of the most prevalent skin and skin structure pathogens. These findings support the clinical use of the approved dosing regimen of 1g ertapenem BID for the treatment of skin and skin structure infections.

To date, PK information, determined in e.g. microdialysis experiments, is frequently linked to the MIC in order to evaluate dose-concentration-response relationships. However, as stated

previously, the MIC suffers from numerous drawbacks. To overcome these limitations, other approaches, such as, time-kill curves have been suggested for evaluating the PD outcome. In order to characterize the experimental time-kill curves, an appropriate PK/PD model can be simultaneously fitted to the data. Once determined, the PD parameters can be linked to PK profiles of different doses and dosing regimens to predict and compare the respective clinical outcome.

The third specific goal of this thesis work was to establish and validate an appropriate PK/PD model that allows characterizing the antimicrobial activity of oxazolidinones, determined in time-kill curve experiments, against MRSA. Results of this study indicate that the identified susceptibility-based two-subpopulation model was appropriate to describe the oxazolidinone effect on MRSA over time. When simultaneously fitted to the data, comparison of the corresponding EC_{50} values revealed that RWJ-416457 is approximately 3.4-fold more potent than the first-in-class representative linezolid. In combination with appropriate PK data, this model can be used to guide the pre-clinical development process of new oxazolidinone antibiotics and, subsequently, to select an appropriate dose for clinical trials.

In summary, the proper application of PK/PD principles throughout drug development and in the clinic supports the establishment of effective dosing regimens and helps to prevent the emergence of resistance. However, the complex dynamic interaction between a host, a pathogen and the infection process has not been completely understood (236). To date, the immune system is seen predominantly as a defence mechanism of the body against infections. Little is known about its impact on the manifestation of clinical symptoms. Therefore, in future approaches patient-, disease and immune status should be taken into greater consideration (Figure 6-5) (166, 167).

Most comprehensive assessments of interactions between pathogen, host and antibiotic can be achieved by integrating individual PK/PD profiles into modeling and support the establishment of effective dosage regimens for treatment (73, 174, 196). However, clinical practice often differs from this ideal situation when treatment is started out empirically to improve the status of the patient (131, 233). Yet, for success in treatment, eradication of the pathogen should be regarded as the primary endpoint in order to avoid emergence and spread of resistant strains (58, 93). Combined efforts will be needed to achieve this goal and meet the challenge of multi-drug-resistant microbe threats in the clinic as well as in the community. Hence, not only rethinking of antimicrobial treatment and prescribing standards but also a change in patient care/management will be necessary (60, 86, 265). In drug development, PK and PD criteria can be used to predict bacteriologic efficacy. However, they should be confirmed during all phases of antimicrobial development and throughout clinical use in response to changing resistance patterns (7, 57, 113, 131, 238).

Identifying new compounds is one potent strategy but not the only one. If new compounds are derived from existing drug classes, cross-resistance can occur (7, 267). Hence, it is essential that existing drug classes are used in optimized ways. For example, new dosage forms of existing compounds (e.g. liposomal antimicrobial agents), drug combinations and advanced modeling and simulation tools need to be developed in order the improve PK/PD and establish effective dosing regimens (86, 181, 220).

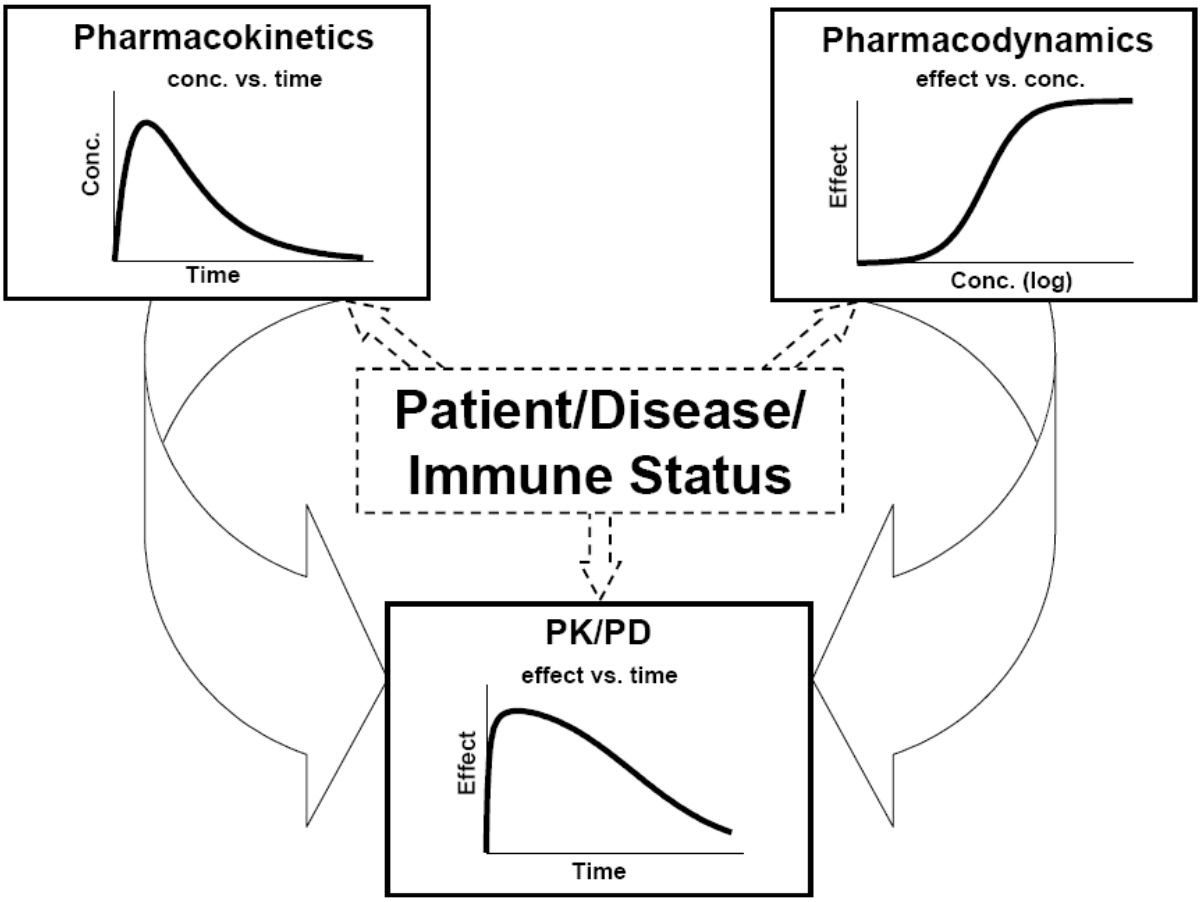

Figure 7-1. Interplay between pharmacokinetics, pharmacodynamics, patient and disease

LIST OF REFERENCES

1. Allegranzi, B., A. Cazzadori, G. Di Perri, S. Bonora, M. Berti, L. Franchino, A. Biglino, A. Cipriani, and E. Concia. 2000. Concentrations of single-dose meropenem (1 g iv) in bronchoalveolar lavage and epithelial lining fluid. J Antimicrob Chemother 46:319-22.

2. Ambrose, P. G. 2006. Monte Carlo simulation in the evaluation of susceptibility breakpoints: predicting the future: insights from the society of infectious diseases pharmacists. Pharmacotherapy 26:129-34.

3. Ambrose, P. G., S. M. Bhavnani, B. B. Cirincione, M. Piedmonte, and T. H. Grasela. 2003. Gatifloxacin and the elderly: pharmacokinetic-pharmacodynamic rationale for a potential age-related dose reduction. J Antimicrob Chemother 52:435-40.

4. Ambrose, P. G., S. M. Bhavnani, and R. C. Owens, Jr. 2003. Clinical pharmacodynamics of quinolones. Infect Dis Clin North Am 17:529-43.

5. Ambrose, P. G., and D. M. Grasela. 2000. The use of Monte Carlo simulation to examine pharmacodynamic variance of drugs: fluoroquinolone pharmacodynamics against Streptococcus pneumoniae. Diagn Microbiol Infect Dis 38:151-7.

6. Andes, D., posting date. Animal Model PK/PD: A Tool for Drug Development. [Online.]

7. Andes, D. 2001. Pharmacokinetic and pharmacodynamic properties of antimicrobials in the therapy of respiratory tract infections. Curr Opin Infect Dis 14:165-72.

8. Andes, D., and W. A. Craig. 2002. Pharmacodynamics of the new fluoroquinolone gatifloxacin in murine thigh and lung infection models. Antimicrob Agents Chemother 46:1665-70.

9. Bahlmann, L., M. Misfeld, S. Klaus, A. Leptien, M. Heringlake, P. Schmucker, H. H. Sievers, U. Ungerstedt, and E. G. Kraatz. 2004. Myocardial redox state during coronary artery bypass grafting assessed with microdialysis. Intensive Care Med 30:889-94.

10. Balaban, N. Q., J. Merrin, R. Chait, L. Kowalik, and S. Leibler. 2004. Bacterial persistence as a phenotypic switch. Science 305:1622-5.

11. Bantar, C., C. Schell, G. Posse, A. Limansky, V. Ballerini, and L. Mobilia. 2008. Comparative time-kill study of doxycycline, tigecycline, sulbactam, and imipenem against several clones of Acinetobacter baumannii. Diagn Microbiol Infect Dis. 61:309-14

12. Barre, J., J. M. Chamouard, G. Houin, and J. P. Tillement. 1985. Equilibrium dialysis, ultrafiltration, and ultracentrifugation compared for determining the plasma-protein-binding characteristics of valproic acid. Clin Chem 31:60-4.

13. Barre, J., F. Didey, F. Delion, and J. P. Tillement. 1988. Problems in therapeutic drug monitoring: free drug level monitoring. Ther Drug Monit 10:133-43.

14. Benfeldt, E., S. H. Hansen, A. Volund, T. Menne, and V. P. Shah. 2007. Bioequivalence of topical formulations in humans: evaluation by dermal microdialysis sampling and the dermatopharmacokinetic method. J Invest Dermatol 127:170-8.

15. Benfeldt, E., J. Serup, and T. Menne. 1999. Effect of barrier perturbation on cutaneous salicylic acid penetration in human skin: in vivo pharmacokinetics using microdialysis and non-invasive quantification of barrier function. Br J Dermatol 140:739-48.

16. Bito, L., H. Davson, E. Levin, M. Murray, and N. Snider. 1966. The concentrations of free amino acids and other electrolytes in cerebrospinal fluid, in vivo dialysate of brain, and blood plasma of the dog. J Neurochem 13:1057-67.

17. Boelsma, E., C. Anderson, A. M. Karlsson, and M. Ponec. 2000. Microdialysis technique as a method to study the percutaneous penetration of methyl nicotinate through excised human skin, reconstructed epidermis, and human skin in vivo. Pharm Res 17:141-7.

18. Bolinder, J., E. Hagstrom, U. Ungerstedt, and P. Arner. 1989. Microdialysis of subcutaneous adipose tissue in vivo for continuous glucose monitoring in man. Scand J Clin Lab Invest 49:465-74.

19. Borg, N., E. Gotharson, E. Benfeldt, L. Groth, and L. Stahle. 1999. Distribution to the skin of penciclovir after oral famciclovir administration in healthy volunteers: comparison of the suction blister technique and cutaneous microdialysis. Acta Derm Venereol 79:274-7.

20. Boswell, F. J., J. P. Ashby, J. M. Andrews, and R. Wise. 2002. Effect of protein binding on the in vitro activity and pharmacodynamics of faropenem. J Antimicrob Chemother 50:525-32.

21. Boutsiouki, P., J. P. Thompson, and G. F. Clough. 2001. Effects of local blood flow on the percutaneous absorption of the organophosphorus compound malathion: a microdialysis study in man. Arch Toxicol 75:321-8.

22. Box, G. E. P. 1979. Robustness in the strategy of scientific model building. Academic Press, New York.

23. Bratzler, D. W., and P. M. Houck. 2004. Antimicrobial prophylaxis for surgery: an advisory statement from the National Surgical Infection Prevention Project. Clin Infect Dis 38:1706-15.

24. Bratzler, D. W., and P. M. Houck. 2005. Antimicrobial prophylaxis for surgery: an advisory statement from the National Surgical Infection Prevention Project. Am J Surg 189:395-404.

25. Brunner, M., P. Dehghanyar, B. Seigfried, W. Martin, G. Menke, and M. Muller. 2005. Favourable dermal penetration of diclofenac after administration to the skin using a novel spray gel formulation. Br J Clin Pharmacol 60:573-7.

26. Brunner, M., H. Derendorf, and M. Muller. 2005. Microdialysis for in vivo pharmacokinetic/pharmacodynamic characterization of anti-infective drugs. Curr Opin Pharmacol 5:495-9.

27. Brunner, M., U. Hollenstein, S. Delacher, D. Jager, R. Schmid, E. Lackner, A. Georgopoulos, H. G. Eichler, and M. Muller. 1999. Distribution and antimicrobial activity of ciprofloxacin in human soft tissues. Antimicrob Agents Chemother 43:1307-9.

28. Brunner, M., and O. Langer. 2006. Microdialysis versus other techniques for the clinical assessment of in vivo tissue drug distribution. Aaps J 8:E263-71.

29. Brunner, M., H. Stabeta, J. G. Moller, C. Schrolnberger, B. Erovic, U. Hollenstein, M. Zeitlinger, H. G. Eichler, and M. Muller. 2002. Target site concentrations of ciprofloxacin after single intravenous and oral doses. Antimicrob Agents Chemother 46:3724-30.

30. Bur, A., C. Joukhadar, N. Klein, Herkner, G. Mitulovic, R. Schmid, E. Agneter, M. Muller, and M. Brunner. 2005. Effect of exercise on transdermal nicotine release in healthy habitual smokers. Int J Clin Pharmacol Ther 43:239-43.

31. Burian, M., I. Tegeder, M. Seegel, and G. Geisslinger. 2003. Peripheral and central antihyperalgesic effects of diclofenac in a model of human inflammatory pain. Clin Pharmacol Ther 74:113-20.

32. Burke, J. P. 2003. Infection control - a problem for patient safety. N Engl J Med 348:651-6.

33. Burkhardt, O., K. Borner, N. von der Hoh, P. Koppe, M. W. Pletz, C. E. Nord, and H. Lode. 2002. Single- and multiple-dose pharmacokinetics of linezolid and co-amoxiclav in healthy human volunteers. J Antimicrob Chemother 50:707-12.

34. Burkhardt, O., M. Brunner, S. Schmidt, M. Grant, Y. Tang, and H. Derendorf. 2006. Penetration of ertapenem into skeletal muscle and subcutaneous adipose tissue in healthy volunteers measured by in vivo microdialysis. J Antimicrob Chemother. 58:632-6

35. Burkhardt, O., J. Majcher-Peszynska, K. Borner, R. Mundkowski, B. Drewelow, H. Derendorf, and T. Welte. 2005. Penetration of ertapenem into different pulmonary compartments of patients undergoing lung surgery. J Clin Pharmacol 45:659-65.

36. Cafini, F., L. Aguilar, N. Gonzalez, M. J. Gimenez, M. Torrico, L. Alou, D. Sevillano, P. Vallejo, and J. Prieto. 2007. In vitro effect of the presence of human albumin or human serum on the bactericidal activity of daptomycin against strains with the main resistance phenotypes in Gram-positives. J Antimicrob Chemother 59:1185-9.

37. Campion, J. J., P. J. McNamara, and M. E. Evans. 2005. Pharmacodynamic modeling of ciprofloxacin resistance in Staphylococcus aureus. Antimicrob Agents Chemother 49:209-19.

38. Cawello, W. 1997. Connection of pharmacokinetics and pharmacodynamics--how does it work? Int J Clin Pharmacol Ther 35:414-7.

39. Cazzola, M., M. G. Matera, and P. Noschese. 2000. Parenteral antibiotic therapy in the treatment of lower respiratory tract infections. Strategies to minimize the development of antibiotic resistance. Pulm Pharmacol Ther 13:249-56.

40. Cha, R., W. J. Brown, and M. J. Rybak. 2003. Bactericidal activities of daptomycin, quinupristin-dalfopristin, and linezolid against vancomycin-resistant Staphylococcus aureus in an in vitro pharmacodynamic model with simulated endocardial vegetations. Antimicrob Agents Chemother 47:3960-3.

41. Cha, R., and M. J. Rybak. 2004. Influence of protein binding under controlled conditions on the bactericidal activity of daptomycin in an in vitro pharmacodynamic model. J Antimicrob Chemother 54:259-62.

42. Chang, S., D. M. Sievert, J. C. Hageman, M. L. Boulton, F. C. Tenover, F. P. Downes, S. Shah, J. T. Rudrik, G. R. Pupp, W. J. Brown, D. Cardo, and S. K. Fridkin. 2003. Infection with vancomycin-resistant Staphylococcus aureus containing the vanA resistance gene. N Engl J Med 348:1342-7.

43. Chao, C. C., H. Y. Sun, Y. C. Chang, and S. T. Hsieh. 2008. Painful neuropathy with skin denervation after prolonged use of linezolid. J Neurol Neurosurg Psychiatry 79:97-9.

44. Chaurasia, C. S., M. Muller, E. D. Bashaw, E. Benfeldt, J. Bolinder, R. Bullock, P. M. Bungay, E. C. DeLange, H. Derendorf, W. F. Elmquist, M. Hammarlund-Udenaes, C. Joukhadar, D. L. Kellogg, Jr., C. E. Lunte, C. H. Nordstrom, H. Rollema, R. J. Sawchuk, B. W. Cheung, V. P. Shah, L. Stahle, U. Ungerstedt, D. F. Welty, and H. Yeo. 2007. AAPS-FDA Workshop White Paper: microdialysis principles, application, and regulatory perspectives. J Clin Pharmacol 47:589-603.

45. Christensen, H., M. Baker, G. T. Tucker, and A. Rostami-Hodjegan. 2006. Prediction of plasma protein binding displacement and its implications for quantitative assessment of metabolic drug-drug interactions from in vitro data. J Pharm Sci 95:2778-87.

46. Chulavatnatol, S., B. Chindavijak, N. Chierakul, and D. Klomsawat. 2003. Pharmacokinetics of ofloxacin in drug-resistant tuberculosis. J Med Assoc Thai 86:781-8.

47. Colburn, W. A. 2003. Biomarkers in drug discovery and development: from target identification through drug marketing. J Clin Pharmacol 43:329-41.

48. Collison, M. E., P. J. Stout, T. S. Glushko, K. N. Pokela, D. J. Mullins-Hirte, J. R. Racchini, M. A. Walter, S. P. Mecca, J. Rundquist, J. J. Allen, M. E. Hilgers, and T. B. Hoegh. 1999. Analytical characterization of electrochemical biosensor test strips for measurement of glucose in low-volume interstitial fluid samples. Clin Chem 45:1665-73.

49. Craig, W. A. 2001. Does the dose matter? Clin Infect Dis 33:233-7.

50. Craig, W. A. 2001. The hidden impact of antibacterial resistance in respiratory tract infection. Re-evaluating current antibiotic therapy. Respir Med 95:12-9; 26-7.

51. Craig, W. A. 1995. Interrelationship between pharmacokinetics and pharmacodynamics in determining dosage regimens for broad-spectrum cephalosporins. Diagn Microbiol Infect Dis 22:89-96.

52. Craig, W. A. 2003, posting date. Pharmacodynamics of Antimicrobials in Animal Models. [Online.]

53. Craig, W. A. 2002. Pharmacodynamics of antimicrobials: general concepts and applications, p. 1-22, Antimicrobial Pharmacodynamics in Theory and Clinical Practice. Marcel-Dekker, New York.

54. Critchley, I. A., D. F. Sahm, C. Thornsberry, R. S. Blosser-Middleton, M. E. Jones, and J. A. Karlowsky. 2002. Antimicrobial susceptibilities of Streptococcus pyogenes isolated from respiratory and skin and soft tissue infections: United States LIBRA surveillance data from 1999. Diagn Microbiol Infect Dis 42:129-35.

55. Cross, S. E., C. Anderson, and M. S. Roberts. 1998. Topical penetration of commercial salicylate esters and salts using human isolated skin and clinical microdialysis studies. Br J Clin Pharmacol 46:29-35.

56. Cunha, B. A. 2002. Ertapenem. A review of its microbiologic, pharmacokinetic and clinical aspects. Drugs Today (Barc) 38:195-213.

57. Dagan, R. 2003. Achieving bacterial eradication using pharmacokinetic/pharmacodynamic principles. Int J Infect Dis 7:21-6.

58. Dagan, R., K. P. Klugman, W. A. Craig, and F. Baquero. 2001. Evidence to support the rationale that bacterial eradication in respiratory tract infection is an important aim of antimicrobial therapy. J Antimicrob Chemother 47:129-40.

59. Dasgupta, A. 2007. Usefulness of monitoring free (unbound) concentrations of therapeutic drugs in patient management. Clin Chim Acta 377:1-13.

60. Davenport, L. A., P. G. Davey, and J. S. Ker. 2005. An outcome-based approach for teaching prudent antimicrobial prescribing to undergraduate medical students: report of a Working Party of the British Society for Antimicrobial Chemotherapy. J Antimicrob Chemother 56:196-203.

61. Day, R. M., M. Harbord, A. Forbes, and A. W. Segal. 2001. Cantharidin blisters: a technique for investigating leukocyte trafficking and cytokine production at sites of inflammation in humans. J Immunol Methods 257:213-20.

62. de Hoog, M., J. W. Mouton, and J. N. van den Anker. 2005. New dosing strategies for antibacterial agents in the neonate. Semin Fetal Neonatal Med 10:185-94.

63. de Lange, E. C., A. G. de Boer, and D. D. Breimer. 2000. Methodological issues in microdialysis sampling for pharmacokinetic studies. Adv Drug Deliv Rev 45:125-48.

64. Dehghanyar, P., C. Burger, M. Zeitlinger, F. Islinger, F. Kovar, M. Muller, C. Kloft, and C. Joukhadar. 2005. Penetration of linezolid into soft tissues of healthy volunteers after single and multiple doses. Antimicrob Agents Chemother 49:2367-71.

65. Del Mar Fernandez de Gatta Garcia, M., N. Revilla, M. V. Calvo, A. Dominguez-Gil, and A. Sanchez Navarro. 2006. Pharmacokinetic/pharmacodynamic analysis of vancomycin in ICU patients. Intensive Care Med. 33:279-85

66. Delgado, J. M., F. V. DeFeudis, R. H. Roth, D. K. Ryugo, and B. M. Mitruka. 1972. Dialytrode for long term intracerebral perfusion in awake monkeys. Arch Int Pharmacodyn Ther 198:9-21.

67. Derendorf, H., Gramatté, T., Schäfer, H. G. 2002. Pharmakodynamische Modelle, p. 278-282, Pharmakokinetik, Volume 2 ed. Wissenschaftliche Verlagsgesellschaft mbH, Stuttgart.

68. Derendorf, H., L. J. Lesko, P. Chaikin, W. A. Colburn, P. Lee, R. Miller, R. Powell, G. Rhodes, D. Stanski, and J. Venitz. 2000. Pharmacokinetic/pharmacodynamic modeling in drug research and development. J Clin Pharmacol 40:1399-418.

69. Derendorf, H., and B. Meibohm. 1999. Modeling of pharmacokinetic/pharmacodynamic (PK/PD) relationships: concepts and perspectives. Pharm Res 16:176-85.

70. Diekema, D. J., M. A. Pfaller, F. J. Schmitz, J. Smayevsky, J. Bell, R. N. Jones, and M. Beach. 2001. Survey of infections due to Staphylococcus species: frequency of occurrence and antimicrobial susceptibility of isolates collected in the United States, Canada, Latin America, Europe, and the Western Pacific region for the SENTRY Antimicrobial Surveillance Program, 1997-1999. Clin Infect Dis 32 Suppl 2:S114-32.

71. DiNubile, M. J., and B. A. Lipsky. 2004. Complicated infections of skin and skin structures: when the infection is more than skin deep. J Antimicrob Chemother 53 Suppl 2:ii37-50.

72. Dresser, L. D., and M. J. Rybak. 1998. The pharmacologic and bacteriologic properties of oxazolidinones, a new class of synthetic antimicrobials. Pharmacotherapy 18:456-62.

73. Drusano, G. 2001. Pharmacodynamic and pharmacokinetic considerations in antimicrobial selection: focus on telithromycin. Clin Microbiol Infect 7:24-9.

74. Drusano, G. 2001. Pharmacodynamic and pharmacokinetic considerations in antimicrobial selection: focus on telithromycin. Clin Microbiol Infect 7 Suppl 3:24-9.

75. Drusano, G. L. 2004. Antimicrobial pharmacodynamics: critical interactions of 'bug and drug'. Nat Rev Microbiol 2:289-300.

76. Drusano, G. L., D. E. Johnson, M. Rosen, and H. C. Standiford. 1993. Pharmacodynamics of a fluoroquinolone antimicrobial agent in a neutropenic rat model of Pseudomonas sepsis. Antimicrob Agents Chemother 37:483-90.

77. Drusano, G. L., S. L. Preston, C. Hardalo, R. Hare, C. Banfield, D. Andes, O. Vesga, and W. A. Craig. 2001. Use of preclinical data for selection of a phase II/III dose for evernimicin and identification of a preclinical MIC breakpoint. Antimicrob Agents Chemother 45:13-22.

78. Ederoth, P., K. Tunblad, R. Bouw, C. J. Lundberg, U. Ungerstedt, C. H. Nordstrom, and M. Hammarlund-Udenaes. 2004. Blood-brain barrier transport of morphine in patients with severe brain trauma. Br J Clin Pharmacol 57:427-35.

79. Engstrom, M., A. Polito, P. Reinstrup, B. Romner, E. Ryding, U. Ungerstedt, and C. H. Nordstrom. 2005. Intracerebral microdialysis in severe brain trauma: the importance of catheter location. J Neurosurg 102:460-9.

80. Ette, E. I. 1997. Stability and performance of a population pharmacokinetic model. J Clin Pharmacol 37:486-95.

81. FDA May 1, 2007, posting date. Bioequivalence of Topical Dermatological Products. [Online.]

82. FDA February 21, 2003, posting date. CDER News Along the Pike. [Online.]

83. FDA March 8, 2001, posting date. Guidance for Industry: Bioavailability and Bioequivalence Studies for Orally Administered Drug Products — General Considerations. [Online.]

84. FDA March 16 2004, posting date. Innovation or Stagnation - Challenge and Opportunity on the Critical Path to New Medical Products. [Online.]

85. FDA July 8, 2003, posting date. Summary of an FDA workshop, "Innovative Systems for Delivery of Drugs and Biologics: Scientific, Clinical and Regulatory Challenges". [Online.]

86. Finch, R. G. 2004. Introduction: standards of antibacterial performance. Clin Microbiol Infect 10:1-5.

87. Foleno, B. D., D. Abbanat, R. M. Goldschmidt, R. K. Flamm, S. D. Paget, G. C. Webb, E. Wira, M. J. Macielag, and K. Bush. 2007. In vitro antibacterial activity of the pyrrolopyrazolyl-substituted oxazolidinone RWJ-416457. Antimicrob Agents Chemother 51:361-5.

88. Fontana, R., M. Aldegheri, M. Ligozzi, G. Lo Cascio, and G. Cornaglia. 1998. Interaction of ceftriaxone with penicillin-binding proteins of Escherichia coli in the presence of human serum albumin. J Antimicrob Chemother 42:95-8.

89. Forrest, A., D. E. Nix, C. H. Ballow, T. F. Goss, M. C. Birmingham, and J. J. Schentag. 1993. Pharmacodynamics of intravenous ciprofloxacin in seriously ill patients. Antimicrob Agents Chemother 37:1073-81.

90. Frimodt-Moller, N. 2002. Correlation between pharmacokinetic/pharmacodynamic parameters and efficacy for antibiotics in the treatment of urinary tract infection. Int J Antimicrob Agents 19:546-53.

91. Fuchs, P. C., A. L. Barry, and S. D. Brown. 2001. In vitro activities of ertapenem (MK-0826) against clinical bacterial isolates from 11 North American medical centers. Antimicrob Agents Chemother 45:1915-8.

92. Fung, H. B., J. Y. Chang, and S. Kuczynski. 2003. A practical guide to the treatment of complicated skin and soft tissue infections. Drugs 63:1459-80.

93. Garau, J. 2003. Why do we need to eradicate pathogens in respiratory tract infections? Int J Infect Dis 7:5-12.

94. Gattringer, R., E. Urbauer, F. Traunmuller, M. Zeitlinger, P. Dehghanyar, P. Zeleny, W. Graninger, M. Muller, and C. Joukhadar. 2004. Pharmacokinetics of telithromycin in plasma and soft tissues after single-dose administration to healthy volunteers. Antimicrob Agents Chemother 48:4650-3.

95. Gee, T., R. Ellis, G. Marshall, J. Andrews, J. Ashby, and R. Wise. 2001. Pharmacokinetics and tissue penetration of linezolid following multiple oral doses. Antimicrob Agents Chemother 45:1843-6.

96. Giurini, J. M., and T. E. Lyons. 2005. Diabetic foot complications: diagnosis and management. Int J Low Extrem Wounds 4:171-82.

97. Goldstein, E. J., D. M. Citron, S. Hunt Gerardo, M. Hudspeth, and C. V. Merriam. 1998. Activities of HMR 3004 (RU 64004) and HMR 3647 (RU 66647) compared to those of erythromycin, azithromycin, clarithromycin, roxithromycin, and eight other antimicrobial agents against unusual aerobic and anaerobic human and animal bite pathogens isolated from skin and soft tissue infections in humans. Antimicrob Agents Chemother 42:1127-32.

98. Gordien, J. B., E. Boselli, C. Fleureau, B. Allaouchiche, G. Janvier, O. Lalaude, M. C. Saux, and D. Breilh. 2006. Determination of free ertapenem in plasma and bronchoalveolar lavage by high-performance liquid chromatography with ultraviolet detection. J Chromatogr B Analyt Technol Biomed Life Sci 830:218-23.

99. Graham, D. R., C. Lucasti, O. Malafaia, R. L. Nichols, P. Holtom, N. Q. Perez, A. McAdams, G. L. Woods, T. P. Ceesay, and R. Gesser. 2002. Ertapenem once daily versus piperacillin-tazobactam 4 times per day for treatment of complicated skin and skin-structure infections in adults: results of a prospective, randomized, double-blind multicenter study. Clin Infect Dis 34:1460-8.

100. Gumbo, T., A. Louie, M. R. Deziel, L. M. Parsons, M. Salfinger, and G. L. Drusano. 2004. Selection of a moxifloxacin dose that suppresses drug resistance in Mycobacterium tuberculosis, by use of an in vitro pharmacodynamic infection model and mathematical modeling. J Infect Dis 190:1642-51.

101. Heinze, A., and U. Holzgrabe. 2006. Determination of the extent of protein binding of antibiotics by means of an automated continuous ultrafiltration method. Int J Pharm 311:108-12.

102. Herkner, H., M. R. Muller, N. Kreischitz, B. X. Mayer, M. Frossard, C. Joukhadar, N. Klein, E. Lackner, and M. Muller. 2002. Closed-chest microdialysis to measure antibiotic penetration into human lung tissue. Am J Respir Crit Care Med 165:273-6.

103. Herrera, A. M., D. O. Scott, and C. E. Lunte. 1990. Microdialysis sampling for determination of plasma protein binding of drugs. Pharm Res 7:1077-81.

104. Herrero, I. A., N. C. Issa, and R. Patel. 2002. Nosocomial spread of linezolid-resistant, vancomycin-resistant Enterococcus faecium. N Engl J Med 346:867-9.

105. Heyneman, C. A., C. Lawless-Liday, and G. C. Wall. 2000. Oral versus topical NSAIDs in rheumatic diseases: a comparison. Drugs 60:555-74.

106. Hoban, D. J., G. V. Doern, A. C. Fluit, M. Roussel-Delvallez, and R. N. Jones. 2001. Worldwide prevalence of antimicrobial resistance in Streptococcus pneumoniae, Haemophilus influenzae, and Moraxella catarrhalis in the SENTRY Antimicrobial Surveillance Program, 1997-1999. Clin Infect Dis 32 Suppl 2:S81-93.

107. Hocht, C., J. A. Opezzo, and C. A. Taira. 2004. Microdialysis in drug discovery. Curr Drug Discov Technol 1:269-85.

108. Hodges, G. J., K. Zhao, W. A. Kosiba, and J. M. Johnson. 2006. The involvement of nitric oxide in the cutaneous vasoconstrictor response to local cooling in humans. J Physiol 574:849-57.

109. Holford, N. H., and L. B. Sheiner. 1982. Kinetics of pharmacologic response. Pharmacol Ther 16:143-66.

110. Holford, N. H., and L. B. Sheiner. 1981. Pharmacokinetic and pharmacodynamic modeling in vivo. Crit Rev Bioeng 5:273-322.

111. Huang, Y., and Z. Zhang. 2004. Binding study of drug with bovine serum album using a combined technique of microdialysis with flow-injection chemiluminescent detection. J Pharm Biomed Anal 35:1293-9.

112. Hutschala, D., K. Skhirtladze, C. Kinstner, B. Mayer-Helm, M. Muller, E. Wolner, and E. M. Tschernko. 2007. In vivo microdialysis to measure antibiotic penetration into soft tissue during cardiac surgery. Ann Thorac Surg 84:1605-10.

113. Jacobs, M. R. 2003. How can we predict bacterial eradication? Int J Infect Dis 7:13-20.

114. Jain, R. K. 1994. Barriers to drug delivery in solid tumors. Sci Am 271:58-65.

115. Jain, R. K. 1987. Transport of molecules in the tumor interstitium: a review. Cancer Res 47:3039-51.

116. Jansson, K., M. Jansson, M. Andersson, A. Magnuson, U. Ungerstedt, and L. Norgren. 2005. Normal values and differences between intraperitoneal and subcutaneous microdialysis in patients after non-complicated gastrointestinal surgery. Scand J Clin Lab Invest 65:273-81.

117. Jansson, P. A., J. Fowelin, U. Smith, and P. Lonnroth. 1988. Characterization by microdialysis of intracellular glucose level in subcutaneous tissue in humans. Am J Physiol 255:E218-20.

118. Jones, R. N., J. T. Kirby, M. L. Beach, D. J. Biedenbach, and M. A. Pfaller. 2002. Geographic variations in activity of broad-spectrum beta-lactams against Pseudomonas aeruginosa: summary of the worldwide SENTRY Antimicrobial Surveillance Program (1997-2000). Diagn Microbiol Infect Dis 43:239-43.

119. Joukhadar, C., P. Dehghanyar, F. Traunmuller, R. Sauermann, B. Mayer-Helm, A. Georgopoulos, and M. Muller. 2005. Increase of microcirculatory blood flow enhances penetration of ciprofloxacin into soft tissue. Antimicrob Agents Chemother 49:4149-53.

120. Joukhadar, C., H. Derendorf, and M. Muller. 2001. Microdialysis. A novel tool for clinical studies of anti-infective agents. Eur J Clin Pharmacol 57:211-9.

121. Joukhadar, C., N. Klein, R. M. Mader, C. Schrolnberger, B. Rizovski, E. Heere-Ress, H. Pehamberger, N. Strauchmann, B. Jansen, and M. Muller. 2001. Penetration of dacarbazine and its active metabolite 5-aminoimidazole-4-carboxamide into cutaneous metastases of human malignant melanoma. Cancer 92:2190-6.

122. Joukhadar, C., and M. Muller. 2005. Microdialysis: current applications in clinical pharmacokinetic studies and its potential role in the future. Clin Pharmacokinet 44:895-913.

123. Jumbe, N., A. Louie, R. Leary, W. Liu, M. R. Deziel, V. H. Tam, R. Bachhawat, C. Freeman, J. B. Kahn, K. Bush, M. N. Dudley, M. H. Miller, and G. L. Drusano. 2003. Application of a mathematical model to prevent in vivo amplification of antibiotic-resistant bacterial populations during therapy. J Clin Invest 112:275-85.

124. Kaplan, A. H., P. H. Gilligan, and R. R. Facklam. 1988. Recovery of resistant enterococci during vancomycin prophylaxis. J Clin Microbiol 26:1216-8.

125. Kashuba, A. D., A. N. Nafziger, G. L. Drusano, and J. S. Bertino, Jr. 1999. Optimizing aminoglycoside therapy for nosocomial pneumonia caused by gram-negative bacteria. Antimicrob Agents Chemother 43:623-9.

126. Katsube, T., Y. Yamano, and Y. Yano. 2008. Pharmacokinetic-pharmacodynamic modeling and simulation for in vivo bactericidal effect in murine infection model. J Pharm Sci 97:1606-14.

127. Kearns, G. L., S. M. Abdel-Rahman, J. L. Blumer, M. D. Reed, L. P. James, R. F. Jacobs, J. A. Bradley, I. R. Welshman, G. L. Jungbluth, and D. J. Stalker. 2000. Single dose pharmacokinetics of linezolid in infants and children. Pediatr Infect Dis J 19:1178-84.

128. Khair, O. A., J. M. Andrews, D. Honeybourne, G. Jevons, F. Vacheron, and R. Wise. 2001. Lung concentrations of telithromycin after oral dosing. J Antimicrob Chemother 47:837-40.

129. Khunvichai A., H. M., Karmann M., Joliff L., Rand K., Derendorf H. 2001. Presented at the 41st Annual Interscience Conference on Antimicrobial Agents and Chemotherapy, Chicago, USA, 2001.

130. Khunvichai A., K. M., Hirt M., Joliffe L., Derendorf H. 2003. Presented at the 32nd Annual Meeting of the American College of Clinical Pharmacology, Tampa, USA.

131. Klugman, K. P. 2003. Implications for antimicrobial prescribing of strategies based on bacterial eradication. Int J Infect Dis 7:S27-31.

132. Koal, T., M. Deters, K. Resch, and V. Kaever. 2006. Quantification of the carbapenem antibiotic ertapenem in human plasma by a validated liquid chromatography-mass spectrometry method. Clin Chim Acta 364:239-45.

133. Kovar, A., T. Dalla Costa, and H. Derendorf. 1997. Comparison of plasma and free tissue levels of ceftriaxone in rats by microdialysis. J Pharm Sci 86:52-6.

134. Kreilgaard, M. 2002. Assessment of cutaneous drug delivery using microdialysis. Adv Drug Deliv Rev 54 Suppl 1:S99-121.

135. Kreilgaard, M., M. J. Kemme, J. Burggraaf, R. C. Schoemaker, and A. F. Cohen. 2001. Influence of a microemulsion vehicle on cutaneous bioequivalence of a lipophilic model drug assessed by microdialysis and pharmacodynamics. Pharm Res 18:593-9.

136. Kunin, C. M., W. A. Craig, M. Kornguth, and R. Monson. 1973. Influence of binding on the pharmacologic activity of antibiotics. Ann N Y Acad Sci 226:214-24.

137. Kuti, J. L., P. K. Dandekar, C. H. Nightingale, and D. P. Nicolau. 2003. Use of Monte Carlo simulation to design an optimized pharmacodynamic dosing strategy for meropenem. J Clin Pharmacol 43:1116-23.

138. Kuti, J. L., N. R. Florea, C. H. Nightingale, and D. P. Nicolau. 2004. Pharmacodynamics of meropenem and imipenem against Enterobacteriaceae, Acinetobacter baumannii, and Pseudomonas aeruginosa. Pharmacotherapy 24:8-15.

139. Laethem, T., I. De Lepeleire, J. McCrea, J. Zhang, A. Majumdar, D. Musson, D. Rogers, S. Li, M. Guillaume, A. Parneix-Spake, and P. Deutsch. 2003. Tissue penetration by ertapenem, a parenteral carbapenem administered once daily, in suction-induced skin blister fluid in healthy young volunteers. Antimicrob Agents Chemother 47:1439-42.

140. Lang, S. D., G. L. Cameron, and P. R. Mullins. 1981. Anomalous effect of serum on the antimicrobial activity of cefoperazone. Drugs 22 Suppl 1:52-9.

141. Laue, H., T. Valensise, A. Seguin, S. Hawser, S. Lociuro, and K. Islam. 2007. Effect of human plasma on the antimicrobial activity of iclaprim in vitro. J Antimicrob Chemother 60:1388-90.

142. Lee, B. L., M. Sachdeva, and H. F. Chambers. 1991. Effect of protein binding of daptomycin on MIC and antibacterial activity. Antimicrob Agents Chemother 35:2505-8.

143. Lees, P., and F. Shojaee Aliabadi. 2002. Rational dosing of antimicrobial drugs: animals versus humans. Int J Antimicrob Agents 19:269-84.

144. Leggett, J. E., and W. A. Craig. 1989. Enhancing effect of serum ultrafiltrate on the activity of cephalosporins against gram-negative bacilli. Antimicrob Agents Chemother 33:35-40.

145. Leveque, N., S. Makki, J. Hadgraft, and P. Humbert. 2004. Comparison of Franz cells and microdialysis for assessing salicylic acid penetration through human skin. Int J Pharm 269:323-8.

146. Levin, B. R., and D. E. Rozen. 2006. Non-inherited antibiotic resistance. Nat Rev Microbiol 4:556-62.

147. Li, R. C. 2000. New pharmacodynamic parameters for antimicrobial agents. Int J Antimicrob Agents 13:229-35.

148. Li, R. C., M. Zhu, and J. J. Schentag. 1999. Achieving an optimal outcome in the treatment of infections. The role of clinical pharmacokinetics and pharmacodynamics of antimicrobials. Clin Pharmacokinet 37:1-16.

149. Lin, Y. H., V. C. Wu, I. J. Tsai, Y. L. Ho, J. J. Hwang, Y. K. Tsau, C. Y. Wu, K. D. Wu, and P. R. Hsueh. 2006. High frequency of linezolid-associated thrombocytopenia among patients with renal insufficiency. Int J Antimicrob Agents 28:345-51.

150. Lindemann, U., K. Wilken, H. J. Weigmann, H. Schaefer, W. Sterry, and J. Lademann. 2003. Quantification of the horny layer using tape stripping and microscopic techniques. J Biomed Opt 8:601-7.

151. Lipsky, B. A., D. G. Armstrong, D. M. Citron, A. D. Tice, D. E. Morgenstern, and M. A. Abramson. 2005. Ertapenem versus piperacillin/tazobactam for diabetic foot infections (SIDESTEP): prospective, randomised, controlled, double-blinded, multicentre trial. Lancet 366:1695-703.

152. Liu, P., and H. Derendorf. 2003. Antimicrobial tissue concentrations. Infect Dis Clin North Am 17:599-613.

153. Liu Q., L. N., Hintze S., Rand K., Derendorf H. 2002. Presented at the AAPS Annual Meeting and Exposition, Toronto.

154. Livermore, D. M., M. W. Carter, S. Bagel, B. Wiedemann, F. Baquero, E. Loza, H. P. Endtz, N. van Den Braak, C. J. Fernandes, L. Fernandes, N. Frimodt-Moller, L. S. Rasmussen, H. Giamarellou, E. Giamarellos-Bourboulis, V. Jarlier, J. Nguyen, C. E. Nord, M. J. Struelens, C. Nonhoff, J. Turnidge, J. Bell, R. Zbinden, S. Pfister, L. Mixson, and D. L. Shungu. 2001. In vitro activities of ertapenem (MK-0826) against recent clinical bacteria collected in Europe and Australia. Antimicrob Agents Chemother 45:1860-7.

155. Livermore, D. M., K. J. Oakton, M. W. Carter, and M. Warner. 2001. Activity of ertapenem (MK-0826) versus Enterobacteriaceae with potent beta-lactamases. Antimicrob Agents Chemother 45:2831-7.

156. Livermore, D. M., A. M. Sefton, and G. M. Scott. 2003. Properties and potential of ertapenem. J Antimicrob Chemother 52:331-44.

157. Livermore, D. M., M. Warner, S. Mushtaq, S. North, and N. Woodford. 2007. In vitro activity of the oxazolidinone RWJ-416457 against linezolid-resistant and -susceptible staphylococci and enterococci. Antimicrob Agents Chemother 51:1112-4.

158. Lodise, T. P., Jr., D. H. Rhoney, V. H. Tam, P. S. McKinnon, and G. L. Drusano. 2006. Pharmacodynamic profiling of cefepime in plasma and cerebrospinal fluid of hospitalized patients with external ventriculostomies. Diagn Microbiol Infect Dis 54:223-30.

159. Lodise, T. P., B. M. Lomaestro, and G. L. Drusano. 2006. Application of antimicrobial pharmacodynamic concepts into clinical practice: focus on beta-lactam antibiotics: insights from the Society of Infectious Diseases Pharmacists. Pharmacotherapy 26:1320-32.

160. Lomaestro, B. M., and G. L. Drusano. 2005. Pharmacodynamic evaluation of extending the administration time of meropenem using a Monte Carlo simulation. Antimicrob Agents Chemother 49:461-3.

161. Lonnroth, P., P. A. Jansson, and U. Smith. 1987. A microdialysis method allowing characterization of intercellular water space in humans. Am J Physiol 253:E228-31.

162. Lorentzen, H., F. Kallehave, H. J. Kolmos, U. Knigge, J. Bulow, and F. Gottrup. 1996. Gentamicin concentrations in human subcutaneous tissue. Antimicrob Agents Chemother 40:1785-9.

163. Low, D. E., N. Keller, A. Barth, and R. N. Jones. 2001. Clinical prevalence, antimicrobial susceptibility, and geographic resistance patterns of enterococci: results from the SENTRY Antimicrobial Surveillance Program, 1997-1999. Clin Infect Dis 32 Suppl 2:S133-45.

164. Lowdin, E., I. Odenholt, S. Bengtsson, and O. Cars. 1996. Pharmacodynamic effects of sub-MICs of benzylpenicillin against Streptococcus pyogenes in a newly developed in vitro kinetic model. Antimicrob Agents Chemother 40:2478-82.

165. Lowy, F. D. 2003. Antimicrobial resistance: the example of Staphylococcus aureus. J Clin Invest 111:1265-73.

166. Lucini, V., Grosso, S., Pannacci, M., Scaglione, F. 2006. Presented at the Program and abstracts of the 46th Interscience Conference on Antimicrobial Agents and Chemotherapy, San Francisco, USA.

167. MacGowan, A. P. 2004. Elements of design: the knowledge on which we build. Clin Microbiol Infect 10:6-11.

168. MacGowan, A. P. 2003. Pharmacokinetic and pharmacodynamic profile of linezolid in healthy volunteers and patients with Gram-positive infections. J Antimicrob Chemother 51 Suppl 2:ii17-25.

169. MacGowan, A. P., K. E. Bowker, C. M. Tobin, A. R. Noel, A. M. Lovering, and A. H. Thomson. 2008. Pharmacodynamics of vancomycin against MRSA: implications of bacterial inoculum for clinical breakpoints, ECCMID, Barcelona.

170. MacGowan, A. P., A. R. Noel, C. A. Rogers, and K. E. Bowker. 2004. Antibacterial effects of amoxicillin-clavulanate against Streptococcus pneumoniae and Haemophilus influenzae strains for which MICs are high, in an in vitro pharmacokinetic model. Antimicrob Agents Chemother 48:2599-603.

171. Marchese, A., G. Balistreri, E. Tonoli, E. A. Debbia, and G. C. Schito. 2000. Heterogeneous vancomycin resistance in methicillin-resistant Staphylococcus aureus strains isolated in a large Italian hospital. J Clin Microbiol 38:866-9.

172. Marchese, A., L. Gualco, A. M. Schito, E. A. Debbia, and G. C. Schito. 2004. In vitro activity of ertapenem against selected respiratory pathogens. J Antimicrob Chemother 54:944-51.

173. McCleverty, D., R. Lyons, and B. Henry. 2006. Microdialysis sampling and the clinical determination of topical dermal bioequivalence. Int J Pharm 308:1-7.

174. McKinnon, P. S., and S. L. Davis. 2004. Pharmacokinetic and pharmacodynamic issues in the treatment of bacterial infectious diseases. Eur J Clin Microbiol Infect Dis 23:271-88.

175. Meibohm, B., and H. Derendorf. 1997. Basic concepts of pharmacokinetic/pharmacodynamic (PK/PD) modelling. Int J Clin Pharmacol Ther 35:401-13.

176. Meibohm, B., and H. Derendorf. 2002. Pharmacokinetic/pharmacodynamic studies in drug product development. J Pharm Sci 91:18-31.

177. Merrikin, D. J., J. Briant, and G. N. Rolinson. 1983. Effect of protein binding on antibiotic activity in vivo. J Antimicrob Chemother 11:233-8.

178. Miller, R., W. Ewy, B. W. Corrigan, D. Ouellet, D. Hermann, K. G. Kowalski, P. Lockwood, J. R. Koup, S. Donevan, A. El-Kattan, C. S. Li, J. L. Werth, D. E. Feltner, and R. L. Lalonde. 2005. How modeling and simulation have enhanced decision making in new drug development. J Pharmacokinet Pharmacodyn 32:185-97.

179. Mitchell, J. A., P. Akarasereenont, C. Thiemermann, R. J. Flower, and J. R. Vane. 1993. Selectivity of nonsteroidal antiinflammatory drugs as inhibitors of constitutive and inducible cyclooxygenase. Proc Natl Acad Sci U S A 90:11693-7.

180. Moore, R. D., P. S. Lietman, and C. R. Smith. 1987. Clinical response to aminoglycoside therapy: importance of the ratio of peak concentration to minimal inhibitory concentration. J Infect Dis 155:93-9.

181. Moribe, K., and K. Maruyama. 2002. Pharmaceutical design of the liposomal antimicrobial agents for infectious disease. Curr Pharm Des 8:441-54.

182. Mouton, J. W., M. N. Dudley, O. Cars, H. Derendorf, and G. L. Drusano. 2002. Standardization of pharmacokinetic/pharmacodynamic (PK/PD) terminology for anti-infective drugs. Int J Antimicrob Agents 19:355-8.

183. Mouton, J. W., M. N. Dudley, O. Cars, H. Derendorf, and G. L. Drusano. 2005. Standardization of pharmacokinetic/pharmacodynamic (PK/PD) terminology for anti-infective drugs: an update. J Antimicrob Chemother 55:601-7.

184. Mouton, J. W., A. Schmitt-Hoffmann, S. Shapiro, N. Nashed, and N. C. Punt. 2004. Use of Monte Carlo simulations to select therapeutic doses and provisional breakpoints of BAL9141. Antimicrob Agents Chemother 48:1713-8.

185. Mouton, J. W., U. Theuretzbacher, W. A. Craig, P. M. Tulkens, H. Derendorf, and O. Cars. 2008. Tissue concentrations: do we ever learn? J Antimicrob Chemother 61:235-7.

186. Mouton, J. W., D. J. Touzw, A. M. Horrevorts, and A. A. Vinks. 2000. Comparative pharmacokinetics of the carbapenems: clinical implications. Clin Pharmacokinet 39:185-201.

187. Mouton, J. W., and A. A. Vinks. 2005. Pharmacokinetic/pharmacodynamic modelling of antibacterials in vitro and in vivo using bacterial growth and kill kinetics: the minimum inhibitory concentration versus stationary concentration. Clin Pharmacokinet 44:201-10.

188. Mueller, M., A. de la Pena, and H. Derendorf. 2004. Issues in pharmacokinetics and pharmacodynamics of anti-infective agents: kill curves versus MIC. Antimicrob Agents Chemother 48:369-77.

189. Muller, M., M. Brunner, R. Schmid, E. M. Putz, A. Schmiedberger, I. Wallner, and H. G. Eichler. 1998. Comparison of three different experimental methods for the assessment of peripheral compartment pharmacokinetics in humans. Life Sci 62:PL227-34.

190. Muller, M., O. Haag, T. Burgdorff, A. Georgopoulos, W. Weninger, B. Jansen, G. Stanek, H. Pehamberger, E. Agneter, and H. G. Eichler. 1996. Characterization of peripheral-compartment kinetics of antibiotics by in vivo microdialysis in humans. Antimicrob Agents Chemother 40:2703-9.

191. Muller, M., H. Mascher, C. Kikuta, S. Schafer, M. Brunner, G. Dorner, and H. G. Eichler. 1997. Diclofenac concentrations in defined tissue layers after topical administration. Clin Pharmacol Ther 62:293-9.

192. Muller, M., R. Schmid, A. Georgopoulos, A. Buxbaum, C. Wasicek, and H. G. Eichler. 1995. Application of microdialysis to clinical pharmacokinetics in humans. Clin Pharmacol Ther 57:371-80.

193. Muller, M., H. Stass, M. Brunner, J. G. Moller, E. Lackner, and H. G. Eichler. 1999. Penetration of moxifloxacin into peripheral compartments in humans. Antimicrob Agents Chemother 43:2345-9.

194. Neuhauser, M. M., J. L. Prause, L. H. Danziger, and S. L. Pendland. 2003. In vitro bactericidal activities of ABT-773 against ermB strains of Streptococcus pneumoniae. Antimicrob Agents Chemother 47:1132-4.

195. Nichols, R. L., posting date. Preventing Surgical Site Infections: A Surgeon's Perspective. [Online.]

196. Nicolau, D. P. 2003. Optimizing outcomes with antimicrobial therapy through pharmacodynamic profiling. J Infect Chemother 9:292-6.

197. Nicolau, D. P., and P. G. Ambrose. 2001. Pharmacodynamic profiling of levofloxacin and gatifloxacin using Monte Carlo simulation for community-acquired isolates of Streptococcus pneumoniae. Am J Med 111:13-18; 36-38.

198. Nielsen, E. I., A. Viberg, E. Lowdin, O. Cars, M. O. Karlsson, and M. Sandstrom. 2006. A Semi-Mechanistic Pharmacokinetic/Pharmacodynamic Model for the Assessment of Activity of Antibacterial Agents from Time-Kill Curve Experiments. Antimicrob Agents Chemother 51:128-36.

199. Nix, D. E., A. K. Majumdar, and M. J. DiNubile. 2004. Pharmacokinetics and pharmacodynamics of ertapenem: an overview for clinicians. J Antimicrob Chemother 53 Suppl 2:ii23-8.

200. Nix, D. E., K. R. Matthias, and E. C. Ferguson. 2004. Effect of ertapenem protein binding on killing of bacteria. Antimicrob Agents Chemother 48:3419-24.

201. Noel, A. R., K. E. Bowker, and A. P. Macgowan. 2005. Pharmacodynamics of moxifloxacin against anaerobes studied in an in vitro pharmacokinetic model. Antimicrob Agents Chemother 49:4234-9.

202. Nolting, A., T. Dalla Costa, K. H. Rand, and H. Derendorf. 1996. Pharmacokinetic-pharmacodynamic modeling of the antibiotic effect of piperacillin in vitro. Pharm Res 13:91-6.

203. Noreddin, A. M., D. J. Hoban, and G. G. Zhanel. 2005. Comparison of gatifloxacin and levofloxacin administered at various dosing regimens to hospitalised patients with community-acquired pneumonia: pharmacodynamic target attainment study using North American surveillance data for Streptococcus pneumoniae. Int J Antimicrob Agents 26:120-5.

204. Nowak, G., J. Ungerstedt, J. Wernerman, U. Ungerstedt, and B. G. Ericzon. 2002. Clinical experience in continuous graft monitoring with microdialysis early after liver transplantation. Br J Surg 89:1169-75.

205. Odenholt, I., and O. Cars. 2006. Pharmacodynamics of moxifloxacin and levofloxacin against Streptococcus pneumoniae, Staphylococcus aureus, Klebsiella pneumoniae and Escherichia coli: simulation of human plasma concentrations after intravenous dosage in an in vitro kinetic model. J Antimicrob Chemother 58:960-5.

206. Odenholt, I., O. Cars, and E. Lowdin. 2004. Pharmacodynamic studies of amoxicillin against Streptococcus pneumoniae: comparison of a new pharmacokinetically enhanced formulation (2000 mg twice daily) with standard dosage regimens. J Antimicrob Chemother 54:1062-6.

207. Olson, R. J., and J. B. Justice, Jr. 1993. Quantitative microdialysis under transient conditions. Anal Chem 65:1017-22.

208. Palavecino, E. 2004. Community-acquired methicillin-resistant Staphylococcus aureus infections. Clin Lab Med 24:403-18.

209. Palumbi, S. R. 2001. Humans as the world's greatest evolutionary force. Science 293:1786-90.

210. Pearson, R. D., R. T. Steigbigel, H. T. Davis, and S. W. Chapman. 1980. Method of reliable determination of minimal lethal antibiotic concentrations. Antimicrob Agents Chemother 18:699-708.

211. Perry, T. R., and J. J. Schentag. 2001. Clinical use of ceftriaxone: a pharmacokinetic-pharmacodynamic perspective on the impact of minimum inhibitory concentration and serum protein binding. Clin Pharmacokinet 40:685-94.

212. Popick, A. C., W. G. Crouthamel, and I. Bekersky. 1987. Plasma protein binding of ceftriaxone. Xenobiotica 17:1139-45.

213. Presant, C. A., W. Wolf, V. Waluch, C. Wiseman, P. Kennedy, D. Blayney, and R. R. Brechner. 1994. Association of intratumoral pharmacokinetics of fluorouracil with clinical response. Lancet 343:1184-7.

214. Preston, S. L., G. L. Drusano, A. L. Berman, C. L. Fowler, A. T. Chow, B. Dornseif, V. Reichl, J. Natarajan, and M. Corrado. 1998. Pharmacodynamics of levofloxacin: a new paradigm for early clinical trials. Jama 279:125-9.

215. Radermacher, J., D. Jentsch, M. A. Scholl, T. Lustinetz, and J. C. Frolich. 1991. Diclofenac concentrations in synovial fluid and plasma after cutaneous application in inflammatory and degenerative joint disease. Br J Clin Pharmacol 31:537-41.

216. Regoes, R. R., C. Wiuff, R. M. Zappala, K. N. Garner, F. Baquero, and B. R. Levin. 2004. Pharmacodynamic functions: a multiparameter approach to the design of antibiotic treatment regimens. Antimicrob Agents Chemother 48:3670-6.

217. Riess, W., K. Schmid, L. Botta, K. Kobayashi, J. Moppert, W. Schneider, A. Sioufi, A. Strusberg, and M. Tomasi. 1986. [The percutaneous absorption of diclofenac]. Arzneimittelforschung 36:1092-6.

218. Riond, J. L., and J. E. Riviere. 1989. Doxycycline binding to plasma albumin of several species. J Vet Pharmacol Ther 12:253-60.

219. Riviere, J. E., and P. L. Williams. 1992. Pharmacokinetic implications of changing blood flow in skin. J Pharm Sci 81:601-2.

220. Rodvold, K. A. 2001. Pharmacodynamics of antiinfective therapy: taking what we know to the patient's bedside. Pharmacotherapy 21:319-330.

221. Rollins, D. 1990. Clinical Pharmacokinetics, Eighteenth Edition ed. Mack Publishing Company.

222. Ryan, D. M. 1993. Pharmacokinetics of antibiotics in natural and experimental superficial compartments in animals and humans. J Antimicrob Chemother 31 Suppl D:1-16.

223. Rybak, M. J. 2006. Pharmacodynamics: relation to antimicrobial resistance. Am J Infect Control 34:38-45; 64-73.

224. Scaglione, F., G. Demartini, M. M. Arcidiacono, S. Dugnani, and F. Fraschini. 1998. Influence of protein binding on the pharmacodynamics of ceftazidime or ceftriaxone against gram-positive and gram-negative bacteria in an in vitro infection model. J Chemother 10:29-34.

225. Scaglione, F., and L. Paraboni. 2006. Influence of pharmacokinetics/pharmacodynamics of antibacterials in their dosing regimen selection. Expert Rev Anti Infect Ther 4:479-90.

226. Schaper, K. J., S. Schubert, and A. Dalhoff. 2005. Kinetics and quantification of antibacterial effects of beta-lactams, macrolides, and quinolones against gram-positive and gram-negative RTI pathogens. Infection 33:3-14.

227. Schito, G. C. 2006. The importance of the development of antibiotic resistance in Staphylococcus aureus. Clin Microbiol Infect 12 Suppl 1:3-8.

228. Schmidt, S., A. Barbour, M. Sahre, K. H. Rand, and H. Derendorf. 2008. PK/PD: new insights for antibacterial and antiviral applications. Curr Opin Pharmacol.

229. Schmidt, S., E. Schuck, V. Kumar, O. Burkhardt, and H. Derendorf. 2007. Integration of pharmacokinetic/pharmacodynamic modeling and simulation in the development of new anti-infective agents - minimum inhibitory concentration versus time-kill curves. Expert Opin. Drug Discov. 2:849-860.

230. Schuck, E. L., A. Dalhoff, H. Stass, and H. Derendorf. 2005. Pharmacokinetic/pharmacodynamic (PK/PD) evaluation of a once-daily treatment using ciprofloxacin in an extended-release dosage form. Infection 33:22-8.

231. Schuck, E. L., and H. Derendorf. 2005. Pharmacokinetic/pharmacodynamic evaluation of anti-infective agents. Expert Rev Anti Infect Ther 3:361-73.

232. Sevillano, D., M. J. Gimenez, L. Alou, L. Aguilar, F. Cafini, M. Torrico, N. Gonzalez, O. Echeverria, P. Coronel, and J. Prieto. 2007. Effects of human albumin and serum on the in vitro bactericidal activity of cefditoren against penicillin-resistant Streptococcus pneumoniae. J Antimicrob Chemother 60:156-8.

233. Shefet, D., E. Robenshtok, M. Paul, and L. Leibovici. 2005. Empirical atypical coverage for inpatients with community-acquired pneumonia: systematic review of randomized controlled trials. Arch Intern Med 165:1992-2000.

234. Singh, P., and M. S. Roberts. 1994. Effects of vasoconstriction on dermal pharmacokinetics and local tissue distribution of compounds. J Pharm Sci 83:783-91.

235. Singh, P., and M. S. Roberts. 1994. Skin permeability and local tissue concentrations of nonsteroidal anti-inflammatory drugs after topical application. J Pharmacol Exp Ther 268:144-51.

236. Smith, H. 1998. What happens to bacterial pathogens in vivo? Trends Microbiol 6:239-43.

237. Smith, P. F., B. Tsuji, B. M. Booker, A. Forrest, S. Bajic, P. Kelchlin, S. M. Bhavnani, R. N. Jones, and P. G. Ambrose. 2006. Pharmacodynamics of cefprozil against Haemophilus influenzae in an in vitro pharmacodynamic model. Diagn Microbiol Infect Dis 56:379-386.

238. Song, J. H. 2003. Introduction: the goals of antimicrobial therapy. Int J Infect Dis 7:1-4.

239. Soriano, A., O. Miro, and J. Mensa. 2005. Mitochondrial toxicity associated with linezolid. N Engl J Med 353:2305-6.

240. Stagni, G., D. O'Donnell, Y. J. Liu, D. L. Kellogg, T. Morgan, and A. M. Shepherd. 2000. Intradermal microdialysis: kinetics of iontophoretically delivered propranolol in forearm dermis. J Control Release 63:331-9.

241. Stahl, M., R. Bouw, A. Jackson, and V. Pay. 2002. Human microdialysis. Curr Pharm Biotechnol 3:165-78.

242. Stahle, L., P. Arner, and U. Ungerstedt. 1991. Drug distribution studies with microdialysis. III: Extracellular concentration of caffeine in adipose tissue in man. Life Sci 49:1853-8.

243. Stalker, D. J., G. L. Jungbluth, N. K. Hopkins, and D. H. Batts. 2003. Pharmacokinetics and tolerance of single- and multiple-dose oral or intravenous linezolid, an oxazolidinone antibiotic, in healthy volunteers. J Antimicrob Chemother 51:1239-46.

244. Stoeckel, K. 1981. Pharmacokinetics of Rocephin, a highly active new cephalosporin with an exceptionally long biological half-life. Chemotherapy 27:42-6.

245. Stoeckel, K., P. J. McNamara, R. Brandt, H. Plozza-Nottebrock, and W. H. Ziegler. 1981. Effects of concentration-dependent plasma protein binding on ceftriaxone kinetics. Clin Pharmacol Ther 29:650-7.

246. Suh, B., W. A. Craig, A. C. England, and R. L. Elliott. 1981. Effect of free fatty acids on protein binding of antimicrobial agents. J Infect Dis 143:609-16.

247. Svensson, C. K., M. N. Woodruff, J. G. Baxter, and D. Lalka. 1986. Free drug concentration monitoring in clinical practice. Rationale and current status. Clin Pharmacokinet 11:450-69.

248. Tam, V. H., P. S. McKinnon, R. L. Akins, G. L. Drusano, and M. J. Rybak. 2003. Pharmacokinetics and pharmacodynamics of cefepime in patients with various degrees of renal function. Antimicrob Agents Chemother 47:1853-61.

249. Tam, V. H., A. N. Schilling, K. Poole, and M. Nikolaou. 2007. Mathematical modelling response of Pseudomonas aeruginosa to meropenem. J Antimicrob Chemother 60:1302-9.

250. Tegeder, I., L. Brautigam, M. Podda, S. Meier, R. Kaufmann, G. Geisslinger, and M. Grundmann-Kollmann. 2002. Time course of 8-methoxypsoralen concentrations in skin and plasma after topical (bath and cream) and oral administration of 8-methoxypsoralen. Clin Pharmacol Ther 71:153-61.

251. Theuretzbacher, U. 2007. Tissue penetration of antibacterial agents: how should this be incorporated into pharmacodynamic analyses? Curr Opin Pharmacol 7:498-504.

252. Thomas, J. K., A. Forrest, S. M. Bhavnani, J. M. Hyatt, A. Cheng, C. H. Ballow, and J. J. Schentag. 1998. Pharmacodynamic evaluation of factors associated with the development of bacterial resistance in acutely ill patients during therapy. Antimicrob Agents Chemother 42:521-7.

253. Thorsen, K., A. O. Kristoffersson, U. H. Lerner, and R. P. Lorentzon. 1996. In situ microdialysis in bone tissue. Stimulation of prostaglandin E2 release by weight-bearing mechanical loading. J Clin Invest 98:2446-9.

254. Tomaselli, F., A. Maier, V. Matzi, F. M. Smolle-Juttner, and P. Dittrich. 2004. Penetration of meropenem into pneumonic human lung tissue as measured by in vivo microdialysis. Antimicrob Agents Chemother 48:2228-32.

255. Toutain, P. L., and A. Bousquet-Melou. 2002. Free drug fraction vs free drug concentration: a matter of frequent confusion. J Vet Pharmacol Ther 25:460-3.

256. Toutain, P. L., J. R. del Castillo, and A. Bousquet-Melou. 2002. The pharmacokinetic-pharmacodynamic approach to a rational dosage regimen for antibiotics. Res Vet Sci 73:105-14.

257. Travers, K., and M. Barza. 2002. Morbidity of infections caused by antimicrobial-resistant bacteria. Clin Infect Dis 34 Suppl 3:S131-4.

258. Treyaprasert, W., S. Schmidt, K. H. Rand, U. Suvanakoot, and H. Derendorf. 2006. Pharmacokinetic/pharmacodynamic modeling of in vitro activity of azithromycin against four different bacterial strains. Int J Antimicrob Agents. 29:263-70

259. Tsiodras, S., H. S. Gold, G. Sakoulas, G. M. Eliopoulos, C. Wennersten, L. Venkataraman, R. C. Moellering, and M. J. Ferraro. 2001. Linezolid resistance in a clinical isolate of Staphylococcus aureus. Lancet 358:207-8.

260. Ungerstedt, U., and C. Pycock. 1974. Functional correlates of dopamine neurotransmission. Bull Schweiz Akad Med Wiss 30:44-55.

261. Van der Auwera, P., and J. Klastersky. 1990. Study of the influence of protein binding on serum bactericidal titres and killing rates in volunteers receiving ceftazidime, cefotaxime and ceftriaxone. J Hosp Infect 15 Suppl A:23-34.

262. Veronese, F. M., R. Bevilacqua, E. Boccu, and C. A. Benassi. 1977. Drug-protein interaction: the binding of cephalosporins to albumins. Farmaco [Sci] 32:303-10.

263. Vilar-Compte, D., R. Roldan-Marin, C. Robles-Vidal, and P. Volkow. 2006. Surgical site infection (SSI) rates among patients who underwent mastectomy after the introduction of SSI prevention policies. Infect Control Hosp Epidemiol 27:829-34.

264. Walker, K. J., A. J. Larsson, R. A. Zabinski, and J. C. Rotschafer. 1994. Evaluation of antimicrobial activities of clarithromycin and 14-hydroxyclarithromycin against three strains of Haemophilus influenzae by using an in vitro pharmacodynamic model. Antimicrob Agents Chemother 38:2003-7.

265. Weber, D. J. 2006. Collateral damage and what the future might hold. The need to balance prudent antibiotic utilization and stewardship with effective patient management. Int J Infect Dis 10:17-24.

266. Wennberg, A. M., O. Larko, P. Lonnroth, G. Larson, and A. L. Krogstad. 2000. Delta-aminolevulinic acid in superficial basal cell carcinomas and normal skin-a microdialysis and perfusion study. Clin Exp Dermatol 25:317-22.

267. Weston, J. S. 2002. Treatment of gram-positive infections: past, present, and future. Crit Care Nurs Clin North Am 14:17-29.

268. White, R. 2001. What in vitro models of infection can and cannot do. Pharmacotherapy 21:292-301.

269. White, R. L., M. B. Kays, T. A. Armstrong, and L. V. Friedrich. 1990. Effects of supraphysiologic temperature and broth dilution on serum protein binding. Antimicrob Agents Chemother 34:1257-8.

270. WHO January, 2002, posting date. Antimicrobial Resistance. [Online.]

271. Winokur, P. L., R. Canton, J. M. Casellas, and N. Legakis. 2001. Variations in the prevalence of strains expressing an extended-spectrum beta-lactamase phenotype and characterization of isolates from Europe, the Americas, and the Western Pacific region. Clin Infect Dis 32 Suppl 2:S94-103.

272. Wispelwey, B. 2005. Clinical implications of pharmacokinetics and pharmacodynamics of fluoroquinolones. Clin Infect Dis 41:127-35.

273. Wittau, M., E. Wagner, V. Kaever, T. Koal, D. Henne-Bruns, and R. Isenmann. 2006. Intraabdominal tissue concentration of ertapenem. J Antimicrob Chemother 57:312-6.

274. Yamaguchi, K., and A. Ohno. 1992. [Considerations on MRSA infections in relation to modern chemotherapy]. Nippon Rinsho 50:923-31.

275. Yano, Y., T. Oguma, H. Nagata, and S. Sasaki. 1998. Application of logistic growth model to pharmacodynamic analysis of in vitro bactericidal kinetics. J Pharm Sci 87:1177-83.

276. Yassin, H. M., and L. L. Dever. 2001. Telithromycin: a new ketolide antimicrobial for treatment of respiratory tract infections. Expert Opin Investig Drugs 10:353-67.

277. Yuk, J. H., C. H. Nightingale, and R. Quintiliani. 1989. Clinical pharmacokinetics of ceftriaxone. Clin Pharmacokinet 17:223-35.

278. Zeitlinger, M., M. Muller, and C. Joukhadar. 2005. Lung microdialysis--a powerful tool for the determination of exogenous and endogenous compounds in the lower respiratory tract (mini-review). Aaps J 7:E600-8.

279. Zeitlinger, M., R. Sauermann, M. Fille, J. Hausdorfer, I. Leitner, and M. Muller. 2008. Plasma protein binding of fluoroquinolones affects antimicrobial activity. J Antimicrob Chemother 61:561-7.

280. Zeitlinger, M. A., R. Sauermann, F. Traunmuller, A. Georgopoulos, M. Muller, and C. Joukhadar. 2004. Impact of plasma protein binding on antimicrobial activity using time-killing curves. J Antimicrob Chemother 54:876-80.

281. Zhanel, G. G., C. Johanson, J. M. Embil, A. Noreddin, A. Gin, L. Vercaigne, and D. J. Hoban. 2005. Ertapenem: review of a new carbapenem. Expert Rev Anti Infect Ther 3:23-39.

282. Zurenko, G. E., B. H. Yagi, R. D. Schaadt, J. W. Allison, J. O. Kilburn, S. E. Glickman, D. K. Hutchinson, M. R. Barbachyn, and S. J. Brickner. 1996. In vitro activities of U-100592 and U-100766, novel oxazolidinone antibacterial agents. Antimicrob Agents Chemother 40:839-45.

BIOGRAPHICAL SKETCH

Stephan Schmidt was born in 1978, in Sonneberg, Germany. The elder of two sons, he grew up mostly in Sonneberg and received his high school degree from the Arnold-Gymnasium in Neustadt bei Coburg, Germany, in 1998. He earned his B.S. in pharmaceutical sciences from the Friedrich-Alexander University in Erlangen, Germany, in 2004. On completion of his practical pharmaceutical training year, he was granted his license to practice as a pharmacist in Germany in 2005. In May 2005, he joined the Ph.D. program at the University of Florida, College of Pharmacy, in the Department of Pharmaceutics. Under the supervision of Dr. Hartmut Derendorf, distinguished professor and chair, he focused his research work on the "pharmacokinetics and pharmacodynamics of oxazolidinones and beta-lactams." During his time at the University of Florida, he has been an active member of the American Association of Pharmaceutical Scientists (AAPS), American Society for Microbiology (ASM), American College of Clinical Pharmacology (ACCP), Student Outreach Committee (SOC) of ACCP and received multiple national and international awards and travel grants.

Upon completion of his Ph.D. program, Stephan will join Prof. Meindert Danhof's group at the Leiden University in the Netherlands for a 3-year post-doctoral fellowship under the supervision of Dr. Oscar Della Pasqua.